Dissertation zur Erlangung des Doktorgrades
der Fakultät für Chemie und Pharmazie
der Ludwig-Maximilians-Universität München

The ERBB receptor network and the role of the LRIG protein family in skin during development, homeostasis and tumorigenesis

Christine Hösl
aus
Mainburg, Deutschland

2019

Erklärung

Diese Dissertation wurde im Sinne von § 7 der Promotionsordnung vom 28. November 2011 von Herrn Prof. Dr. Eckhard Wolf betreut und von Herrn PD Dr. Dietmar Martin von der Fakultät für Chemie und Pharmazie vertreten.

Eidesstattliche Versicherung

Diese Dissertation wurde eigenständig und ohne unerlaubte Hilfe erarbeitet.

München, 02. August 2019

Christine Hösl

Dissertation eingereicht am	02. August 2019
1. Gutachter:	PD Dr. Dietmar Martin
2. Gutachter:	Prof. Dr. Eckhard Wolf
Mündliche Prüfung am	13. September 2019

The ERBB receptor network and the role of the LRIG protein family in skin during development, homeostasis and tumorigenesis

Christine Hoesl

Publications

During my doctoral research, I worked on the following publications which are published or in the process of being published:

The receptor tyrosine kinase ERBB4 is expressed in skin keratinocytes and influences epidermal proliferation.

C. Hoesl, J.M. Röhrl, M.R. Schneider, M. Dahlhoff

Biochimica et Biophysica Acta - General Subjects, April 2018

DOI: 10.1016/j.bbagen.2018.01.017

The transmembrane protein LRIG2 increases tumor progression in skin carcinogenesis

C. Hoesl, T. Fröhlich, J.E. Hundt, H. Kneitz, M. Goebeler, R. Wolf, M.R. Schneider, M. Dahlhoff

Molecular Oncology, October 2019

DOI: 10.1002/1878-0261.12579

Epidermal overexpression of LRIG1 disturbs development and homeostasis in skin by disrupting the ERBB system

C. Hoesl, J.E. Hundt, C. Rose, R. Wolf, M.R. Schneider, M. Dahlhoff

Journal of Dermatological Science, revision submitted September 2019, under review

The secretome of skin cancer cells activates the mTOR/MYC pathway in healthy keratinocytes and converts them into tumorigenic cells

C. Hoesl, E. Zanuttigh, T. Fröhlich, J. Philippou-Massier, S. Krebs, H. Blum, M. Dahlhoff

FEBS Journal, submitted September 2019, under review

The first three manuscripts are presented as part of this thesis.

Conferences

Parts of this work have been presented at the following conferences:

43th Annual meeting of the Arbeitsgemeinschaft Dermatologische Forschung, Vienna, Austria (2016)

> ***Poster presentation*** "The LRIG-Family - Regulators of ERBB signaling in skin during development, homeostasis and tumorigenesis"

15th Meeting of the Dermato-Endocrinologie-group, Vienna, Austria (2016)

> ***Talk*** "The LRIG-Family - Regulators of ERBB signaling in skin during development, homeostasis and tumorigenesis"

81th Cold Spring Harbor Symposium: Targeting Cancer, Cold Spring Harbor, NY, USA (2016)

> ***Poster presentation*** "LRIG2 – friend or foe in skin tumorigenesis"

46th Annual meeting of the European Society for Dermatological Research, Munich, Germany (2016)

> ***Poster presentation & poster price*** "LRIG2 – friend or foe in skin tumorigenesis" and "LRIG1 a regulator of ERBB signaling in skin during development and homeostasis"

44th Annual meeting of the Arbeitsgemeinschaft Dermatologische Forschung, Göttingen, Germany (2017)

Poster presentation "LRIG2 – friend or foe in skin tumorigenesis"

47th Annual meeting of the European Society for Dermatological Research, Salzburg, Austria (2017)

Poster presentation "The transmembrane protein LRIG1 regulates receptor tyrosine kinases in skin development and homeostasis"

Mechanisms and Models of Cancer, Cold Spring Harbor, NY, USA (2018)

Poster presentation "The Janus face of LRIG1 in skin cancer" and "LRIG2 – f riend or foe in skin tumorigenesis"
*Supported by the **DAAD stipend** to support congress travels.*

46th Annual meeting of the Arbeitsgemeinschaft Dermatologische Forschung, Munich, Germany (2019)

Poster presentation "The transmembrane proteins LRIG1 and LRIG2 differentially affect skin carcinogenesis"

Summary

The skin, the outermost layer of the human body, is a highly versatile organ and is regulated very tightly. Epidermal dysregulation can cause over 3000 skin diseases, among them non-melanoma skin cancer (NMSC). NMSC occurs more commonly than all other tumors combined. High cumulative sun exposure and a history of sunburns are the causes of 90% of NMSC incidences. Ultraviolet radiation also increases erythroblastic leukemia viral oncogene homolog (ERBB) receptor signaling as it is found in various tumors. The ERBB receptor family comprises four receptor tyrosine kinases: EGFR/ERBB1/HER1, ERBB2/HER2/neu, ERBB3/HER3 and ERBB4/HER4. The ERBB system represents a very complex signaling network regulating pivotal cellular processes like proliferation, differentiation, apoptosis and motility. They also play important roles during skin development, homeostasis and tumorigenesis. Deletion of the autonomous epidermal growth factor receptor (EGFR) as well as its activation causes a severe phenotype in murine epidermis. Furthermore, EGFR triggers carcinogenesis in the skin, as observed in several other tumors. In contrast, ERBB2 and ERBB3 deficiency have no major impact on skin homeostasis, whereas both receptors are involved in NMSC promotion. The second autonomous receptor of the ERBB family, ERBB4, is involved in crucial evolutionary processes such as the development of the heart and the central nervous system, and it is implicated in various epithelial tumors. However, the presence and role of ERBB4 in the skin has been debated for many years. Therefore, we investigated the function of ERBB4

in the skin *in vitro* and *in vivo* in human skin tissue samples and a skin-specific ERBB4 knockout mouse model. We analyzed receptor expression in the human keratinocyte cell line HaCaT and in the skin epidermoid carcinoma cell line A431 and found ERBB4 expression and activation upon epidermal growth factor stimulation in both. We uncovered the expression and localization of ERBB4 in human tissue samples in the basal epidermis and developed a skin-specific ERBB4 knockout mouse model, showing a decreased epidermal thickness and a reduced proliferation rate. Taken together, our findings not only proved the expression of ERBB4 in the skin, or more precisely, in the basal layer of human and murine epidermis, they also showed the influence of the receptor on epidermal homeostasis by affecting proliferation.

ERBB receptors are regulated by positive and negative feedback loop mechanisms, comprising ligand activation, receptor recycling, degradation and compartmentalization, but also the synthesis of new regulatory molecules like leucine-rich repeats and immunoglobulin-like domains proteins (LRIG). LRIG proteins belong to a single-pass transmembrane protein family that includes three homologous proteins in vertebrates (LRIG1-3). Due to their potential as prognostic factors in various cancer types, LRIG proteins aroused attention. LRIG1 is the best-studied member of the protein family. It promotes stem cell quiescence in the skin, intestine and stomach and influences the ERBB signaling network by inducing ubiquitination and therefore the degradation of EGFR. Research on LRIG2 and LRIG3 is currently much less advanced. However, regarding tumorigenesis, LRIG2 is mostly related to poor prognosis, while LRIG3 and LRIG1 are thought to be tumor suppressors. Molecular mechanisms, in particular their role in the skin, are not yet understood completely.

Using the Tet-Off system, we generated inducible, skin-specific transgenic (TG) mouse lines overexpressing LRIG1-3 to investigate their function in skin development, homeostasis and tumorigenesis *in vivo*. This thesis presents the impact of LRIG1 and LRIG2 on the epidermis and pilosebaceous unit.

Skin-specific overexpression of LRIG1 in mice revealed a severe phenotype during epidermal development and homeostasis. LRIG1 excess during embryogenesis caused postnatal lethality, possibly due to a disrupted skin barrier. Newborn LRIG1-TG mice showed altered epidermal differentiation and hair follicle morphogenesis. Additionally, the ERBB system was affected by LRIG1 overexpression at birth. However, inhibition of LRIG1 overexpression until birth by doxycycline enabled TG mice to survive. LRIG1 excess disturbed skin homeostasis and resulted in a severe alopecia phenotype, showing decreased ERBB signaling and a profoundly impaired hair follicle cycle. In contrast,

neurogenic locus notch homolog protein (NOTCH) signaling, which is involved in cell fate decisions, was activated and the expression of stem cell markers of the bulge and the sebaceous gland was increased in adult LRIG1-TG mice. In conclusion, the LRIG1-TG mouse model revealed a remarkable effect of LRIG1 on skin development and homeostasis, influencing the ERBB system as well as NOTCH signaling and epidermal stem cells.

In contrast to LRIG1, LRIG2-TG mice showed no impact on skin development or homeostasis. Nevertheless, we found that thrombospondin-1 (THBS1) interacts with LRIG2 in adult TG mice. THBS1 is an important player in angiogenesis and tumorigenesis, influencing the extracellular matrix. *In vitro* studies showed increased LRIG2 expression in epidermal cancer cell lines (A431 and A375) compared to human keratinocytes (HaCaT). The evaluation of human tissue samples of patients with cutaneous squamous cell carcinoma (cSCC) also revealed LRIG2 expression in these tumors. Further, 12-O-tetra-decanoylphorbol-13-acetate (TPA)-induced epidermal dysplasia elucidated severely increased inflammation due to an LRIG2 excess in TG mice, indicating a potential tumorigenic function of LRIG2. To investigate the role of LRIG2 during skin tumorigenesis, we applied a two-stage chemical carcinogenesis protocol to LRIG2-TG mice and controls using the tumor initiating agent 7,12-dimethylbenz(a)anthracene, and the tumor promoting agent TPA. LRIG2-TG mice showed a significantly increased tumor progression and an early onset of cSCC with a concomitant inactivation of the tumor suppressor phosphatidylinositol 3,4,5-triphosphate 3-phosphatase and dual specificity protein phosphatase PTEN. In addition, we found activated EGFR/ERBB4-mitogen activated protein kinase (MAPK) signaling in LRIG2-TG mice during tumorigenesis. Summarizing, our study revealed an intriguing impact of LRIG2 excess on skin tumor progression but not initiation, confirming a possible function of LRIG2 as an oncoprotein as previously reported for cervical SCC.

To conclude, our findings reveal that LRIG proteins are also involved in feedback loop mechanisms of the ERBB receptors in the skin. We showed a tremendous impact of LRIG1 on skin development and homeostasis and the influence of LRIG2 on skin tumorigenesis. Additionally, we identified ERBB4 receptor expression in the basal layer of the epidermis and found that ERBB4 affects epidermal proliferation. In summary, the present thesis provides important insights into the interplay of ERBB receptors and LRIG proteins in skin development, homeostasis and tumorigenesis

Zusammenfassung

Die Haut ist die äußerste Schicht des Körpers und steht in ständiger Interaktion mit der Umwelt. Sie ist ein sehr vielseitiges Organ und unterliegt sehr strengen Regulationsmechanismen. Epidermale Fehlregulationen können weit über 3000 Hauterkrankungen verursachen, darunter der nicht-melanozytäre Hautkrebs, zudem auch das Plattenepithelkarzinom der Haut zählt, auch „weißer Hautkrebs“ genannt. Weißer Hautkrebs tritt häufiger auf als alle anderen Tumorarten zusammen. Hohe kumulative Sonneneinstrahlung und eine Vorgeschichte von Sonnenbränden sind die Hauptursachen für 90% der weißen Hautkrebsinzidenzen. Ultraviolette Strahlung erhöht die Signaltransduktion der ERBB (*erythroblastic leukemia viral oncogene homolog*) Rezeptoren, wie es in verschiedenen Tumoren vorkommt. Die ERBB-Rezeptorfamilie umfasst vier Rezeptor-Tyrosinkinasen: EGFR/ERBB1/HER1, ERBB2/HER2/neu, ERBB3/HER3 und ERBB4/HER4. Das ERBB-System stellt ein sehr komplexes Signalnetzwerk dar, das zentrale zelluläre Prozesse wie Proliferation, Differenzierung, Apoptose und Motilität steuert. Diese spielen auch bei der Morphogenese, der Homöostase und der Tumorgenese der Haut eine wichtige Rolle. Die Deletion des autonomen EGFR (*epidermal growth factor receptor*) sowie dessen Aktivierung verursacht einen ausgeprägten Phänotyp in der murinen Epidermis. Darüber hinaus ist der EGFR auch in die Hautkarzinogenese involviert, was auch bei vielen anderen Tumoren beobachtet wurde. Im Gegensatz dazu hat die Deletion von ERBB2 und ERBB3 keinen großen

Einfluss auf die Homöostase der Haut, allerdings sind beide Rezeptoren an der Entstehung des Plattenepithelkarzinoms der Haut beteiligt. Der zweite autonome Rezeptor der ERBB-Familie, ERBB4, ist an entscheidenden embryonalen Prozessen wie der Entwicklung des Herzens und des zentralen Nervensystems beteiligt, allerdings auch an verschiedenen epithelialen Tumorarten. Über die Expression und die Rolle von ERBB4 in der Haut wird seit vielen Jahren diskutiert. Aus diesem Grund haben wir die Funktion von ERBB4 in der Haut *in vitro* und *in vivo* an humanen Hautproben und einem hautspezifischen ERBB4 Knockout-Mausmodell näher charakterisiert. Wir haben die Rezeptorexpression in der humanen Keratinozyten-Zelllinie HaCaT und in der epidermoid-Karzinom-Zelllinie A431 analysiert und konnten die Expression sowie eine Aktivierung von ERBB4 durch eine Stimulation mit EGF (*epidermal growth factor*) in beiden Zelllinien nachweisen. Außerdem konnten wir die Expression von ERBB4 in humaner Haut in der basalen Schicht der Epidermis lokalisieren. Die hautspezifischen ERBB4 Knockout-Mäuse zeigten eine geringere Epidermisdicke mit einer geringeren Proliferationsrate. Zusammenfassend konnten wir nicht nur die Expression von ERBB4 in der Haut nachweisen, sondern auch den Einfluss des Rezeptors auf die epidermale Homöostase durch seine Wirkung auf die Proliferation der Keratinozyten in der Haut.

ERBB-Rezeptoren werden durch positive und negative *Feedbackloop* Mechanismen reguliert, die die Aktivierung von Liganden, das Recycling, den Abbau und die Kompartimentierung von Rezeptoren, aber auch die Synthese neuer regulatorischer Moleküle veranlassen. Zu diesen *Feedbackloop* Proteinen zählen auch die LRIG (*leucine-rich repeats and immunoglobulin-like domains*) Proteine. Die LRIG Proteine gehören zu einer *Singlepass*-Transmembranproteinfamilie, die in Wirbeltieren drei homologe Proteine umfasst (LRIG1-3). Aufgrund ihres Potenzials als prognostische Faktoren bei verschiedenen Krebsarten erregten die LRIG Proteine große Aufmerksamkeit. LRIG1 ist das am meisten untersuchte Mitglied der Proteinfamilie. Es verhindert die Teilung von Stammzellen in der Haut, im Darm und im Magen und beeinflusst das ERBB-Signalnetzwerk indem es die Ubiquitinierung und damit den Abbau des EGFRs induziert. LRIG2 und LRIG3 sind bisher nur wenig analysiert und charakterisiert worden. In Bezug auf die Tumorgenese ist die Expression von LRIG2 jedoch meist mit einer schlechten Prognose verbunden, während LRIG3 und LRIG1 als Tumorsuppressoren gelten. Molekulare Mechanismen, insbesondere ihre Rolle in der Haut, sind noch nicht vollständig verstanden.

Um die Funktion der LRIG Proteine in der Morphogenese, Homöostase und Tumorgenese der Haut *in vivo* zu untersuchen haben wir unter Verwendung des Tet-Off-Systems induzierbare, hautspezifische, transgene (TG) Mauslinien, die LRIG1-3 überexprimieren,

generiert. Diese Arbeit befasst sich mit den Auswirkungen von LRIG1 und LRIG2 auf die Epidermis und den Haarfollikel sowie die Talgdrüse.

Die hautspezifische Überexpression von LRIG1 bei Mäusen zeigte einen apparenten Phänotyp während der epidermalen Entwicklung und Homöostase. Eine Überexpression von LRIG1 während der Embryogenese ist postnatal letal, was möglicherweise auf eine gestörte Hautbarriere zurückzuführen ist. Neugeborene LRIG1-TG Mäuse zeigten eine gestörte epidermale Differenzierung und Morphogenese der Haarfollikel. Das ERBB-System war bei diesen Tieren durch die Überexpression von LRIG1 stark verändert. Jedoch konnte eine Hemmung der LRIG1-Überexpression bis zur Geburt durch Doxycyclin das Überleben von TG Mäusen sichern. Die LRIG1 Überexpression führte bei adulten Mäusen zu einer gestörten Homöostase der Haut und zu einer schweren Alopezie, mit einer verminderten ERBB-Signaltransduktion und einem stark beeinträchtigten Haarfollikelzyklus. Im Gegensatz dazu war die NOTCH (*neurogenic locus notch homolog protein*) Signaltransduktion, welche an der Bestimmung des Schicksals der Zelle beteiligt ist, bei adulten LRIG1-TG Mäusen aktiviert und die Expression von Stammzellmarkern der *Bulge* und der Talgdrüse erhöht.

Im Gegensatz zu LRIG1-TG Mäusen zeigten LRIG2-TG Mäuse keinen Einfluss auf die Morphogenese oder Homöostase der Haut. Wir konnten aber zeigen, dass THBS1 (Thrombospondin-1) mit LRIG2 in TG Mäusen interagiert. THBS1 ist ein wichtiger Akteur in der Angiogenese und Tumorgenese und beeinflusst die extrazelluläre Matrix. Unsere *in vitro* Studien zeigten eine erhöhte LRIG2-Expression in epidermalen Tumorzelllinien (A431 und A375) im Vergleich zu humanen Keratinozyten (HaCaT). Die Auswertung von humanen Patientenproben mit kutanem Plattenepithelkarzinom zeigte ebenfalls eine LRIG2-Expression in diesen Tumoren. An einer mittels TPA (12-O-Tetra-decanoylphorbol-13-acetat) induzierten epidermalen Dysplasie konnten wir an LRIG2-TG Mäusen eine starke Entzündungsreaktion nachweisen, was auf eine mögliche Funktion von LRIG2 in der Tumorgenese hinweist. Um die Rolle von LRIG2 bei der Tumorgenese des Plattenepithelkarzinoms der Haut näher zu charakterisieren, haben wir eine zweistufige chemische Hautkarzinogenese bei LRIG2-TG Mäusen und Kontrolltieren induziert, bei welchem die tumorinitiierende Substanz 7,12 Dimethylbenz(a)anthracen und das tumorfördernde Mittel TPA verwendet wurden. LRIG2-TG Mäuse zeigten eine signifikant erhöhte Tumorprogression und eine frühe Entstehung von kutanen Plattenepithelkarzinomen mit einer gleichzeitigen Inaktivierung des Tumorsuppressors PTEN (*3,4,5-triphosphate 3-phosphatase and dual specificity protein phosphatase PTEN*). Zusätzlich fanden wir eine aktivierte EGFR/ERBB4-MAPK (*mitogen activated protein kinase*) Signaltransduktion in LRIG2-TG Mäusen während der Tumorgenese.

Zusammenfassend lässt sich sagen, dass unsere Studie einen Einfluss von LRIG2 auf die Progression von Hauttumoren, aber nicht auf ihre Initiation zeigte. Dies bestätigt eine mögliche Funktion von LRIG2 als Onkoprotein, wie sie bereits beim zervikalen Plattenepithelkarzinom berichtet wurde.

Abschließend konnten wir in unseren Untersuchungen zeigen, dass die LRIG Proteine auch in der Haut wichtige *Feedbackloop* Mechanismen für die ERBB Rezeptoren erfüllen. Das LRIG1-TG Mausmodell wies einen starken Einfluss der LRIG1 Überexpression auf die epidermale Entwicklung und Homöostase auf. Die LRIG2 Überexpression in TG Mäusen dagegen zeigte einen Einfluss auf die Hautkarzinogenese. Ebenfalls identifizierten wir die Expression des ERBB4 Rezeptors in der Basalschicht der Epidermis und konnten seine Beteiligung an der epidermalen Proliferation nachweisen. Die vorliegende Arbeit zeigt wichtige Erkenntnisse über das Zusammenspiel der ERBB Rezeptoren und LRIG Proteine während der Morphogenese, Homöostase und Tumorgenese der Haut.

Table of contents

Chapter 1 Background

1-1 The skin as an outstanding organ to study biological processes

1-1.1 The skin and the interfollicular epidermis

The skin is one of the most important organs of the human body, it makes up to 15% of our total body weight[1] and is, with 25 m^2, the third largest organ in humans after the gut and the lung[2]. Since it represents the outermost layer of the body, the skin acts as a protective barrier against water loss and environmental influences such as ultraviolet (UV) radiation or infections[3-5]. Besides these, vitamin D production, thermoregulation and sensory perception are also crucial functions of the skin[3,6]. The skin is constituted of three main layers: the epidermis, the dermis and the hypodermis (Figure 1-1)[7]. The latter is the deepest layer and consists mainly of loose connective tissue. The hypodermis provides anchorage of the skin to the underlying fascia as well as blood vessels and nerves. The middle layer represents the dermis with the epidermal appendages. The dermis contains sweat glands and hair follicles (HFs) with sebaceous glands (SGs), the arrector pili muscles (APM), which attach to each HF, many sensory neurons and blood vessels, supplying

nutrients to the skin. Last, the outermost layer of the skin is the interfollicular epidermis (IFE), normally comprising four layers in different stages of differentiation: *stratum basale*, *stratum spinosum*, *stratum granulosum* and *stratum corneum* (Figure 1-1)[3,7,8].

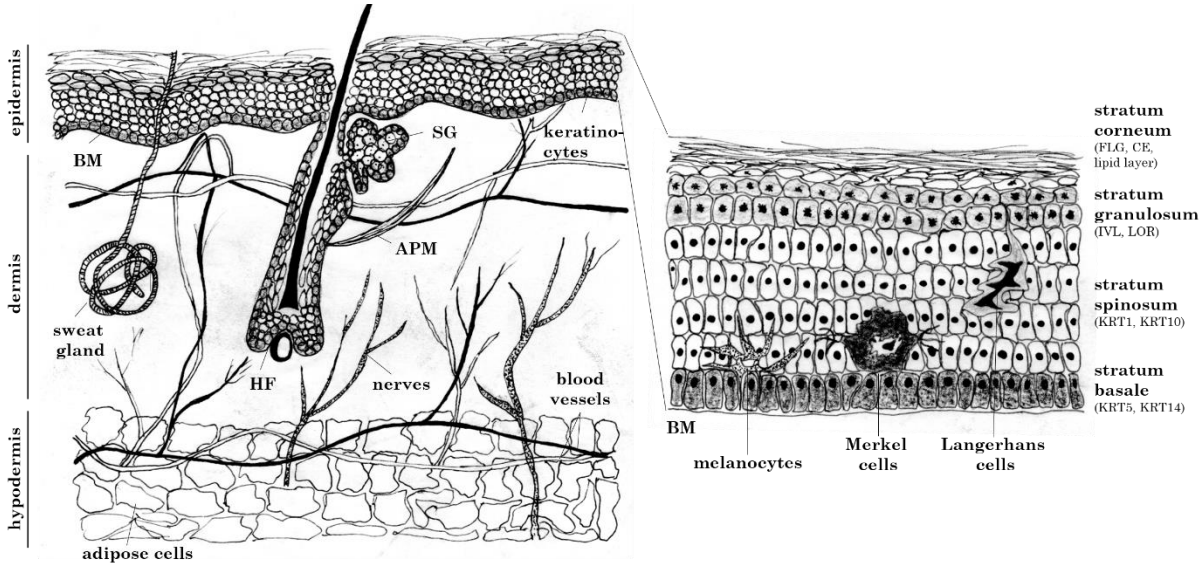

Figure 1-1 The skin, the epidermis and its appendages.
Schematic representation of the skin, depicting the hypodermis with adipose tissue, blood vessels and nerves, the dermis containing the pilosebaceous unit, sweat gland and blood vessels and nerves and the epidermis, enlarged on the right, showing the cell layers with specific differentiation markers (in brackets) and the different cell types residing in the epidermis. BM, basement membrane; HF, hair follicle; APM, arrector pili muscle; SG, sebaceous gland; FLG, filaggrin; CE, cornified envelope; IVL, involucrin; LOR, loricrin; KRT, keratin.

Approximately 20 different cell types reside within the skin[3]. Keratinocytes are the most abundant cells of the IFE, expressing specific proteins depending on their differentiation stage[9]. Yet, the IFE also hosts melanin producing melanocytes[10], which protect epidermal cells against UV light induced DNA damage[11], Langerhans cells, important for the epidermal immune response and skin barrier[12] and Merkel cells, responsible for the touch sensory function of the skin[9,13-15]. Keratinocytes in the basal epidermis are attached to the underlying basement membrane (BM). The BM is rich in extracellular matrix (ECM) and growth factors and influences migration, proliferation, apoptosis and thus, also tumorigenesis of basal cells due to different stimuli[4]. The basal cells express keratin (KRT) 5 or 14 until they differentiate into the suprabasal layer (*stratum spinosum*), expressing KRT1 and KRT10[5,16,17]. During differentiation, the keratinocytes undergo actin-dependent delamination due to a polarized cytoskeleton network[18]. Basal cells lose their adhesion to the BM and are pushed upwards[4]. Involucrin (IVL) or loricrin (LOR) are markers for the *stratum granulosum*[19,20] and keratohyalin granules and filaggrin (FLG) are present in terminally differentiated cells[21]. Dead, enucleated keratinocytes with keratin filaments and proteins crosslinked by transglutaminases build the cornified envelope (CE) which is surrounded by a lipid envelope[22]. The CE is crucial in

regard to the protective function of the skin as it represents the impermeable barrier for microbes and prevents the loss of essential fluids[4,5]. Terminally differentiated cells scale off the epidermal surface and are replaced by new differentiating cells[3,4]. For the constantly self-renewal of the skin and in response to environmental influences and injury epidermal stem cells (SCs) are necessary, differentiating into multiple epidermal linages[3,23-25]. Various models about epidermal proliferation and differentiation were developed in this context: the presence of epidermal proliferative units (EPU)[26], the asymmetric division or the symmetric division of SCs[4]. The hypotheses of the EPUs and the symmetric division suggest the existence of transit amplifying or progenitor cells (PCs), which divide for certain times before they differentiate[4,26,27]. Terminal differentiation is controlled by several signaling pathways, such as epidermal growth factor receptor (EGFR)[28] or neurogenic locus notch homolog protein (NOTCH)[29], and takes approximately four weeks in humans[4]. However, regarding the skin as a protective barrier, the pilosebaceous unit also has to be considered in addition to the IFE. Microbes in particular reside on the entire skin appendage surface and influence its homeostasis[2,30].

1-1.2 The hair follicle and its cycle

Besides the IFE, HFs are also involved in maintaining the skin's integrity. The HFs play an important role in interacting with microbes and influencing the absorbance of UV radiation, skin moisture, thermoregulation and sensory function[30]. A perpetual cycle of

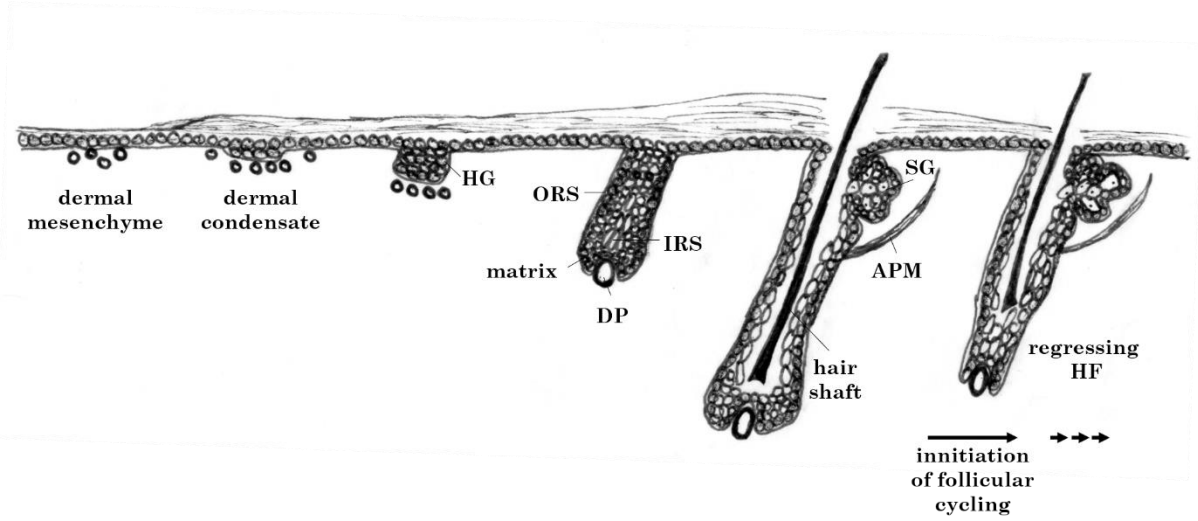

Figure 1-2 Hair follicle morphogenesis.
HF development is initiated by the formation of DP and HG and mediated by various epidermal and mesenchymal signals. The HF with ORS, IRS, SG and APM is formed by highly proliferative matrix cells. After the first HF has developed, it undergoes regression and enters the first follicular cycle. Increase and decrease of epidermal thickness is shown. HG, hair germ; ORS, outer root sheath; IRS, inner root sheath; DP, dermal papilla; SG, sebaceous gland; APM, arrector pili muscle; HF, hair follicle.

HF growth and degeneration is responsible for hair growth and regeneration throughout life[3,4,31]. The hair morphogenesis starts during development, assessing all HFs, thus no HFs are formed postnatally. The epithelial-mesenchymal interaction between the dermal condensate, the precursor of the dermal papilla (DP), and the epidermis induces the formation of the first hair germ (HG). Epidermal cells start to proliferate and grow downward and build the HF with the outer root sheath (ORS). The ORS continues the IFE and remains in contact with the BM, expressing KRT5 and KRT14 likewise[3]. At the base of the developing HF, the matrix resides, comprising highly proliferative, proliferation marker protein Ki-67 (MKI67) positive keratinocytes. Matrix cells change their gene expression profile due to the contact with the DP and build the inner root sheath (IRS), expressing trans-acting T-cell-specific transcription factor GATA-3 (GATA3)[32]. The companion layer, positive for KRT6, and the hair shaft are formed. When matrix cells stop to proliferate, they undergo apoptosis and two thirds of the HF are degraded[33,34]. The retracting BM pulls the DP upward to the bulge, which is located at the lowest permanent part of the HF, expressing hematopoietic progenitor cell antigen CD34 (CD34)[35]. Slowly cycling SCs[36], which are necessary for the regeneration of HFs, reside in the bulge and can also give rise to the IFE and SG[37-39]. Further, the secondary HG arises and interacts with the DP to activate the bulge SCs. Thus, the development and growth of the new HF and its hair is initiated and the hair cycle is induced[31,40-42]. The new hair can emerge through the same orifice at the skin surface. The infundibulum (INF) represents an additional SC compartment in the HF, expressing leucine-rich repeats and immunoglobulin-like domains 1 (LRIG1). However, under homeostatic conditions, these SCs are only involved in the maintenance of the IFE and SG[43,44]. SGs are established at birth in the upper part of the HFs. Differentiated and degenerated sebocytes in the SGs release lipids and sebum and thereby ensure the maintenance of skin moisture[4]. These cells also have to be reproduced by SCs, residing at the base of SGs, to sustain epidermal integrity[27]. PCs in the SGs express PR domain zinc finger protein 1 (BLIMP1)[45] and

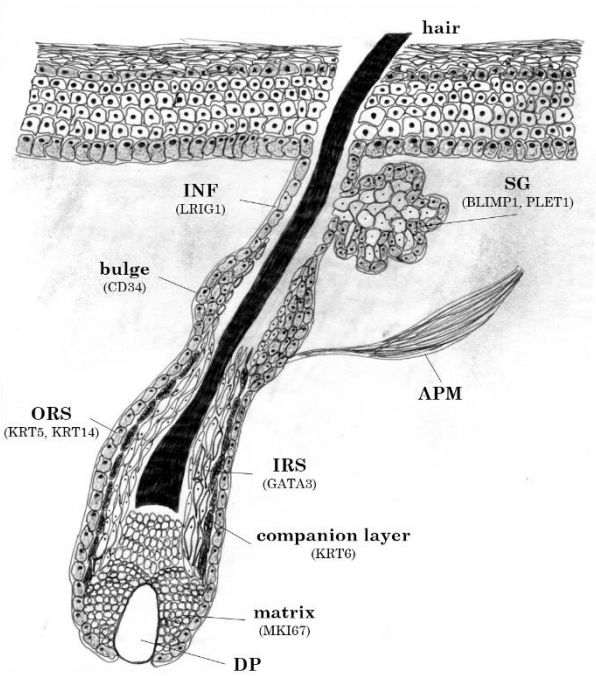

Figure 1-3 Structure of the hair follicle.
Structure of a HF with its different compartments and specific markers in brackets. INF, infundibulum; ORS, outer root sheath; IRS, inner root sheath; DP, dermal papilla; APM, arrector pili muscle; SG, sebaceous gland.

placenta-expressed transcript 1 protein (PLET1)[46]. In conclusion, every skin compartment, the IFE[27,47], the HF with the bulge[36] and the INF[43,44], and the SG[45,48], has its own reservoir of bi- or multipotent SCs which are able to give rise to the epithelial cell linages[49-51]. These reservoirs are referred to as niches and provide an appropriate microenvironment to maintain the balance between proliferation and differentiation[52,53]. The distinct SC niches have different capacities and are involved in individual processes during homeostasis and tissue regeneration[27,37-39,43-45]. However, the molecular mechanisms are far from being fully understood. The morphogenesis of HFs and the compartments of HFs with the specific markers are shown in Figure 1-2 and Figure 1-3.

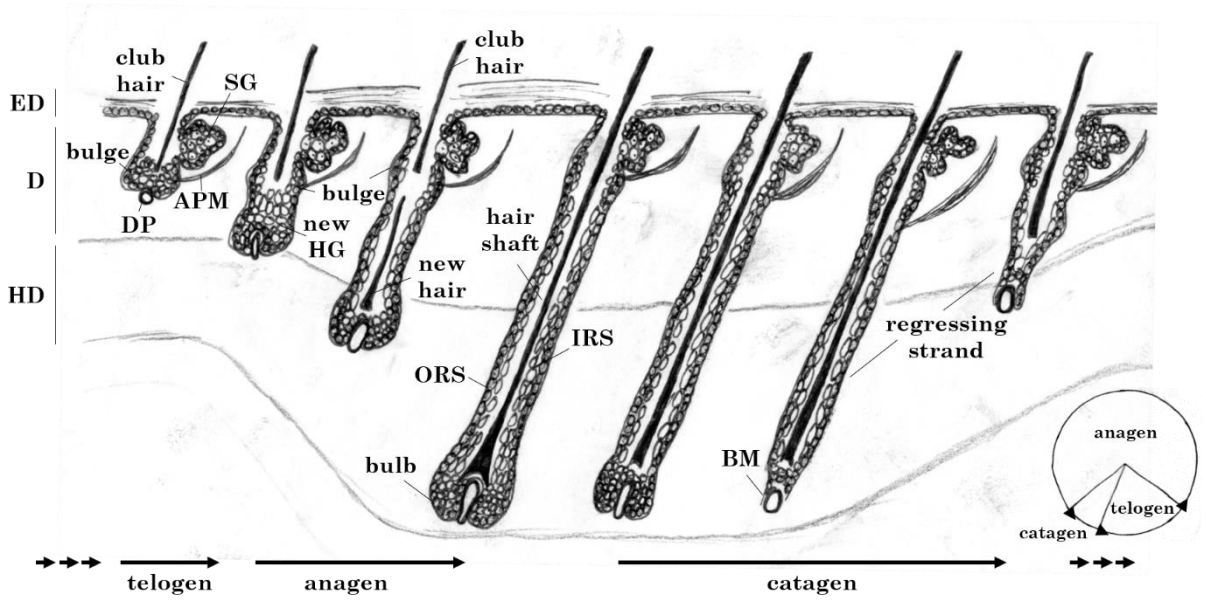

Figure 1-4 The hair follicle cycle.
Different morphological substages of HFs during resting (telogen), growth (anagen) and apoptosis-driven regression (catagen) phase are shown. The pie chart illustrates the proportion of time the HF spends in each stage. Increasing and decreasing length and localization of HF during the HF cycle is depicted. The hair cycle repeats itself throughout a lifetime. ED, epidermis; D, dermis; HD, hypodermis; DP, dermal papilla; APM, arrector pili muscle; SG, sebaceous gland; HG, hair germ; ORS, outer root sheath; IRS, inner root sheath; BM, basement membrane. (adopted from Muller-Rover *et. al*[31])

The HF cycle is divided into three distinct stages: catagen, telogen and anagen[31,54]. The catagen stage is referred to as the regression phase, in which the hair shaft shrinks due to apoptosis and the HF can renew itself[33,34]. Regression is followed by the telogen stage, also called the resting phase. However, telogen stage represents more the "master-switch"[55] stage of HF cycling, where bulge SCs are regulated to prepare HF regeneration and the subsequent growth phase[36,39] as well as tissue renewal upon injury[55,56]. Additionally, in telogen stage the club hair is anchored and maintained[57]. During anagen, HFs grow downward and build a new hair[58]. Figure 1-4 depicts several criteria, which

allow the assignment of HFs to the different stages, including the length of HFs, their location in the skin as well as the thickness of the IFE[31].

In summary, the variety and complexity of the skin require precise regulation and coordination of epidermal pathways, otherwise more than 3000 skin disorders may occur[59]. These properties make the skin to an outstanding organ to study biological processes and molecular mechanisms, including SC biology.

1-2 Non-melanoma skin cancer

The frequency of non-melanoma skin cancer (NMSC) incidences is higher than of all other cancers combined[60,61]. In the Caucasian population, NMSC is even the most common type of cancer with up to three million new cases per year worldwide[62,63]. NMSC arises from keratinocytes, and depending on the keratinocyte cell type, the tumor group is subdivided into basal cell carcinomas (BCC) (70% of NMSC)[64], squamous cell carcinomas (SCC) (25% of NMSC)[65,66] and some other rare skin tumors like actinic keratoses (AKs) or Bowen's disease (SCC *in situ*)[67,68]. The molecular biological causes for the development of skin cancer are DNA damages, gene mutations or disturbed repair mechanisms[69,70]. Fair skin, genetic susceptibility, age and sex influence NMSC incidence intrinsically[71], whereas tobacco smoking[72], human immunodeficiency virus (HIV) infection[73] or immunosuppression[74] are extrinsic risk factors. In immunosuppressed patients for instance, NMSC incidence is increased tremendously and cutaneous SCC (cSCC) seems to be more aggressive and tends to metastasize[69,74]. However, UV irradiation is the major risk factor of NMSC[75,76], which predominantly causes mutations in the tumor suppressor gene cellular tumor antigen p53 (*TP53*)[77,78]. cSCC incidences increase with the time patients spent in the sun, whereas the relation in BCC is more complex[79], pointing to the very distinct molecular mechanisms of both cancers. While disturbed hedgehog signaling leads to the *de novo* development of BCC[80], cSCC is thought to arise from precursor lesions in a multi-stage model owing to genomic instability[69,81]. The mutational pattern in cSCC is very complex and the link to the dysregulation of one particular pathway is not yet found[82]. However, it was shown that the expression of the EGFR, a member of the erythroblastic leukemia viral oncogene homolog (ERBB) receptor family, and its ligands were altered in both cancer types[83-86]. UV radiation causes the upregulation of EGFR[87] and ERBB2[88], another receptor of the ERBB family, while the inhibition of EGFR results in the prevention of UV-induced skin carcinogenesis[89]. Although the chances of recovery are

95%[90], cSCC is more likely to metastasize than BCC, also leading to death (metastatic rate: 0.1–9.9%; 75% of deaths due to NMSC[68])[69,81]. Besides radiotherapy and conventional chemotherapy, there are currently only few non-surgical treatment opportunities available[71]. One promising treatment alternative for NMSC is an EGFR targeted therapy[91], which is also found in many other epithelial tumors, such as non-small cell lung cancer (NSCLC) or colorectal cancer[92]. However, patients treated with monoclonal antibodies against EGFR or with small-molecule tyrosine kinase inhibitors show severe side effects such as inflammatory skin rashes, acneiform eruption, skin dryness leading to eczema and fissures, pruritus, hair abnormalities, hyperpigmentation and mucosal changes[93,94]. Although, these adverse reactions are not life-threatening, they have an enormous psychological as well as physiological impact on the patient's quality of life, which can also limit the therapy[85]. Thus, the research into new and more specific targets is required to improve the treatment of NMSC in the skin.

1-3 The ERBB signaling network

1-3.1 The ERBB receptor family

The ERBB receptor family comprises four receptor tyrosine kinases (RTKs): EGFR/ERBB1/HER1[95], ERBB2/HER2/neu[96], ERBB3/HER3[97] and ERBB4/HER4[98]. They are composed of an extracellular ligand-binding domain, a single hydrophobic transmembrane domain and a cytoplasmic tail with a kinase domain and tyrosine auto-phosphorylation sites[95,99,100] (see Figure 1-5).

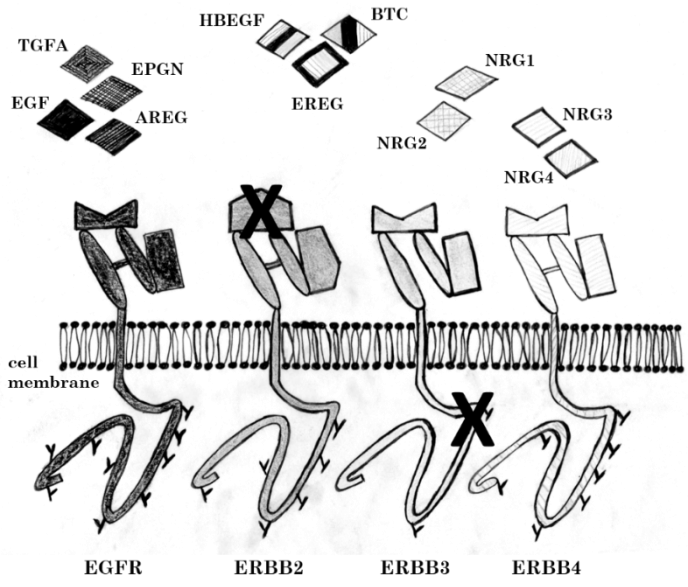

Figure 1-5 ERBB receptors and their ligands.
Receptor tyrosine kinases EGFR, ERBB2, ERBB3 and ERBB4 and their ligands. EGFR specifically binds EGF, TGFA, EPGN and AREG. EREG, HBEGF and BTC bind EGFR and ERBB4. NRG1 and NRG2 are bound by ERBB3 and ERBB4. NRG3 and NRG4 are specific ERBB4 ligands. ERBB2 has no ligand binding domain and ERBB3 lacks kinase activity (indicated by **X**). **Y** depicts different phosphorylation sites of the receptors.

The ERBB signaling pathway is involved in many pivotal processes during life such as proliferation, differentiation or apoptosis[101]. Upon ligand binding, receptors form homo- or heterodimers and due to auto-phosphorylation of the cytosolic domain a variety of signaling cascades can be induced[99,101].

Eleven ligands of the ERBB receptor family are known: amphiregulin (AREG), betacellulin (BTC), epidermal growth factor (EGF), epigen (EPGN), epiregulin (EREG), heparin-binding EGF-like growth factor (HBEGF), neuregulins (NRG1-4) and transforming growth factor alpha (TGFA)[102-104]. These ligands are located in the cell membrane as precursors and are composed of an EGF motif containing cysteine repeats with an N-terminal extension and a C-terminal membrane-anchoring region[105,106]. The activation and release of the growth factor is triggered by a myriad of signals from different stimuli including the shedding by metalloproteases like a disintegrin and metalloproteinase domain-containing proteins (ADAMs)[107]. Paracrine, autocrine but also juxtacrine receptor activation is possible[108]. The ligands show binding specificity to certain receptors of the ERBB family and regulate receptor activation by their binding strength[85]. While EGF, TGFA, EPGN and AREG specifically bind EGFR, BTC, HBEGF and EREG bind EGFR and ERBB4. NRG1 and NRG2 bind ERBB3 and ERBB4, and NRG3 and NRG4 are specific ERBB4 ligands[99,109]. Ligand binding of ERBB receptors causes conformational changes inducing receptor homo- or heterodimerization and thereafter the activation of a variety of downstream signaling cascades[110,111]. While EGFR and ERBB4 are two autonomous receptors that can form homodimers and heterodimers with each of the three other receptors, ERBB2 is an orphan receptor[101,112]. The structure of ERBB2 is similar to the ligand-bound form of EGFR, which might be the reason for the inability to bind ligands and form homodimers[113]. However, ERBB2 is the favored partner for heterodimerization, especially for the second non-autonomous receptor ERBB3[114,115], which lacks kinase activity[116,117]. Heterodimers in general, and especially those with the ERBB2 receptor[115], are more mitogenic than homodimers and are related to many pathological processes. This is due to a higher affinity and specificity of the receptor heterodimers to the ligands and their resulting decelerated dissociation[99,101]. Receptor dimerization leads to the phosphorylation of characteristic tyrosines and the recruitment of several phosphorylation-specific substrate proteins with a proto-oncogene tyrosine-protein kinase Src (SRC) homology (SH) 2 domain and a phosphotyrosine binding domain. Due to the large number of possible adaptor proteins, several downstream signaling pathways can be initiated[85,99,101,109,118]. The most prominent downstream pathway upon EGFR activation is the recruitment of growth-factor-receptor bound-2 (GRB2) and son of sevenless

homolog 1 (SOS), which bind directly, or through association with the adaptor molecule Shc transforming protein (SHC), to specific docking sites on the receptor. GTPase Ras (RAS) is then recruited and activates the mitogen-activated protein kinase (MAPK) cascades, which are responsible for cell cycle entry, survival and proliferation in keratinocytes[85,92,119]. Indirectly, EGFR can also activate the phosphatidylinositol 3-kinase (PI3K) – RAC-alpha serine/threonine-protein kinase (AKT)/ protein kinase B (PKB) cascade involved in cell survival by RAS or by dimerization with the ERBB3 receptor[92,99]. Unoccupied ERBB receptors are internalized and recycled back to the cell surface[120]. On the contrary, activated receptors alter their trafficking behavior. Upon ligand binding, EGFR is more rapidly internalized through clatherin-coated pits than the other receptor family members[121,122]. Thus, EGFR signaling occurs mainly in endosomal compartments while the other ERBBs act primarily at their membrane bound localization[123]. Additionally, ERBB heterodimers recycle back to the cell surface more frequently than homodimers, which causes enhanced receptor signaling and point to their increased mitogenic character[124]. Endosomal signaling cascades are distinct from the pathways induced at the membrane, but include also cell proliferation or survival[99,123]. Receptor endocytosis and down-regulation seems to be an EGFR specific feature and is impaired in all other receptor family members[122,125]. Recruitment of the E3 ubiquitin-protein ligase CBL (CBL) and the neural precursor cell expressed developmentally downregulated protein 8 (NEDD8) induces ubiquitination and lysosomal degradation of EGFR[126,127]. Besides endosomal signaling and lysosomal receptor down-regulation, the ERBB system is also involved in transcriptional control mechanisms by nuclear receptor translocation[128-132]. EGFR together with the transcriptional cofactor signal transducer and activator of transcription 3 (STAT3) can induce transcription in the nucleus of highly proliferative cells[133]. EGFR has no DNA binding domain, whereas ERBB2 can directly interact with the cyclooxygenase enzyme prostaglandin G/H synthase 2 (PTGS2) promoter in the nucleus and stimulate its transcription, often observed in human cancer types like colon and breast cancer[134]. Transcriptional mechanisms were also shown for nuclear ERBB3[135] and ERBB4[136,137], mainly in proliferating cells pointing to a role during tumorigenesis. ERBB4 represents an exception among its family members as it can be shed from the cell membrane extracellularly by ADAM17[107] and intracellularly by gamma-secretase[138] and can further induce juxtacrine as well as nuclear signaling. The resulting intracellular domain (ICD) translocates to the nucleus[138] to activate the transcription of different target genes together with STAT5[139] or transcriptional coactivator YAP1 (YAP1)[140,141]. Whereas phosphorylated YAP1 can constrain ERBB4 in the cytoplasm and thus prevents its function in transcriptional regulation[141]. Additionally, ERBB4 is the only receptor that has

six different splice isoforms which induce various intracellular signaling pathways[142,143]. Four tissue-specifically expressed isoforms differ in their extracellular juxtamembrane domain (JM-a-d): 23 amino acids in the extracellular domain (ECD) of JM-a are replaced by 13 amino acids in the JM-b variant, JM-c shows deletion of the entire JM region, whereas JM-d comprises both, the JM-a and the JM-b sequence[132,142]. The JM-a specific sequence is essential for receptor cleavage[132]. If this region is lacking, ADAM17 is not able to shed the ERBB4 ECD, thereby impeding gamma-secretase to cleave ERBB4 intracellularly. Consequently, nuclear translocation of the ICD of ERBB4 is prevented and its transcriptional activity inhibited[144,145]. The other two isoforms of ERBB4, CYT-1 and CYT-2, differ in their cytoplasmic tail in the PI3K binding domain and have no impact on nuclear translocation. However, due to sixteen missing amino acids in the binding domain for PI3K in the CYT-2 isoform only CYT-1 can activate the PI3K pathway[146].

ERBB signaling is tissue-dependent, thus the next chapter will give a short overview about the ERBB network in the skin.

1-3.2 ERBB receptors in the skin and skin pathogenesis

In the 80s of the last century ERBB receptors were discovered and became a focus of biological research. More and more indications arose that ERBBs play a pivotal role in skin development and homeostasis and that their dysregulation results in pathogenesis, including psoriasis[147-152], disturbed wound healing[153-155], melanoma[154,156-158] and NMSC[83,84,154,159,160] (see Chapter 1-2)[85]. In humans EGFR[86,161,162] and ERBB3[155,161,163] are most abundant in the basal layer of the epidermis, while ERBB2 is mainly located in the suprabasal layer[161,164]. Although ERBB4 expression has been reported in human embryonic and adult skin[165], detection is very difficult and contradictory in the field and was therefore examined in more detail as part of this thesis (see Chapter 2). EGFR seems to be involved in the terminal differentiation by maintaining the proliferative capacity of epidermal PCs[28]. Further, the transition from anagen to catagen in the HF cycle is also influenced by EGFR[166,167]. The loss of EGFR[168,169] in mice led to alopecia, while the skin-specific deletion of ERBB2[170] and ERBB3[154] resulted in no obvious phenotype. However, ERBB2 excess during homeostasis causes severe alopecia and the concomitant delayed keratinocyte differentiation and spontaneous formation of papillomata indicate a function of ERBB2 in tumor initiation[171-174]. Besides, ERBB2 and ERBB3 are involved in tumor promotion[154,170], and EGFR is an important player during tumor development and

progression in the skin. Disturbed EGFR signaling revealed a decreased tumor burden and papillomata expressing no EGFR were smaller and showed decreased proliferation, resulting in cell cycle arrest[175-178]. In regard to carcinogenesis, the expression of ERBB receptors as well as their ligands can be a prognostic factor. Thus, the investigation of the underlying mechanisms is crucial to understand their impact on tumor development and progression and to develop better tumor therapies[99,179].

The ERBB system represents one of the most complex signaling networks in biology with high redundancy, which shows precise regulation of ligands, receptors, adaptor molecules and compartmentalization, including receptor endocytosis, degradation or recycling. Therefore, positive and negative feedback mechanisms are pivotal to maintain homeostasis, and are often disturbed in cancer[99,180].

1-3.3 **Feedback loop regulation of ERBB receptors**

To maintain cellular function, the duration, amplitude and frequency of signals within the ERBB network are regulated by positive or negative feedback loop mechanisms. The positive ERBB regulation includes the extension and amplification of the signal by trans[181]- or secondary[182] phosphorylation of the receptor, by receptor recycling[183] as well as by ligand activation[184]. Autocrine or paracrine activation of ERBBs initiate the RAS-MAPK pathway, which may lead to the transcription of new ligands[101]. Further, the cross-talk with other signaling pathways, which activate metalloproteases, can induce the proteolytic release of ligands and thus transactivate ERBBs[185]. In turn, an excess of ligands leads to ERBB degradation, as observed in BCC[86]. However, the ligand-induced degradation is delayed due to the limited capacity of clathrin-mediated endocytosis[99]. Contrary, ERBB receptors are negatively regulated through receptor dephosphorylation by protein tyrosine-specific phosphatases such as density-enhanced phosphatase-1 (DEP1)[186] or protein tyrosine phosphatase-1B (PTP1B)[187], which influence receptor endocytosis at different sites along the endocytotic pathway resulting either in recycling or degradation of the receptor[99,184]. In addition, further receptor degradation pathways, catalytic inactivation, conformational changes, which induce steric inhibition, as well as receptor translocation or compartmentalization are further possible mechanisms for negative feedback loop regulation of ERBBs[99,184]. Moreover, signaling regulators like sprouty (SPRY)[188-191] or LRIG1[192] are newly synthesized due to ERBB activation and thereby induce a late regulatory response. While SPRY has a dual function by preventing

receptor degradation and increasing MAPK activation[191], LRIG1 is involved in the negative feedback loop of EGFR by inducing receptor ubiquitination and degradation through CBL recruitment (see Chapter 1-4.1)[188,193]. These feedback mechanisms are responsible for the steady state of the ERBB network and dysregulation is observed in many tumors[194]. Especially negative feedback mechanisms are often attenuated during carcinogenesis, leading to uncontrolled receptor activation[195-198]. LRIG proteins arose attention regarding their potential to regulate signaling of RTKs like the ERBBs, but also due to their role as prognostic tumor markers in various cancers (see Chapter 1-4).

1-4 The LRIG protein family

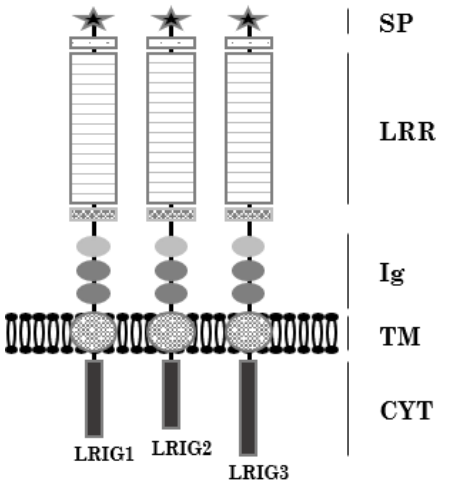

Figure 1-6 Schematic structure of LRIG proteins.
SP, signal peptide; LRR, leucine-rich repeats with cysteine-rich N- and C-flanking domains; Ig, immunoglobulin-like domains; TM, transmembrane domain; CYT, cytoplasmic tail. (adopted from Simion *et. al*[204])

The LRIG proteins are single-pass transmembrane proteins, first discovered in 1996 in the central nervous system (CNS) of *Drosophila melanogaster*, named kekkon (Kek) 1 and 2[199]. At the same time, Suzuki *et al.* described the murine orthologues LRIG1 in P19 embryonal carcinoma cells, involved in neural differentiation[200]. In vertebrates the LRIG single-pass transmembrane protein family consists of three members, LRIG1[200,201], LRIG2[202,203] and LRIG3[203]. They all share the following structure: a signal peptide, 15 tandem leucine-rich repeats (LRR) with cysteine-rich N- and C-flanking domains, three immunoglobulin-like domains (Ig), a transmembrane domain, and a cytoplasmic tail (Figure 1-6)[203,204]. Like in *Drosophila*, the ECDs of the LRIGs are highly conserved, whereas the intracellular regions are more distinct[203]. LRRs and Ig domains are often involved in protein recognition processes[205,206]. The murine protein family shows 80-87% similarity to human homologs and all three members are widely expressed in all tissues analyzed so far[203]. While the *LRIG1* transcript is highly expressed in brain, liver, lung, small intestine and stomach[203,207], the mRNA of *LRIG2* is most strongly expressed in ovary, uterus and skin[203]. *LRIG3* transcripts are most abundant in stomach, thyroid and skin[203,207]. All LRIG proteins are involved in very diverse cellular processes, such as tumorigenesis[207-209], psoriasis[210], and complex tissue morphogenesis[200,211,212], but only little

is known about the underlying molecular mechanisms. Especially, the function of LRIGs as prognostic factors is currently widely discussed in the research field[207], which emphasizes the importance of understanding their impact on cellular processes.

1-4.1 **LRIG1**

The first described and best studied member of the LRIG transmembrane protein family is *LRIG1*[200], located at chromosome 3p14.3[201] in humans, a region often deleted in many cancers[213]. LRIG1 is known to be a negative regulator of RTKs, such as ERBBs[192,193,214], hepatocyte growth factor receptor (MET)[215], proto-oncogene tyrosine-protein kinase receptor Ret (RET)[216] or platelet-derived growth factor receptor alpha (PDGFRA)[212]. Different mechanisms of receptor regulation were postulated. In case of RET, it was shown that LRIG1 prevents ligand binding and thus receptor activation[216]. Contrary, regarding ERBB receptor signaling, LRIG1 interacts with the extracellular region of EGFR and promotes its lysosomal degradation by the recruitment of the E3 ubiquitin ligase to induce ubiquitination[192,193]. The same mechanism was shown for MET[215]. Additionally, since LRIG1 can be shed from the cell surface, it can also act in a non-cell-autonomous manner and suppress proliferation of neighboring cells[217,218]. However, the ECD of LRIG1 influences paracrine EGFR signaling but does not induce receptor degradation[218], referring to different regulatory mechanisms. Another important feature of LRIG1 is its function in adult SCs. In the epidermis, more specifically in the isthmus adjacent to the INF and SG[43], as well as in the small intestine[219] and stomach[220], LRIG1 was shown to promote SC quiescence. Suzuki *et al.* also reported the expression of *LRIG1* mRNA and LRIG1 protein in the basal layers of HFs and to a lesser extend in the IFE, clustered in patches[221]. Loss of LRIG1 in the skin leads to a growth advantage in the basal layer together with EGFR upregulation and induction of committed PCs[222]. LRIG1 knockout (KO) mice developed psoriasis and revealed increased proliferation in the skin[221]. In the intestine, the deletion of LRIG1 causes the development of neoplasia and highly penetrant duodenal adenomas[219]. These current findings suggest the involvement of LRIG1 in several crucial feedback loop mechanisms of growth factor receptors, like proliferation, differentiation or apoptosis but also tumorigenesis[223,224]. Nevertheless, further studies are needed to elucidate the molecular function of LRIG1 in more detail.

1-4.2 **LRIG2**

LRIG2 is the most poorly studied member of the LRIG family, located at chromosome 1p13, which is implicated in various cancers[202,213] such as SCC, breast cancer[207,213] and oligodendroglioma[225]. LRIG2 shows high structural similarity to LRIG1 and Kek1[226]. The ECD of LRIG2 is responsible for its function and promotes cell proliferation and the inhibition of apoptosis[227]. LRIG2 seems to play an important role during development, as LRIG2 deficient mice show a transiently reduced growth rate and an increased spontaneous mortality rate[212]. Xiao *et al.* showed that LRIG2 interacts with EGFR and enhances EGFR/PI3K/AKT signaling[227], but EGFR or ERBB2 expression seems not to be influenced by LRIG2[224]. Mutations of LRIG2 are related to urofacial syndrome (UFS)[228] and many other pathologies[225,227,229-231]. In summary, LRIG2 appears to have a mitogenic function, but the molecular mechanisms still have to be analyzed tissue-specifically.

1-4.3 **LRIG3**

The last described member of the LRIG family is LRIG3[203]. Genes in close proximity to the *LRIG3* gene, at the chromosomal region 12q13[203], are highly expressed in several tumors[232-234], indicating a function of LRIG3 in cancer. LRIG3 is involved in crucial developmental processes like neural crest formation in Xenopus embryos[211], mammalian morphogenesis of the inner ear[235] or the regulation of heart function[236] and blood cholesterol levels[237]. Irrespectively of the large differences in the ICD[203], LRIG3 shows a higher homology to LRIG1 than to LRIG2[238], and the expression of both overlaps during development[235]. However, LRIG1 and LRIG3 are functionally distinct and oppose one another in HEK293T cells, and the ratio of both LRIGs is important for ERBB receptor regulation[224]. While LRIG1 is able to decrease LRIG2, LRIG3 and ERBB receptor expression, LRIG3 has no direct effect on LRIG1 expression but interacts with and stabilizes the ERBBs, thereby increasing their expression and influencing receptor binding ability[224,238]. Additionally, the ICD of LRIG3 contains SH2 and SH3 domains which enable the transmembrane protein to bind to activated ERBB receptors[238], whereas the ECD seems to have a unique function and decreases ERBB3 receptor expression[224]. In contrast, the down-regulation of LRIG3 in glioblastoma cells or cervical SCC resulted in increased EGFR expression and activation[239,240]. The current findings indicate a tissue-

specific impact of LRIG3 on ERBB signaling and also a function as tumor suppressor as observed in prostate cancer[241].

1-4.4 LRIGs – prognostic factors in carcinogenesis

The chromosomal regions, where the three *LRIG* genes are located at are often implicated in cancer[201-203]. In addition, recent studies showed a correlation between *LRIG* transcripts or LRIG protein expression and cancer prognosis[207]. Despite their opposing function, both, LRIG1 and LRIG3, appear to rather act as tumor suppressors during carcinogenesis, while LRIG2 expression is mainly related to poor prognosis in various types of cancer[207,209]. Patients with SCC of the uterine cervix revealed high LRIG2 expression in the tumors and decreased survival prognosis[242,243], whereas high LRIG1 expression in those patients was related to prolonged survival[229]. Loss of LRIG3 in cervical SCC led to increased proliferation[239], but its expression had no prognostic value[244]. Contrary, there is no impact of LRIG2 on uterine cervical adenocarcinoma[242], however, patients with high LRIG3 expression revealed good prognosis[245]. In addition, in NSCLC, LRIG1 expression correlated with patient survival[246] and LRIG3 was downregulated at initial stages[247]. In contrast, high cytoplasmic LRIG2 expression in patients with NSCLC revealed poor survival[230], similar to esophageal carcinoma patients[231]. In cSCC, LRIG1 upregulation is related to better prognosis and more differentiated tumors, while patients with low LRIG1 expression show metastasis and decreased survival[248]. These findings indicate that the role of *LRIG* transcripts and LRIG proteins must be carefully examined tissue-specifically to evaluate their prognostic impact. The prognostic value of LRIGs is often also associated with ERBB signaling. In ERBB2 positive breast cancer *LRIG1* is downregulated[249] and the suppression of LRIG1 leads to further ERBB2 upregulation[214]. Inversely, the overexpression of LRIG1 in bladder cancer directly influences EGFR activity and stops tumor growth[250]. In head and neck cancer, it was shown that LRIG1 suppresses the expression of ERBB ligands and matrix- metalloproteinases (MMPs) causing decreased ERBB/MAPK signaling and ECM remodeling[251]. Since LRIG1 expression in the brain is very high[203], loss of *Lrig1* in glioma in mice results in very aggressive tumors but ectopic LRIG1 can decrease tumor invasion[252]. Glioblastoma often express a constitutively active but poorly ubiquitinated mutant form of the EGFR (EGFRvIII) causing disturbed receptor trafficking to lysosomes and nonattenuated oncogenic signaling[253]. Ectopic LRIG1 expression induces the decrease of tumor cell proliferation, survival, motility and invasion CBL-independently[254]. LRIG3 overexpression also decreased EGFR activation and

attenuated downstream RAS/MAPK and PI3K/AKT signaling in glioblastoma[255]. This was consistent with the knockdown of LRIG3 in glioblastoma cells, which resulted in the upregulation of EGFR and thus in increased proliferation[240]. Holmlund *et al.* was the first who associated LRIG expression with a negative effect on survival. He postulated the opposing function of LRIG2 and LRIG1 in oligodendroglioma, showing the relation between cytoplasmic LRIG2 expression and poor prognosis[225]. Furthermore, LRIG2 expression correlated with glioma grade and it was shown that glioblastoma cells release the soluble ECD of LRIG2, which is functional in tumor progression[227]. Additionally, the loss of LRIG2 led to the protection against platelet-derived growth factor subunit B (PDGFB)-induced glioma in mice[212]. The impact of LRIG2 on the ERBB network during carcinogenesis is so far not well analyzed and therefore investigated in this thesis (see Chapter 4). In conclusion, LRIG proteins seem to represent tissue-specific, prognostic factors in various tumors where both expression and localization seem to play a role. Thus, in regard to tumor therapy, LRIGs might be promising targets and initial steps have been taken to develop new strategies for cancer treatment[207]. The identification of interaction partners and especially the influence of LRIGs on the ERBB system would be very important in respect to prospective therapy approaches.

Chapter 2 The receptor tyrosine kinase ERBB4 is expressed in skin keratinocytes and influences epidermal proliferation

2-1 Aim

ERBB receptors are crucial players during skin development, homeostasis but also tumorigenesis and are often dysregulated in various cancers[85,99,101,180]. Consequently, the understanding of how ERBB receptors cooperate is crucial for future therapeutic strategies. EGFR KO mice show a severe epidermal phenotype, developing alopecia, hyperplasia of the IFE and SG and inflammation[168]. Additionally, EGFR is involved in NMSC[84] as well as in melanoma[158] and influences tumor development and progression in the skin[175-178]. Skin-specific ERBB2 and ERBB3 KO mice also revealed a tumor progressive function in the 7,12-dimethylbenz(a)anthracene (DMBA)/12-O-tetra-decanoylphorbol-13-acetate (TPA) carcinogenesis model[154,170], while they show no obvious phenotype under homeostatic conditions. However, the ERBB receptor family consists of four members, but in contrast to EGFR, ERBB2 and ERBB3, ERBB4 expression was not unambiguously detected in the skin. Nevertheless, ERBB4 is involved in many crucial processes like the development of the heart, the CNS[256] and the mammary gland (MG)[256,257] and also in

epithelial tumorigenesis, such as NSCLC[258], breast cancer[259-261] or colorectal cancers[262]. Especially the overexpression of ERBB4 in oral[263] and head and neck[159] SCC as well as in melanoma[156,157] has drawn our attention to a role of the receptor in skin and skin tumorigenesis. Although the analysis of ERBB4 in the skin is difficult and reports are inconsistent in the literature, Srinivasan *et al.* showed ERBB4 expression in human embryonic and adult skin[165]. Further, Panchal *et al.* revealed the increase of ERBB4 in murine skin due to the transgenic (TG) overexpression of its specific ligand, NGR3, leading to epidermal hyperplasia[264]. Taking these findings into account, a role of ERBB4 in the skin or during skin pathogenesis is very likely. Therefore, we hypothesized that ERBB4 is involved in skin homeostasis or tumorigenesis. The weak expression of ERBB4 in healthy skin, together with the existence of several isoforms of the receptor[142,143], make its detection in the epidermis very challenging, which might also be the reason for the common overlooking of epidermal ERBB4. In the following study, our aim was to analyze the impact of ERBB4 on skin *in vitro*, in human keratinocytes HaCaT and in the human skin epidermoid carcinoma cell line A431, as well as *in vivo*, in human and murine epidermis during homeostasis. We generated a skin-specific ERBB4 KO mouse model and investigated the effect of ERBB4 on skin morphology and cell biology in more detail.

2-2 Study

This work was published in Biochimica et Biophysica Acta - General Subjects in April 2018.[161]

Authors: **C. Hoesl**, J.M. Röhrl, M.R. Schneider, M. Dahlhoff

Author contribution: *Study design and manuscript preparation:* MD; *Data analysis:* CH and JMR; *Data interpretation and manuscript preparation:* MRS;

BBA - General Subjects 1862 (2018) 958–966

Contents lists available at ScienceDirect

BBA - General Subjects

journal homepage: www.elsevier.com/locate/bbagen

The receptor tyrosine kinase ERBB4 is expressed in skin keratinocytes and influences epidermal proliferation

Christine Hoesl, Jennifer M. Röhrl, Marlon R. Schneider, Maik Dahlhoff*

Institute of Molecular Animal Breeding and Biotechnology, Gene Center, LMU Munich, Munich, Germany

ARTICLE INFO

Keywords:
HaCaT
A431
EGFR
ERBB4
Knockout
Mouse model

ABSTRACT

Background: The epidermal growth factor receptor (EGFR) and associated receptors ERBB2 and ERBB3 are important for skin development and homeostasis. To date, ERBB4 could not be unambiguously identified in the epidermis. The aim of this study was to analyze the ERBB-receptor family with a special focus on ERBB4 *in vitro* in human keratinocytes and *in vivo* in human and murine epidermis.

Methods: We compared the transcript levels of all ERBB-receptors and the seven EGFR-ligands in HaCaT and A431 cells. ERBB-receptor activity was analyzed after epidermal growth factor (EGF) stimulation by Western blot analysis. The location of the receptors was investigated by immunofluorescence in human keratinocytes and skin. Finally, we investigated the function of ERBB4 in the epidermis of skin-specific ERBB4-knockout mice.

Results: After EGF stimulation, all ligands were upregulated except for epigen. Expression levels of EGFR were unchanged, but all other ERBB-receptors were down-regulated after EGF stimulation, although all ERBB-receptors were phosphorylated. We detected ERBB4 at mRNA and protein levels in both human epidermal cell lines and in the basal layer of human and murine epidermis. Skin-specific ERBB4-knockout mice revealed a significantly reduced epidermal thickness with a decreased proliferation rate.

Conclusions: ERBB4 is expressed in the basal layer of human epidermis and cultured keratinocytes as well as in murine epidermis. Moreover, ERBB4 is phosphorylated in HaCaT cells due to EGF stimulation, and its deletion in murine epidermis affects skin thickness by decreasing proliferation.

General significance: ERBB4 is expressed in human keratinocytes and plays a role in murine skin homeostasis.

1. Introduction

The epidermal growth factor receptor (EGFR, ERBB1, HER1) and its ligands play an important role in skin homeostasis, and their deregulation promptly affects keratinocyte proliferation and differentiation, potentially resulting in inflammatory or hyperproliferative responses [1]. EGFR belongs to a family of receptor tyrosine kinase (RTK) receptors that also includes ERBB2 (NEU, HER2), ERBB3 (HER3), and ERBB4 (HER4) [2,3]. While evidence for a key role of EGFR in skin pathophysiology is ample, considerably less is known about the functions of the structurally related ERBB receptors in this tissue.

ERBB2, a ligand-less receptor, is co-expressed with EGFR in the epidermal basal layer and in proliferative cells of the pilosebaceous unit [4]. ERBB2 is activated by UV irradiation and increases UV induced skin tumorigenesis by suppressing S-phase arrest [5]. ERBB2 is overexpressed in several types of cancer, including human non-melanoma skin cancer [6,7], and transgenic overexpression of ERBB2 causes epidermal and follicular hyperplasia and spontaneous tumor formation [4,8–11]. Deletion of ERBB2 in HaCaT cells [12] and murine skin deteriorates wound healing and decreases tumor burden in a multistage chemical carcinogenesis protocol in ERBB2 knockout mice [13]. ERBB3 is expressed in all epidermal layers, with highest levels in the suprabasal and spinous layers [4,14]. ERBB3 has a potential involvement in wound repair [15,16], and it has an important function in chemically-induced skin tumorigenesis in mice [17]. So far, ERBB4 expression analysis in the skin resulted in contradictory findings. ERBB4 expression was not detectable in human [14,18] or murine [4] epidermis, and also not in human primary keratinocytes [19] and A431 [20,21]. Nevertheless, other groups detected ERBB4 in human epidermis [21], in A431 cells, although only a weak signal was observed [18], and not unambiguously identified in HaCaT cells [19]. Notably, Panchal and colleagues detected ERBB4 in murine epidermis and hair follicles [22]. This group overexpressed neuregulin 3 (NRG3), a highly specific ERBB4 ligand, under the control of the keratin 14 promoter in the skin, and observed a dramatically thickened epidermis.

The aim of this work was to study the ERBB receptors and their

* Corresponding author at: Gene Center, LMU Munich, Feodor-Lynen-Str. 25, 81377 Munich, Germany.
E-mail address: dahlhoff@lmb.uni-muenchen.de (M. Dahlhoff).

https://doi.org/10.1016/j.bbagen.2018.01.017
Received 26 October 2017; Received in revised form 17 January 2018; Accepted 23 January 2018

ligands in the human keratinocyte cell line HaCaT, representing normal keratinocytes, and in the human skin epidermoid carcinoma cell line A431, which represents a squamous cell carcinoma. As EGFR, ERBB2, and ERBB3 are established receptors regulating skin homeostasis and tumorigenesis, we focused on the neglected ERBB4 receptor. Although in the past some studies investigated ERBB receptors and some of their ligands in these cell lines, to date no publication is available in which all ERBB receptors and all EGFR ligands are analyzed in both lines and directly compared to each other. We clearly detected ERBB4 expression in established keratinocyte cell lines, human and murine epidermis using three different antibodies. Generation of skin-specific ERBB4 knockout mice revealed that ERBB4 is dispensable for skin development, but it is involved in epidermal proliferation and homeostasis.

2. Materials and methods

2.1. Cell culture

HaCaT keratinocytes and A431 cells were cultured in DMEM® medium (Biochrom, Berlin, Germany) supplemented with 10% fetal calf serum (FCS, Biochrom) and 1% penicillin/streptomycin (Biochrom). For starvation, cells were cultured in the medium indicated above without FCS for 12 h and were stimulated with 100 ng/ml EGF (R&D systems, Wiesbaden-Nordenstadt, Germany) for the indicated periods of time.

2.2. Mice

Mice carrying floxed *Erbb4* alleles [23] or expressing cre recombinase under the keratin 5 promoter have been described previously [24]. Genotyping of transgenic mice was done by PCR using the following primers *P20*: 5′-CAAATGCTCTCTCTGTTCTTTGTGTCTG-3′; *P22*: 5′-TTTTGCCAAGTTCTAATTCCATCAGAAGC-3′; *P23*: 5′-TATTGT GTTCATCTATCATTGCAACCCAG-3′; *K5Cre-Fw*: 5′-AATCGCCATCTTCC AGCAG-3′; *K5Cre-Rv*: 5′-GATCGCTGCCAGGATATACG-3′. Mouse strains were maintained in the C57BL/6N background under specific pathogen-free conditions and had access to water and standard rodent diet (V1534, Ssniff, Soest, Germany) *ad libitum*. All experiments were approved by the Committee on Animal Health and Care of the state of Upper Bavaria (Regierung von Oberbayern, Germany). Genotyping of mouse lines was performed according to the original publications. Eight-week-old *Erbb4*^{del} females and control littermates were dissected for further investigations. After euthanasia, skin samples were fixed in 4% paraformaldehyde (PFA, Sigma, Taufkirchen, Germany), dehydrated, and embedded in paraffin or snap-frozen and stored at −80 °C until use.

2.3. Quantitative RT-PCR

For RNA analysis the starved cells were stimulated with EGF for 2 h. Total RNA was isolated with TRIZOL reagent (Invitrogen, Darmstadt, Germany) and 1 μg of RNA samples were reverse-transcribed in a final volume of 20 μl using RevertAid Reverse Transcriptase (Thermo Scientific, Schwerte, Germany) according to the manufacturer's instructions. Quantitative RT-PCR was carried out in a LightCycler®480 (Roche, Mannheim, Germany) using the primers listed in Supplementary Table S1 (0.5 μM), 1 μl cDNA, 0.2 μM probe (Universal ProbeLibrary Set, Roche), and the LightCycler® 480 Probes Master Mix (Roche) in a final volume of 10 μl. Cycle conditions were 95 °C for 5 min for the first cycle, followed by 45 cycles at 95 °C for 10 s, 60 °C for 15 s, and 72 °C for 1 s. Transcript copy numbers were normalized to histone H3 (*H3F3A*) (Fig. 1) or peptidyl-prolyl cis-trans isomerase a (*PPIA*) (Fig. S3) mRNA copies. The ΔCt value of the sample was determined by subtracting the average Ct value of the target gene from the average Ct value of the *H3F3A* gene. For each primer pair we performed no-template control and no-RT control assays, which produced negligible signals that were usually > 40 in Ct value. Experiments were performed in duplicates for each sample. All primers and probes are listed in Supplementary Table S1. For qualitative mRNA expression of human *ERBB4*, RT-PCR using reagents from Qiagen (Hilden, Germany) were performed. The final reaction volume was 20 μl, and cycle conditions were 94 °C for 5 min, followed by 35 cycles at 94 °C for 1 min, 60 °C for 1 min, and 72 °C for 1 min. Following primers were employed: *ERBB4* forward primer 5′-GAGCAAGAATTGACTCGAATAGG-3′ and reverse primer 5′-TTCCTGACATGGGGGTGTAG-3′; *JM* forward primer 5′-TCC AGATGGCTTACAGGG-3′ and reverse primer 5′-TCTCATTAAGAATCTT AATAGC-3′; *CYT* forward primer 5′-ATCTCTTGGATGAAGAGGATT-3′ and reverse primer 5′-TTGTCTCGCATAGGAGTCAT-3′; *GAPDH* forward primer 5′-TCATCAACGGGAAGCCCATCAC-3′ and reverse primer 5′-AGACTCCACGACATACTCAGCACCG-3′.

2.4. Western blot analysis

For Western blot experiments the starved cells were stimulated with EGF for 10 min. Protein of cells and murine tissue was extracted using Laemmli-extraction-buffer, and the protein concentration was estimated *via* bicinchoninic acid protein assay. 25 μg of total protein were separated by 10% SDS-PAGE and transferred to PVDF membranes (Millipore, Schwalbach, Germany) by semidry blotting. Membranes were blocked in 5% w/v fat-free milk powder (Roth, Karlsruhe, Germany) for 1 h at room temperature (RT). After washing in Tris-buffered saline solution (TBS) with 0.1% Tween20 (Sigma) (TBS-T), membranes were incubated over night at 4 °C in 5% w/v BSA (Sigma) in TBS-T with the appropriated primary antibody. All primary and secondary antibodies and their dilutions are listed in Supplementary Table S2. After washing, membranes were incubated in 5% w/v fat-free milk powder with a horseradish peroxidase-labeled secondary antibody. Signals were detected using an enhanced chemiluminescence detection reagent (GE Healthcare, Munich, Germany) and appropriated X-ray films (GE Healthcare).

2.5. Immunofluorescence

For *in vitro* immunofluorescence stainings, cells were grown on cover slips and fixed for 15 min in 4% PFA in phosphate buffered saline (PBS). After fixation, the cells were permeabilized for 10 min with 0.5% Triton X-100 (Roth) in PBS and then washed with PBS. Cover slips were incubated for 2 h at RT with primary antibodies listed in Supplementary Table S3. Sections were washed and incubated with secondary antibody together with Alexa Fluor 594 conjugated Phalloidin (Thermo Fisher Scientific, Waltham, MA, USA, #A-12381). All sections were mounted with Vectashield (Vector Laboratories, Burlingame, CA, USA) with DAPI and stored at 4 °C.

Biopsy sample (normal femoral skin from a female, Caucasian, 52 years old patient and healthy frontal skin) obtained after informed consent were kindly provided by R. Wolf, M.D. (Klinik für Dermatologie und Allergologie, Universitätsklinikum Giessen-Marburg, Marburg, Germany). Human and murine samples were embedded in Tissue-Tek O.C.T. (VWR, Darmstadt, Germany), frozen on dry ice and cryosectioned (10 μm). After fixation for 15 min at RT in 4% PFA in PBS sections were washed with TBS-T and blocked in blocking buffer (5% donkey serum (Millipore), 0.1% Tween20 in TBS) for 2 h at RT. For immunolabeling the primary and secondary antibodies listed in Supplementary Table S3 were used. Sections were incubated with primary antibody in staining buffer (2.5% donkey serum, 0.1% Tween20 in TBS) at 4 °C over night. After washing with 0.1% TBS-T tissue sections were incubated with appropriate fluorescent secondary antibodies in staining buffer for 1–2 h at RT and nuclei were additionally stained with 4′,6-diamidino-2-phenylindole (DAPI) for 5 min at RT. At last, sections were mounted with Vectashield with DAPI after washing with 0.1% TBS-T. Images were acquired using Zeiss LSM710 laser-scanning confocal microscope (Carl Zeiss MicroImaging) with a 40× water

objective. Representative single Z-planes are presented. RGB images were assembled using Fiji (ImageJ) software.

2.6. Immunohistochemistry

Skin samples were fixed in 4% PFA, dehydrated, and embedded in paraffin. For target retrieval the sections were deparaffinized and boiled in a microwave for 20 min in 10 mM citrate buffer (pH 6.0). Tissue sections were incubated with anti-Ki67 antibody over night at 4 °C followed by incubation with a biotin linked secondary antibody for 1 h at RT. Slides were incubated for 30 min with an avidin-biotin-enzyme complex solution (Vector Laboratories), 3,3′-diaminobenzidine (KemEnTec, Copenhagen, Denmark) was used as a chromogen. Counterstaining was performed with hematoxylin. At last, sections were

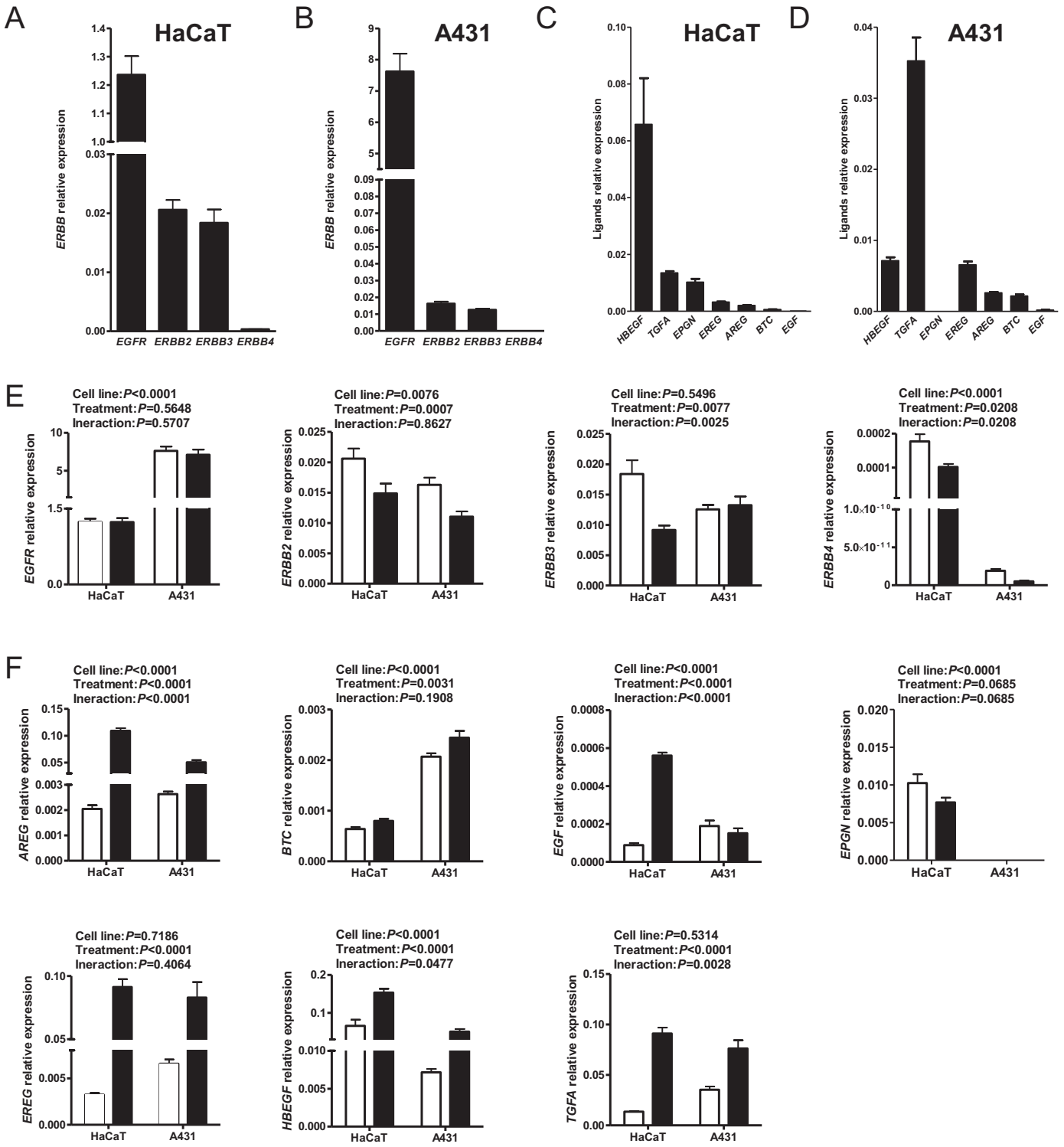

Fig. 1. Abundance and regulation of EGFR/ERBB family members in HaCaT and A431 cells. Relative expression of ERBB receptors (A) and EGFR ligands (C) in HaCaT and A431 cells (B, D). (E) Analysis of receptor transcript levels by quantitative RT-PCR in non-treated and EGF treated HaCaT and A431 cells (n = 6 samples/group). (F) Expression of the EGFR ligands in HaCaT and A431cell lines non-treated and treated with EGF for 2 h (n = 6 samples/group). Expression levels are relative to *H3F3A* expression. Data are presented as means ± SEM, and were analyzed by 2-way ANOVAs. In E and F: white columns represent non-stimulated cells, and black columns represent EGF stimulated cells.

dehydrated using 50%, 70%, 90%, and 100% ethanol and xylene and mounted with Histokitt (Hecht-Assistant, Sondheim, Germany). All antibodies are listed in Supplementary Table S3. Proliferation rate was measured on Ki67-stained sections by counting 20 visual fields for each animal. Both, Ki67-positive and negative nuclei were counted on pictures taken with a 200 magnification lens and a Leica DFC425C digital camera (Leica Microsystems, Wetzlar, Germany) covering a length of 13 mm skin.

2.7. Morphometric analysis

Epidermal thickness was analyzed in four female Erbb4^{del} mice and control littermates. For the quantitative evaluation of epidermal thickness, two different sections from the back skin of each animal were stained with H&E. Pictures covering a length of 26 mm of epidermis (distributed over a total length of 10.4 cm of back skin) were taken with a 200× magnification lens using a Leica DFC425C digital camera (Leica Microsystems) per animal. Epidermal thickness was investigated on 40 pictures on 10 constantly distributed measuring points per picture, resulting in a total of 400 measuring points per animal. The Leica Application Suite 4.4.0 software (Leica Microsystems) was used for the measurements.

2.8. Data pretreatment and statistical analysis

Data are presented as means ± SEM and compared by Student's *t*-test (GraphPad Prism version 5.0 for Windows, GraphPad Software, San Diego, CA, USA). Differences were considered to be statistically significant if $P < 0.05$. Ct values of gene targets of qRT-PCR analysis were shown relative to Ct values of the *H3F3A* or *PPIA* cDNA and compared by 2-way analysis of variance (ANOVA) (GraphPad Prism), for the following parameters: cell line, treatment, and cell line x treatment (interaction).

3. Results

3.1. Expression of ERBB receptors and EGFR ligands in HaCaT and A431 cells

We employed quantitative RT-PCR to characterize the expression of the *ERBB* receptors and the EGFR ligands in human HaCaT and A431 cells. Among the receptors, *EGFR* showed the highest expression level, *ERBB2* as well as *ERBB3* transcript levels were lower (Fig. 1A). Additionally, we were able to detect *ERBB4* gene expression in HaCaT cells (Fig. 1A; E). To evaluate changes in receptor expression during EGFR activation, we treated both cell lines with EGF for 2 h. As shown in Fig. 1E, EGF stimulation of HaCaT cells significantly reduced the transcript levels of all three *ERBB* receptors, but not EGFR. In A431 cells only the transcript levels of *ERBB2* were significantly reduced. The same applied to *ERBB4* transcripts, but this receptor was barely expressed in A431 (Fig. 1B). Evaluation of the transcript levels of the seven EGFR ligands by quantitative RT-PCR demonstrated that heparin-binding EGF-like growth factor (*HBEGF*) was the most abundantly expressed ligand, followed by transforming growth factor alpha (*TGFA*), epigen (*EPGN*), epiregulin (*EREG*), amphiregulin (*AREG*), betacellulin (*BTC*), and *EGF* in HaCaT cells (Fig. 1C). In A431 cells *EPGN* was not expressed, and the most abundant ligand was *TGFA* (Fig. 1D). Treatment with EGF resulted in the upregulation of all ligands, except for *EPGN* in HaCaT cells. In A431 cells results were similar, besides that *EGF* expression levels did not change (Fig. 1F). The receptor and ligand expression data shown in Fig. 1 was determined relative to *H3F3A* expression, these results were confirmed with a second reference gene *PPIA* (Fig. S1). The expression of *ERBB4* was confirmed by RT-PCR. *ERBB4* transcripts were found in non-stimulated and EGF treated HaCaT cells. Additionally, a faint band was visible in A431 cells (Fig. 2A). ERBB4 can be alternatively spliced into four major isoforms

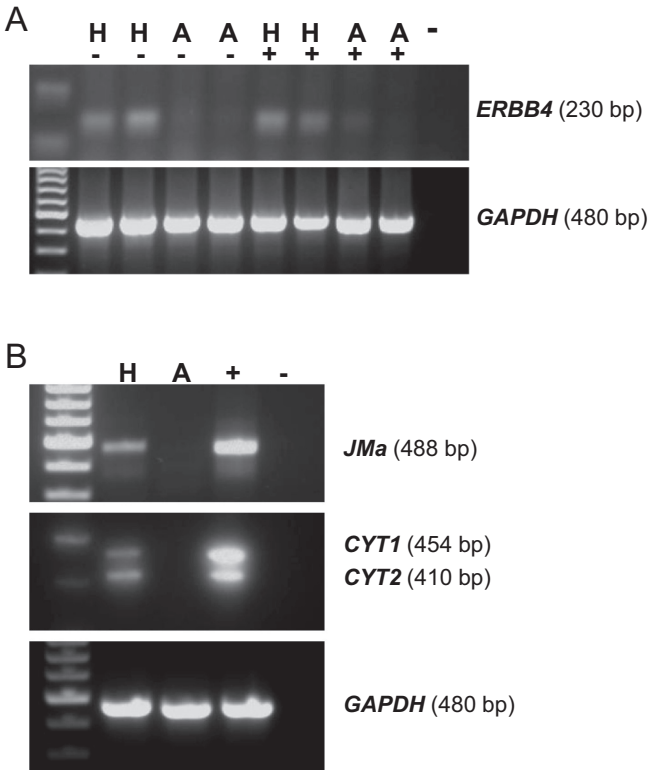

Fig. 2. Gene expression of ERBB4 and its isoforms *in vitro*. (A) Analysis of *ERBB4* transcript levels by RT-PCR in A431 and HaCaT cells. (B) Isoform JM-a and both CYT variants are expressed in HaCaT cells. *GAPDH* serves as loading control. Abbreviations: HaCaT cells (H), A431 cells (A), EGF stimulation for 2 h (+), non-stimulated (−).

with different functions. Two alternative extracellular juxtamembrane isoforms (JM-a and JM-b) and two intracellular cytoplasmic isoforms (CYT-1 and CYT-2) have been described [25]. To clarify which isoforms of ERBB4 are expressed in HaCaT cells, RT-PCR recognizing the JM and CYT region of the *ERBB4*-receptor was performed. HaCaT cells expressed only the cleavable JM-a isoform, but both CYT variants (Fig. 2B).

3.2. Expression of EGFR/ERBB receptors, MAPK, and AKT on protein level in vitro

We next performed Western blot analysis to characterize ERBB receptor expression on protein level in both cell lines. For this, we investigated non-stimulated cells and cells stimulated with EGF for 10 min. We found a much higher amount of EGFR and ERBB2 proteins in A431 cells compared to HaCaT cells. In addition, ERBB3 expression was slightly higher in A431 (Fig. 3A). Also ERBB4 was expressed in both cell lines, and was detected by three different antibodies (Fig. 3G–I). Activated EGFR, phosphorylated at tyrosine residue 1173 and 1068, was detected in stimulated as well as non-stimulated A431 cells and in stimulated HaCaT cells, but not in non-stimulated HaCaT cells (Fig. 3B). The same pattern was found for the activated ERBB2-receptor, phosphorylated at tyrosine residue 877. Phosphorylation of the ERBB2 at tyrosine residue 1221 was barely detectable (Fig. 3C). For phosphorylated ERBB3-receptor at tyrosine 1289, we found a higher signal in A431 cells compared to HaCaT cells (Fig. 3D). One of the main downstream targets of EGFR is mitogen-activated protein kinase (MAPK). MAPK was activated in non-stimulated and EGF treated A431 cells at equal amounts (Fig. 3E). The same results were obtained for phosphorylated RAC-alpha serine/threonine-protein kinase (AKT) (Fig. 3F). In HaCaT cells, MAPK and AKT were only activated under stimulated conditions. Non EGF-treated HaCaT cells showed no phosphorylated ERBB receptors and no kinase activity (Fig. 3E; F).

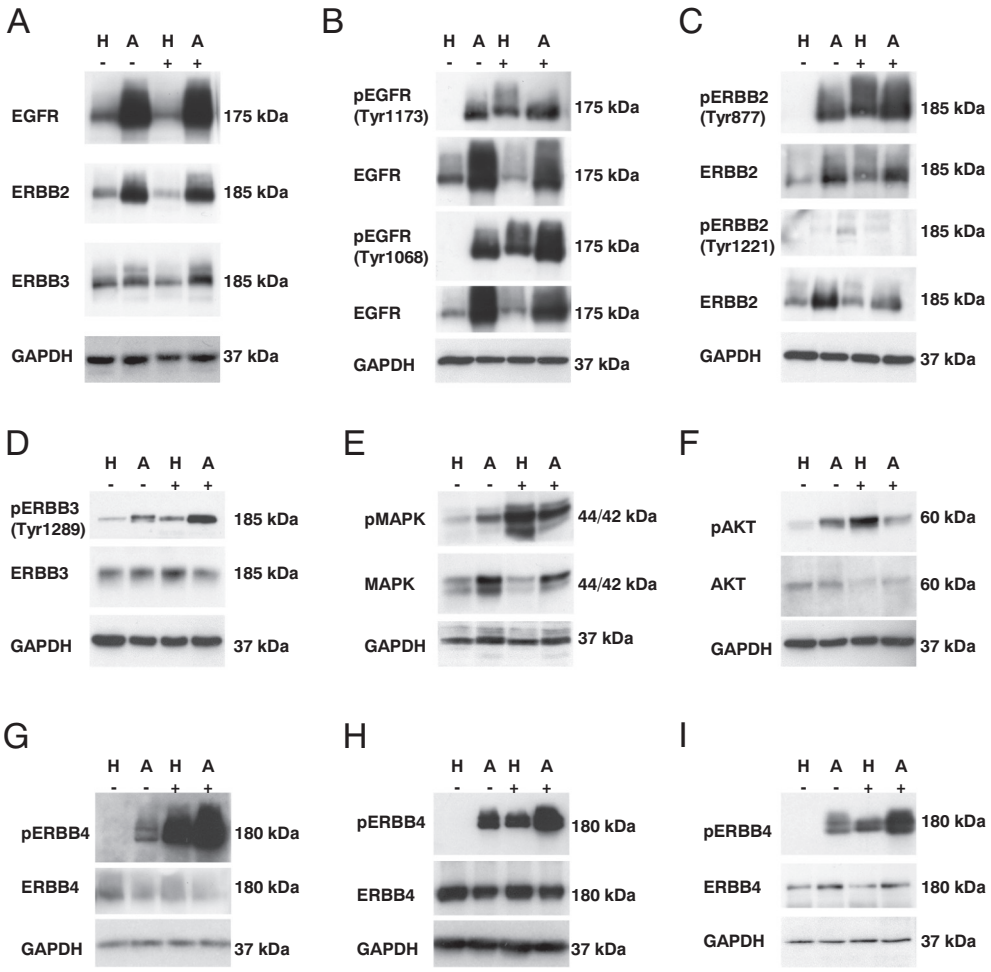

Fig. 3. Activation of ERBB receptors and their downstream targets after EGF stimulation. (A) Western blot analysis showing the expression of the receptors in non-treated and EGF stimulated HaCaT and A431 cells. (B) Western blot analysis show activated EGFR, (C) ERBB2, (D) ERBB3 and phosphorylated (E) MAPK and (F) AKT. The blots were stripped and GAPDH serves as loading control. Phosphorylated and non-phosphorylated ERBB4 was detected with three different antibodies (G) anti-pERBB4 (Cell Signaling #4757) and anti-ERBB4 (Cell Signaling #4795), (H) anti-pERBB4 (Cell Signaling #3790) and anti-ERBB4 (Santa Cruz #283), (I) anti-pERBB4 (Abcam #76132) and anti-ERBB4 (Proteintech #19943-1-AP). Abbreviations: HaCaT cells (H), A431 cells (A), EGF stimulation for 10 min (+), non-stimulated (−).

Next, we investigated the protein expression level of ERBB4 with three different antibodies for phosphorylated and total ERBB4 each. All antibodies provided the same results: ERBB4 seemed to be expressed equally in all four cell samples. Regarding receptor activation, phosphorylated ERBB4 was detected in EGF stimulated HaCaT and A431 cells, in non-stimulated A431 cells, but not in non-treated HaCaT cells (Fig. 3G–I). These findings are in accordance with the expression pattern of the other ERBB family members.

3.3. Immunofluorescence staining of EGFR/ERBB receptors in HaCaT cells and human skin

Next, we analyzed ERBB-receptor expression by immunofluorescence staining. HaCaT cells were stained with antibodies for the different ERBB receptors together with phalloidin to illustrate the cytoplasm (Fig. 4). EGFR, ERBB2, and ERBB4 were located next to the membrane, and ERBB3 was additionally detected diffusely in the cytosol of HaCaT cells. An overview of the cell staining with lower magnification is presented in Fig. S2. To confirm these findings, we stained also healthy human skin. We observed ERBB4 and EGFR expression in the epidermis (Fig. 5), and both receptors were stronger expressed in the basal than in the suprabasal layer. ERBB4 expression was confirmed using four different antibodies showing the same expression pattern in the basal layer of the epidermis (Fig. S3). Contrary to previous reports on murine skin [4], ERBB3 was detected only in the basal layer and ERBB2 in the suprabasal layer of human epidermis (Fig. 5).

3.4. Skin-specific deletion of ERBB4 in mice

Finally, to analyze a possible influence of ERBB4 on skin development and homeostasis we deleted the receptor in murine skin. For this purpose, we crossed mice carrying conditional *Erbb4* alleles [23] with transgenic mice expressing the cre enzyme under the control of the keratin 5 (K5) promoter [24]. The obtained skin-specific ERBB4 knockout mice ($Erbb4^{del}$) were viable, born at Mendelian ratios, and bred normally. We demonstrated that ERBB4 is expressed in the basal layer of the epidermis, but the signal was absent in $Erbb4^{del}$ mice (Fig. 6A). Western blot analysis confirmed the loss of ERBB4 in skin of $Erbb4^{del}$ mice (Fig. 6B). $Erbb4^{del}$ mice showed no macroscopic alterations. Histologically, however, $Erbb4^{del}$ mice revealed a significantly thinner epidermis compared to control animals (Fig. 6C; D). To assess the function of ERBB4 in skin proliferation, we performed a Ki67 staining (Fig. 6E). The epidermal proliferation rate in $Erbb4^{del}$ mice was significantly decreased compared to control littermates (Fig. 6F). We performed Western blot analysis to assess whether the loss of ERBB4 affects the expression of other ERBB receptors in the skin. We found no changes of EGFR, ERBB2, and ERBB3 expression, or their phosphorylation states in $Erbb4^{del}$ mice compared to control littermates (Suppl. Fig. S4). Also, the main ERBB downstream kinases MAPK and AKT were not affected in $Erbb4^{del}$ mice (Suppl. Fig. S4).

4. Discussion

The ERBB receptors and their ligands play an important role in epidermal development, homeostasis, and tumorigenesis [1–3]. In this study, we analyzed the expression of all four members of the ERBB

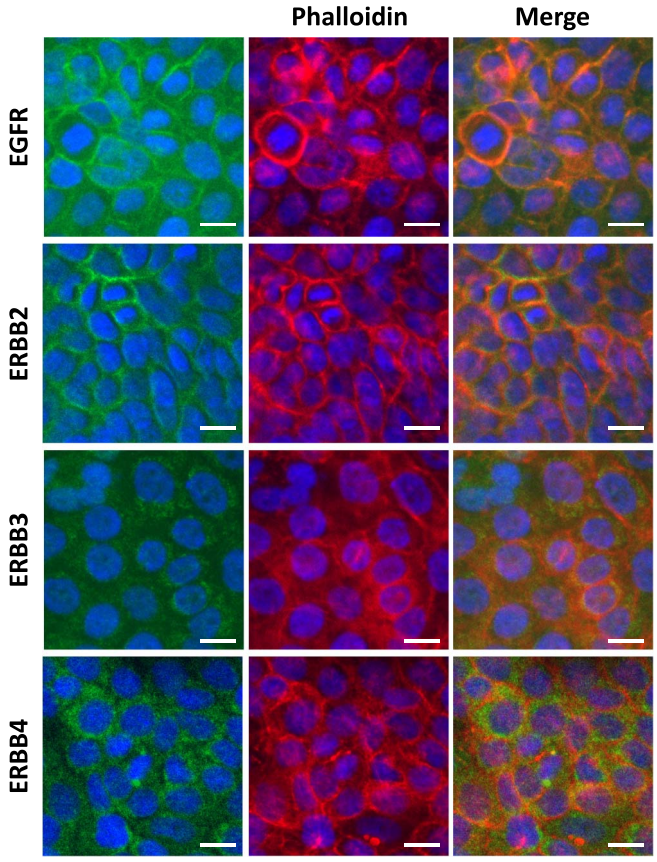

Fig. 4. Immunofluorescence showing the expression of ERBB receptors in HaCaT cells. Receptors were labeled with Alexa Fluor 488 (green), and phalloidin with Alexa Fluor 594 (red), nuclei were stained with DAPI (blue). Merge shows an overlay of all stainings. Pictures were taken with 400× magnification. Scale bars represent 10 µm.

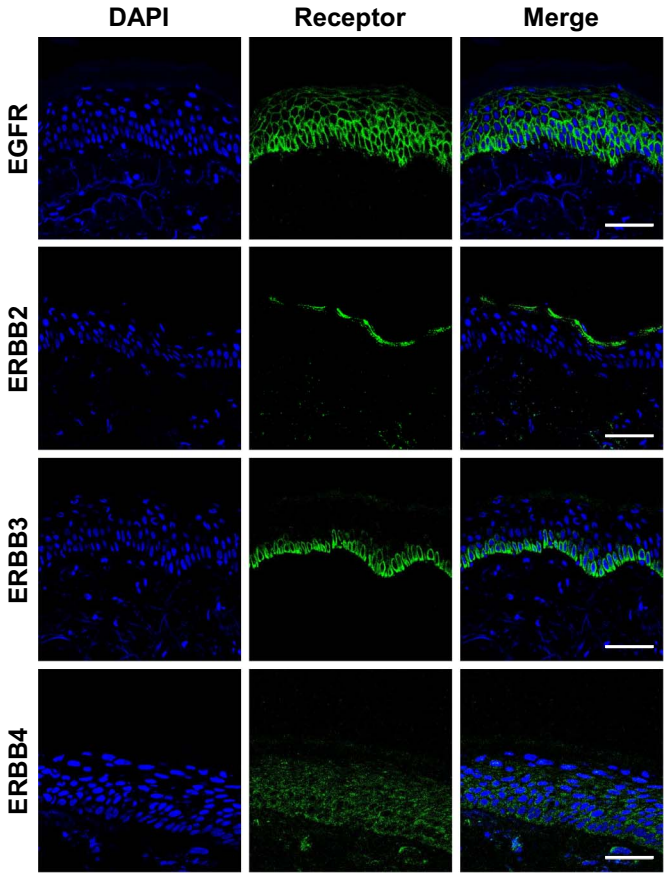

Fig. 5. Localization of ERBB receptors *in vivo*. Immunofluorescence reveals the expression of ERBB receptors in healthy human epidermis. ERBB receptors are shown in green, and the nuclei were stained with DAPI (blue). Merge shows an overlay of both stainings. Scale bars represent 50 µm.

receptor family in epidermal keratinocytes *in vitro* and *in vivo*. We compared the gene expression of *EGFR*, *ERBB2*, *ERBB3*, and *ERBB4* in human HaCaT keratinocytes with malignant epidermal A431 cells, confirming EGFR as the most abundant ERBB receptor for both cell lines. *EGFR* was much higher expressed in A431 than in HaCaT cells, because A431 contain multiple *EGFR* gene amplifications [26]. *ERBB2* and *ERBB3* were expressed in similar amounts in both cell lines, but on protein level ERBB2 was higher expressed in A431 than in HaCaT cells. To our knowledge, this is the first study to investigate all seven EGFR ligands [27], including BTC [28], EREG [29], and the last recognized EGFR ligand EPGN [30,31] in both cell lines. All ligands were upregulated after EGF stimulation, except *EGF* in A431 and *EPGN* in HaCaT cells. EPGN was not expressed in A431 cells, which is in line with previous studies showing that a deletion of epigen in mice has no effect on skin homeostasis [32]. However, a skin-specific overexpression of EPGN revealed hyperplasia of the sebaceous glands and increased expression of the LRIG1-positive stem cell pool in the hair follicle, although no differences in the epidermis were observed [33]. *TGFA*, *HBEGF*, and *AREG* were highly upregulated in both cell lines after EGFR activation, emphasizing their important role in skin homeostasis, wound healing [34–36], psoriasis [37], and tumorigenesis [1,38–41]. Most intriguingly, we found transcripts of *ERBB4* in HaCaT cells, and a very weak signal in A431 cells. These results were also confirmed by standard RT-PCR. Due to alternative splicing, ERBB4 can be expressed in six different isoforms [42]. They vary in their extracellular juxtamembrane (JM) and intracellular cytoplasmic (CYT) domains. We analyzed the four most frequently expressed variants, JM-a and JM-b as well as CYT-1 and CYT-2 and revealed the expression of all isoforms except JM-b. The JM-a isoform is known to be a substrate to regulated intramembrane proteolysis, encoding a cleavage site for matrix metalloproteases (MMPs), like the tumor necrosis factor alpha converting enzyme (TACE), at the cell surface [43–45]. The intracellular domain (ICD) of JM-a can be released by gamma-secretase cleavage [43] and enter the nucleus to act at transcriptional levels [46]. Isoform JM-b contains the alternative exon 15b instead of exon 16 and cannot be shed from the cell surface. Additionally, two further splicing variants for ERBB4 have been reported, JM-c lacking both exons 15b and 16, and JM-d including these both exons, containing the MMP cleavage site [25,47]. Moreover, two cytoplasmatic isoforms exist varying in the presence of exon 26. While the CYT-1 variant contains exon 26 and exhibits a phosphatidyl inositol 3-kinase (PI3-K) binding site, the CYT-2 isoform lacks exon 26 and therefore lacks PI3-K activity [48]. The existence of six different ERBB4 isoforms and additional posttranslational modifications may make it difficult to identify the ERBB4-receptor, especially when it is poorly expressed like in the skin. Consequently, proving evidence of ERBB4 expression in the epidermis is extremely challenging.

Regarding ERBB expression at protein level, we could show that all four RTKs were expressed *in vitro* under stimulated and non-stimulated conditions. In addition, all ERBB receptors were autophosphorylated and therefore activated in A431 tumor cells. In contrast, in HaCaT keratinocytes a stimulus is necessary to activate the ERBB receptors. After stimulation of ERBBs using a known ligand like EGF, autophosphorylation was induced and EGFR, ERBB2, ERBB3, and ERBB4 were activated and affected downstream signal transduction cascades like the MAPK or AKT pathways. EGF is known to bind and activate homo- and heterodimers of all ERBB receptors [19]. These results are in accordance with early studies analyzing A431 [18] and HaCaT cells [19].

Since we could show the presence of all members of the ERBB

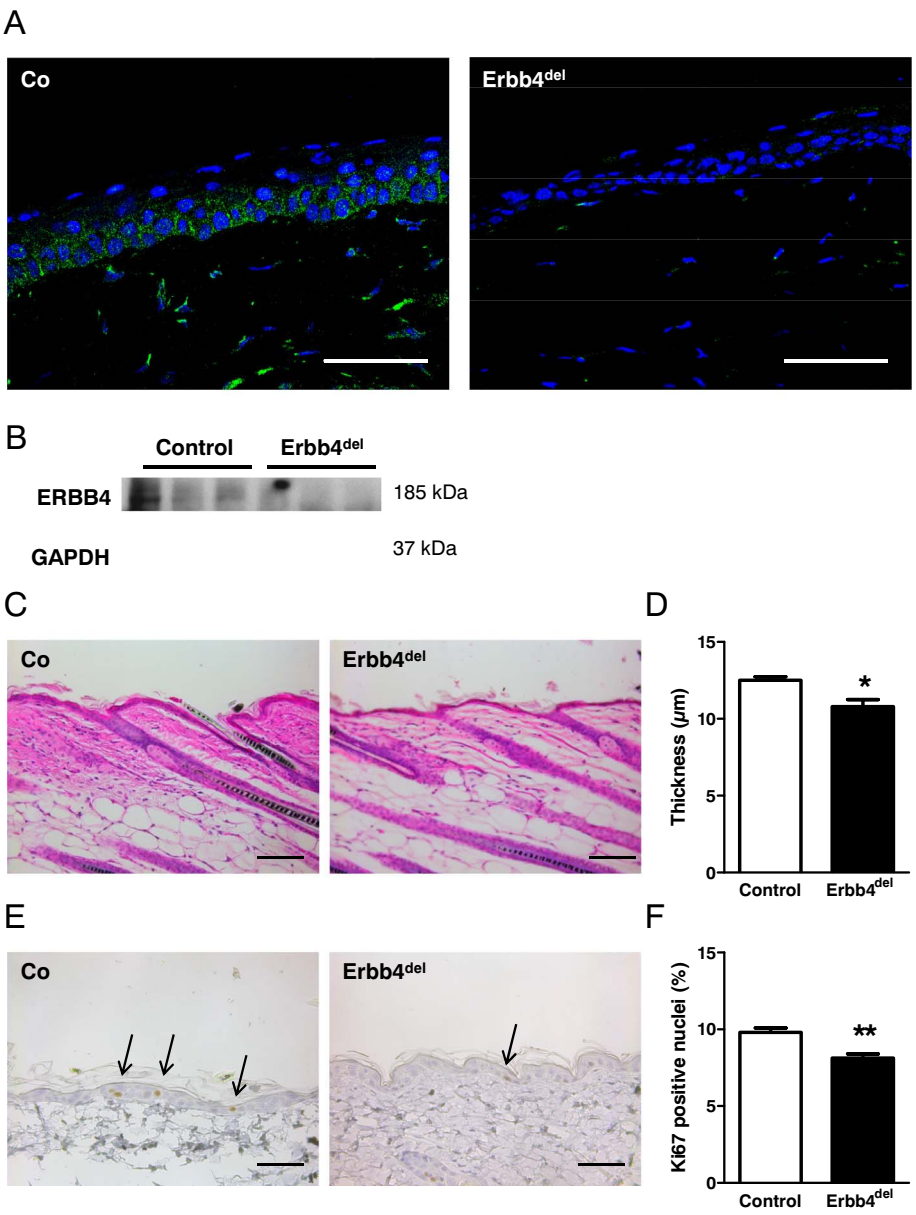

Fig. 6. Erbb4^{del} mice show an influence of ERBB4 on skin homeostasis. (A) ERBB4 expression in the basal layer of murine tail epidermis. Immunofluorescence staining shows ERBB4 in green and nuclei were stained with DAPI in blue. (B) Western blots show a weak band for ERBB4 in control mice and no band in ERBB4-KOs and GAPDH was used as a loading control. (C) H&E staining of back skin of control and Erbb4^{del} mice. (D) Morphometric analysis of epidermal thickness revealed a significantly reduced thinner epidermis in knockout mice. (E) Ki67 staining of murine back skin. (F) Proliferation index is significantly reduced in ERBB4 knockout mice. Data are presented as means ± SEM, and were analyzed by Student's *t*-test ($n = 4$). Scale bars in A and E represent 50 µm, and in C 100 µm.

family *in vitro* and *in vivo* at transcript and protein expression level in human epidermal cells, and the findings about ERBB4 expression in keratinocytes are often contradictory in literature, we decided to study the function of ERBB4 in murine skin. It has been published that ERBB4 is expressed in murine skin, and that skin-specific overexpression of the ERBB4 ligand NRG3 results in epidermal hyperplasia in mice [22]. For further analysis of the function of ERBB4 in murine skin, we developed a skin-specific knockout mouse model for the receptor. Characterization of Erbb4^{del} mice revealed an impact of ERBB4 on skin proliferation. Interestingly, we found no alteration in skin proliferation in Erbb2^{del} [13] and Erbb3^{del} mice [17] under steady-state conditions in our previous studies. However, EGFR is the most abundantly expressed and most important ERBB receptor in the skin and seems to play a critical role during development, homeostasis as well as tumorigenesis. Skin-specific EGFR knockout mice [49,50] develop skin inflammation, hair follicle degeneration and show a deficient skin barrier, reminding symptoms of patients treated with EGFR inhibitors. Frequently, the inhibition of EGFR during cancer therapy is accompanied by skin rash, dry and itchy skin, and microbial infections [51–53]. Evidently, we could show that ERBB4 is expressed in the basal layer of human and murine epidermis, similar to EGFR. Furthermore, Erbb4^{del} mice showed an influence of the ERBB4 receptor on epidermal proliferation and homeostasis. Our current study indicates an even more important role of ERBB4 in skin homeostasis than ERBB2 and ERBB3. Nevertheless, further studies are required to investigate ERBB4 during pathological processes as wound healing, dermatitis or tumorigenesis.

In conclusion, our study reveals that ERBB4 is expressed in the human keratinocyte cell line HaCaT and in human and murine skin. In contrast to skin-specific ERBB2- and ERBB3-knockout mice, the epidermal deletion of ERBB4 reduces the proliferation rate of the epidermis and its thickness. Therefore we conclude that ERBB4 influences skin homeostasis.

Supplementary data to this article can be found online at https://doi.org/10.1016/j.bbagen.2018.01.017.

Transparency document

The Transparency document associated with this article can be found in online version.

Grant support

This work was supported by a grant from the Else Kröner-Fresenius-Stiftung (2014_A173).

Conflict of interest

The authors have no conflict of interest to declare.

Author's contributions

MD contributed to study design and manuscript preparation. CH and JMR contributed to data analysis. MRS contributed to data interpretation and manuscript preparation. All authors read and approved the final manuscript.

Acknowledgements

The authors would like to thank Joseph Millauer and Franziska Kress (genotyping and expression studies) for their expert assistance. The authors acknowledge support by the Else Kröner-Fresenius-Stiftung (2014_A173) to MD and MRS.

References

[1] M.R. Schneider, S. Werner, R. Paus, E. Wolf, Beyond wavy hairs: the epidermal growth factor receptor and its ligands in skin biology and pathology, Am. J. Pathol. 173 (2008) 14–24.
[2] Y. Yarden, M.X. Sliwkowski, Untangling the ErbB signalling network, Nat. Rev. Mol. Cell Biol. 2 (2001) 127–137.
[3] A. Citri, Y. Yarden, EGF-ERBB signalling: towards the systems level, Nat. Rev. Mol. Cell Biol. 7 (2006) 505–516.
[4] K. Kiguchi, D. Bol, S. Carbajal, L. Beltran, S. Moats, K. Chan, J. Jorcano, J. Digiovanni, Constitutive expression of erbB2 in epidermis of transgenic mice results in epidermal hyperproliferation and spontaneous skin tumor development, Oncogene 19 (2000) 4243–4254.
[5] J.G. Madson, D.T. Lynch, J. Svoboda, R. Ophardt, J. Yanagida, S.K. Putta, A. Bowles, C.S. Trempus, R.W. Tennant, L.A. Hansen, Erbb2 suppresses DNA damage-induced checkpoint activation and UV-induced mouse skin tumorigenesis, Am. J. Pathol. 174 (2009) 2357–2366.
[6] G. Krahn, U. Leiter, P. Kaskel, M. Udart, J. Utikal, G. Bezold, R.U. Peter, Coexpression patterns of EGFR, HER2, HER3 and HER4 in non-melanoma skin cancer, Eur. J. Cancer 37 (2001) 251–259.
[7] M.R. Schneider, Y. Yarden, The EGFR-HER2 module: a stem cell approach to understanding a prime target and driver of solid tumors, Oncogene 35 (2016) 2949–2960.
[8] D. Bol, K. Kiguchi, L. Beltran, T. Rupp, S. Moats, I. Gimenez-Conti, J. Jorcano, J. Digiovanni, Severe follicular hyperplasia and spontaneous papilloma formation in transgenic mice expressing the neu oncogene under the control of the bovine keratin 5 promoter, Mol. Carcinog. 21 (1998) 2–12.
[9] W. Xie, X. Wu, L.T. Chow, E. Chin, A.J. Paterson, J.E. Kudlow, Targeted expression of activated erbB-2 to the epidermis of transgenic mice elicits striking developmental abnormalities in the epidermis and hair follicles, Cell Growth Differ. 9 (1998) 313–325.
[10] W. Xie, L.T. Chow, A.J. Paterson, E. Chin, J.E. Kudlow, Conditional expression of the ErbB2 oncogene elicits reversible hyperplasia in stratified epithelia and up-regulation of TGFalpha expression in transgenic mice, Oncogene 18 (1999) 3593–3607.
[11] K. Kiguchi, T. Kitamura, T. Moore, M. Rumi, H.C. Chang, D. Treece, L. Ruffino, K. Connolly, J. Digiovanni, Dual inhibition of both the epidermal growth factor receptor and erbB2 effectively inhibits the promotion of skin tumors during two-stage carcinogenesis, Cancer Prev. Res. (Phila.) 3 (2010) 940–952.
[12] M. Dahlhoff, N. Gaborit, S. Bultmann, H. Leonhardt, Y. Yarden, M.R. Schneider, CRISPR-assisted receptor deletion reveals distinct roles for ERBB2 and ERBB3 in skin keratinocytes, FEBS J. 284 (2017) 3339–3349.
[13] M. Dahlhoff, S. Muzumdar, M. Schafer, M.R. Schneider, ERBB2 is essential for the growth of chemically induced skin tumors in mice, J. Invest Dermatol. 137 (2017) 921–930.
[14] M. Piepkorn, H. Predd, R. Underwood, P. Cook, Proliferation-differentiation relationships in the expression of heparin-binding epidermal growth factor-related factors and erbB receptors by normal and psoriatic human keratinocytes, Arch. Dermatol. Res. 295 (2003) 93–101.
[15] M.I. Okwueze, N.L. Cardwell, A.C. Pollins, L.B. Nanney, Modulation of porcine wound repair with a transfected ErbB3 gene and relevant EGF-like ligands, J. Invest Dermatol. 127 (2006) 1030–1041.
[16] S. Forsberg, O. Rollman, Re-epithelialization from human skin explant cultures is promoted by ligand-activated HER3 receptor, J. Dermatol. Sci. 59 (2010) 7–15.
[17] M. Dahlhoff, M. Schafer, S. Muzumdar, C. Rose, M.R. Schneider, ERBB3 is required for tumor promotion in a mouse model of skin carcinogenesis, Mol. Oncol. 9 (2015) 1825–1833.
[18] S.W. Stoll, S. Kansra, S. Peshick, D.W. Fry, W.R. Leopold, J.F. Wiesen, M. Sibilia, T. Zhang, Z. Werb, R. Derynck, E.F. Wagner, J.T. Elder, Differential utilization and localization of ErbB receptor tyrosine kinases in skin compared to normal and malignant keratinocytes, Neoplasia 3 (2001) 339–350.
[19] M.M. Marques, N. Martinez, I. Rodriguez-Garcia, A. Alonso, EGFR family-mediated signal transduction in the human keratinocyte cell line HaCaT, Exp. Cell Res. 252 (1999) 432–438.
[20] G. Bowers, D. Reardon, T. Hewitt, P. Dent, R.B. Mikkelsen, K. Valerie, G. Lammering, C. Amir, R.K. Schmidt-Ullrich, The relative role of ErbB1-4 receptor tyrosine kinases in radiation signal transduction responses of human carcinoma cells, Oncogene 20 (2001) 1388–1397.
[21] R. Srinivasan, R. Poulsom, H.C. Hurst, W.J. Gullick, Expression of the c-erbB-4/HER4 protein and mRNA in normal human fetal and adult tissues and in a survey of nine solid tumour types, J. Pathol. 185 (1998) 236–245.
[22] H. Panchal, O. Wansbury, S. Parry, A. Ashworth, B. Howard, Neuregulin3 alters cell fate in the epidermis and mammary gland, BMC Dev. Biol. 7 (2007) 105.
[23] W. Long, K.U. Wagner, K.C. Lloyd, N. Binart, J.M. Shillingford, L. Hennighausen, F.E. Jones, Impaired differentiation and lactational failure of Erbb4-deficient mammary glands identify ERBB4 as an obligate mediator of STAT5, Development 130 (2003) 5257–5268.
[24] A. Ramirez, A. Page, A. Gandarillas, J. Zanet, S. Pibre, M. Vidal, L. Tusell, A. Genesca, D.A. Whitaker, D.W. Melton, J.L. Jorcano, A keratin K5Cre transgenic line appropriate for tissue-specific or generalized Cre-mediated recombination, Genesis 39 (2004) 52–57.
[25] V. Veikkolainen, K. Vaparanta, K. Halkilahti, K. Iljin, M. Sundvall, K. Elenius, Function of ERBB4 is determined by alternative splicing, Cell Cycle 10 (2011) 2647–2657.
[26] N. Tebbutt, M.W. Pedersen, T.G. Johns, Targeting the ERBB family in cancer: couples therapy, Nat. Rev. Cancer 13 (2013) 663–673.
[27] M.R. Schneider, E. Wolf, The epidermal growth factor receptor ligands at a glance, J. Cell. Physiol. 218 (2009) 460–466.
[28] M. Dahlhoff, E. Wolf, M.R. Schneider, The ABC of BTC: structural properties and biological roles of betacellulin, Semin. Cell Dev. Biol. 28 (2014) 42–48.
[29] D.J. Riese, R.L. Cullum, Epiregulin: roles in normal physiology and cancer, Semin. Cell Dev. Biol. 28 (2014) 49–56.
[30] L. Strachan, J.G. Murison, R.L. Prestidge, M.A. Sleeman, J.D. Watson, K.D. Kumble, Cloning and biological activity of epigen, a novel member of the epidermal growth factor superfamily, J. Biol. Chem. 276 (2001) 18265–18271.
[31] M.R. Schneider, Y. Yarden, Structure and function of epigen, the last EGFR ligand, Semin. Cell Dev. Biol. 28 (2014) 57–61.
[32] M. Dahlhoff, M. Schafer, E. Wolf, M.R. Schneider, Genetic deletion of the EGFR ligand epigen does not affect mouse embryonic development and tissue homeostasis, Exp. Cell Res. 319 (2013) 529–535.
[33] M. Dahlhoff, D. Frances, J.E. Kloepper, R. Paus, M. Schafer, C. Niemann, M.R. Schneider, Overexpression of epigen during embryonic development induces reversible, epidermal growth factor receptor-dependent sebaceous gland hyperplasia, Mol. Cell. Biol. 34 (2014) 3086–3095.
[34] P.D. Ellis, K.M. Hadfield, J.C. Pascall, K.D. Brown, Heparin-binding epidermal-growth-factor-like growth factor gene expression is induced by scrape-wounding epithelial cell monolayers: involvement of mitogen-activated protein kinase cascades, Biochem. J. 354 (2001) 99–106.
[35] Y. Shirakata, R. Kimura, D. Nanba, R. Iwamoto, S. Tokumaru, C. Morimoto, K. Yokota, M. Nakamura, K. Sayama, E. Mekada, S. Higashiyama, K. Hashimoto, Heparin-binding EGF-like growth factor accelerates keratinocyte migration and skin wound healing, J. Cell Sci. 118 (2005) 2363–2370.
[36] M. Marikovsky, K. Breuing, P.Y. Liu, E. Eriksson, S. Higashiyama, P. Farber, J. Abraham, M. Klagsbrun, Appearance of heparin-binding EGF-like growth factor in wound fluid as a response to injury, Proc. Natl. Acad. Sci. U. S. A. 90 (1993) 3889–3893.
[37] P.W. Cook, M.R. Pittelkow, W.W. Keeble, R. Graves-Deal, R.J. Coffey Jr., G.D. Shipley, Amphiregulin messenger RNA is elevated in psoriatic epidermis and gastrointestinal carcinomas, Cancer Res. 52 (1992) 3224–3227.
[38] A. Imamoto, L.M. Beltran, J. Digiovanni, Evidence for autocrine/paracrine growth stimulation by transforming growth factor-alpha during the process of skin tumor promotion, Mol. Carcinog. 4 (1991) 52–60.
[39] A.A. Dlugosz, C. Cheng, E.K. Williams, N. Darwiche, P.J. Dempsey, B. Mann, A.R. Dunn, R.J. Coffey Jr., S.H. Yuspa, Autocrine transforming growth factor alpha is dispensible for v-rasHa-induced epidermal neoplasia: potential involvement of alternate epidermal growth factor receptor ligands, Cancer Res. 55 (1995) 1883–1893.
[40] L. Rittie, J. Varani, S. Kang, J.J. Voorhees, G.J. Fisher, Retinoid-induced epidermal hyperplasia is mediated by epidermal growth factor receptor activation via specific induction of its ligands heparin-binding EGF and amphiregulin in human skin in vivo, J. Invest Dermatol. 126 (2006) 732–739.
[41] L. Rittie, S. Kansra, S.W. Stoll, Y. Li, J.E. Gudjonsson, Y. Shao, L.E. Michael, G.J. Fisher, T.M. Johnson, J.T. Elder, Differential ErbB1 signaling in squamous cell versus basal cell carcinoma of the skin, Am. J. Pathol. 170 (2007) 2089–2099.
[42] T.T. Junttila, M. Sundvall, J.A. Maatta, K. Elenius, Erbb4 and its isoforms: selective regulation of growth factor responses by naturally occurring receptor variants, Trends Cardiovasc. Med. 10 (2000) 304–310.
[43] C.Y. Ni, M.P. Murphy, T.E. Golde, G. Carpenter, gamma-Secretase cleavage and nuclear localization of ErbB-4 receptor tyrosine kinase, Science (New York, N.Y.) 294 (2001) 2179–2181.
[44] H.J. Lee, K.M. Jung, Y.Z. Huang, L.B. Bennett, J.S. Lee, L. Mei, T.W. Kim, Presenilin-

dependent gamma-secretase-like intramembrane cleavage of ErbB4, J. Biol. Chem. 277 (2002) 6318–6323.
[45] C. Rio, J.D. Buxbaum, J.J. Peschon, G. Corfas, Tumor necrosis factor-alpha-converting enzyme is required for cleavage of erbB4/HER4, J. Biol. Chem. 275 (2000) 10379–10387.
[46] Y.W. Zhang, R. Wang, Q. Liu, H. Zhang, F.F. Liao, H. Xu, Presenilin/gamma-secretase-dependent processing of beta-amyloid precursor protein regulates EGF receptor expression, Proc. Natl. Acad. Sci. U. S. A. 104 (2007) 10613–10618.
[47] R. Gilbertson, R. Hernan, T. Pietsch, L. Pinto, P. Scotting, R. Allibone, D. Ellison, R. Perry, A. Pearson, J. Lunec, Novel ERBB4 juxtamembrane splice variants are frequently expressed in childhood medulloblastoma, Gene Chromosome Cancer 31 (2001) 288–294.
[48] K. Elenius, C.J. Choi, S. Paul, E. Santiestevan, E. Nishi, M. Klagsbrun, Characterization of a naturally occurring ErbB4 isoform that does not bind or activate phosphatidyl inositol 3-kinase, Oncogene 18 (1999) 2607–2615.
[49] B.M. Lichtenberger, P.A. Gerber, M. Holcmann, B.A. Buhren, N. Amberg, V. Smolle, H. Schrumpf, E. Boelke, P. Ansari, C. Mackenzie, A. Wollenberg, A. Kislat, J.W. Fischer, K. Rock, J. Harder, J.M. Schroder, B. Homey, M. Sibilia, Epidermal EGFR controls cutaneous host defense and prevents inflammation, Sci. Transl. Med. 5 (2013) 199ra111.
[50] T.C. Lee, D.W. Threadgill, Generation and validation of mice carrying a conditional allele of the epidermal growth factor receptor, Genesis 47 (2009) 85–92.
[51] F. Ciardiello, G. Tortora, EGFR antagonists in cancer treatment, N. Engl. J. Med. 358 (2008) 1160–1174.
[52] R.E. Eilers Jr., M. Gandhi, J.D. Patel, M.F. Mulcahy, M. Agulnik, T. Hensing, M.E. Lacouture, Dermatologic infections in cancer patients treated with epidermal growth factor receptor inhibitor therapy, J. Natl. Cancer Inst. 102 (2010) 47–53.
[53] M.E. Lacouture, Mechanisms of cutaneous toxicities to EGFR inhibitors, Nat. Rev. Cancer 6 (2006) 803–812.

2-3 Supplementary material

In the following all supplementary figures and tables of the publication "The receptor tyrosine kinase ERBB4 is expressed in skin keratinocytes and influences epidermal proliferation."[161] are depicted.

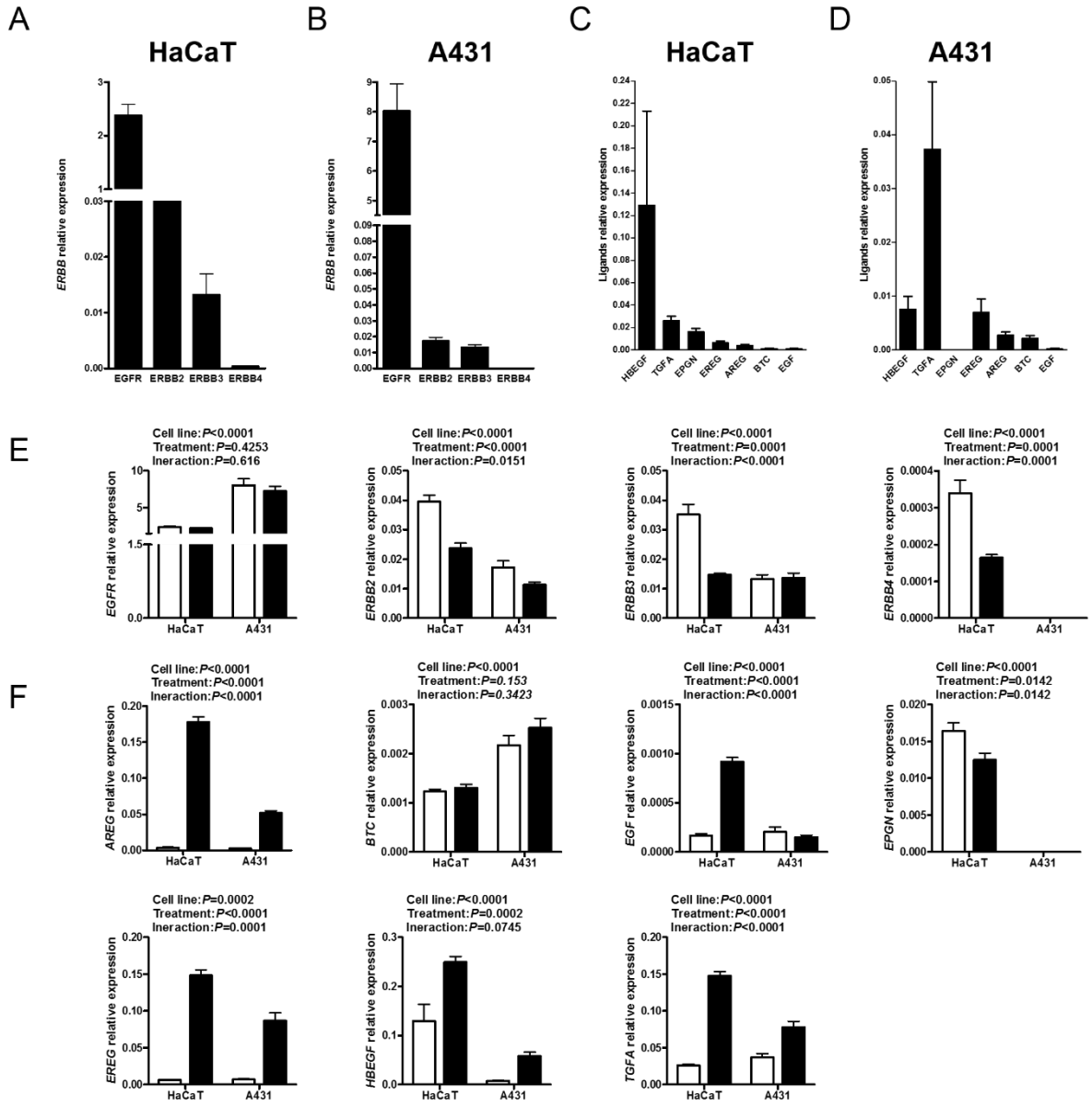

Figure 2-1 Fig. S1. Abundance and regulation of EGFR/ERBB family members in HaCaT and A431 cells.
Relative expression of ERBB receptors **(A)** and EGFR ligands **(C)** in HaCaT and A431 cells **(B,D)**. **(E)** Analysis of receptor transcript levels by quantitative RT-PCR in non-treated and EGF treated cells (n=6 samples/group). **(F)** Expression of the EGFR ligands in HaCaT and A431cell lines non-treated and treated with EGF for 2 h (n=6 samples/group). Expression is relative to *PPIA* expression. Data are presented as means ± SEM, and analyzed by 2-way ANOVAs. In **E** and **F**: white columns are non-stimulated, and black columns are stimulated with EGF.

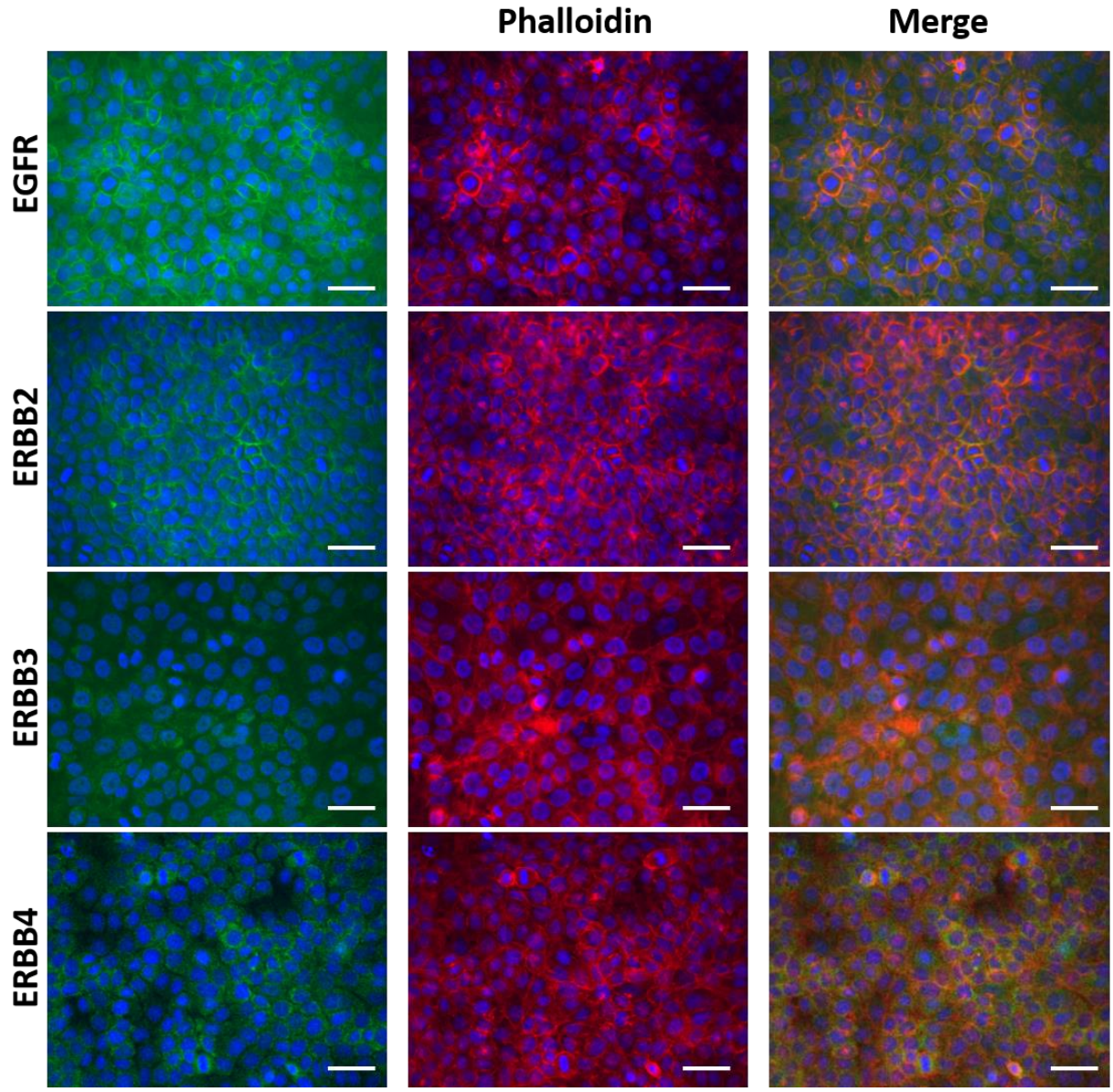

Figure 2-2 Fig. S2. Immunofluorescence showing the expression of ERBB receptors in HaCaT cells. Receptors were labeled with Alexa Fluor 488 (green), and phalloidin with Alexa Fluor 594 (red), nuclei were stained with DAPI (blue). Merge shows an overlay of all staining. Pictures were taken with 400x magnification. Scale bars represent 50 µm.

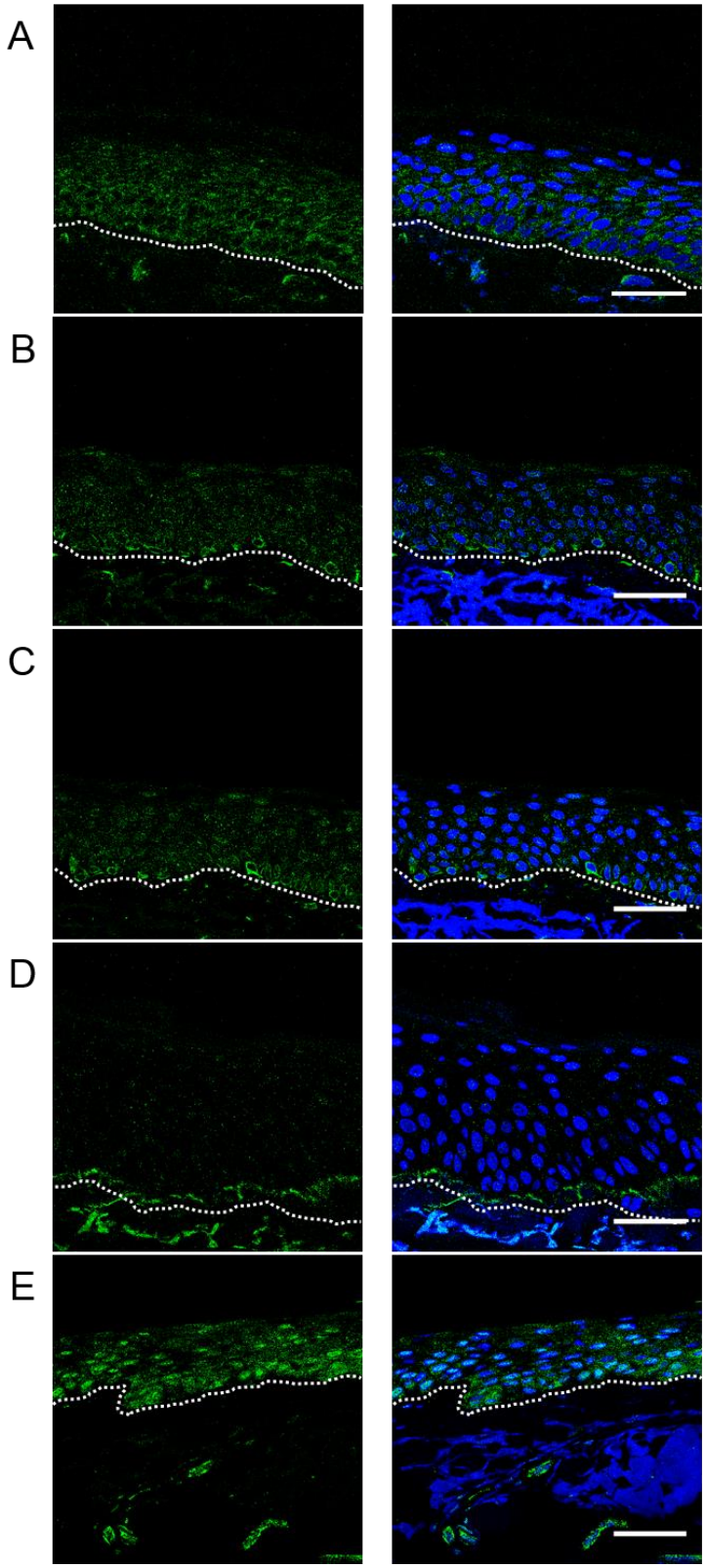

Figure 2-3 Fig. S3. ERBB4 expression in healthy human epidermis.
Receptor expression is shown with five different antibodies. **(A)** Abcam, #19391, **(B)** Fitzgerald, #70R-17129, **(C)** Proteintech, #19943-1-AP, **(D)** Santa Cruz, #8050 and **(E)** Santa Cruz, #283 in green, nuclei were stained with DAPI (blue). Dashed line separates epidermis from dermis. Scale bars represent 50 µm.

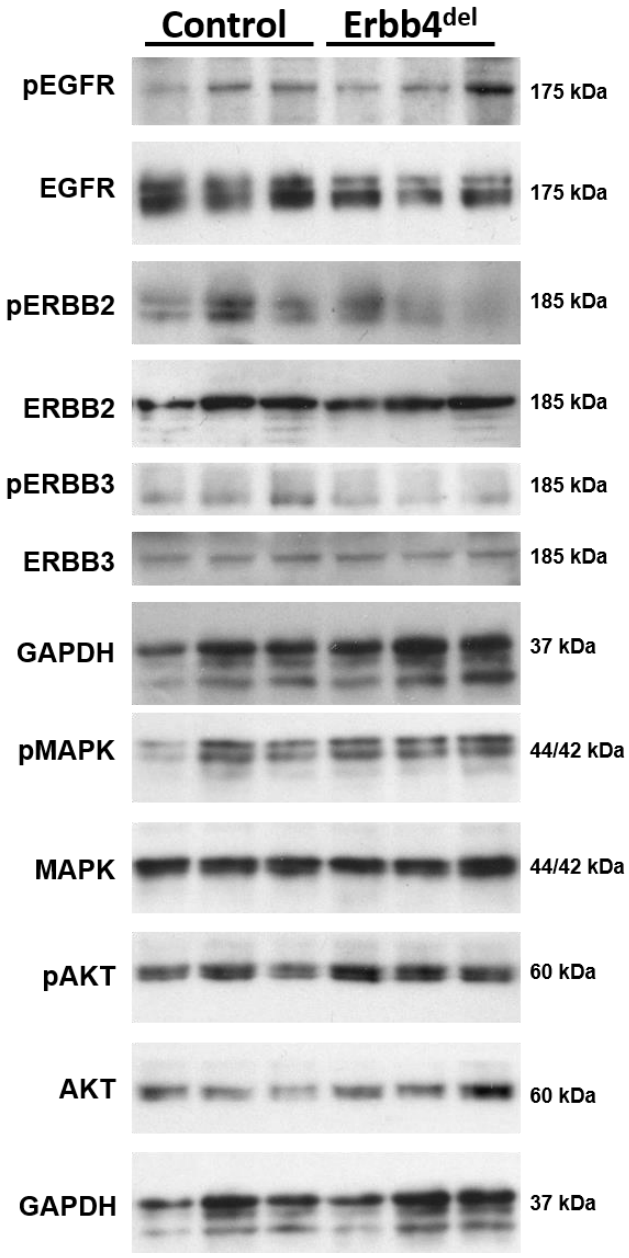

Figure 2-4 Fig. S4. Western blot analysis from Erbb4^{del} back skin and control mice.
The total and phosphorylated levels of EGFR, ERBB2, ERBB3, and of the downstream kinases MAPK and AKT are shown. GAPDH was used as loading control.

Table 2-1 Supplementary Table S1.
Primers and probes employed for quantitative RT-PCR analysis.

AREG	Forward Primer Reverse Primer Probe	5'-cggagaatgcaaatatatagagcac-'3 5'-caccgaaatattcttgctgaca-'3 #38 (cat. no. 04687965001)
BTC	Forward Primer Reverse Primer Probe	5'-actgcatcaaagggagatgc-'3 5'-tctcacaccttgctccaatg-'3 #49 (cat. no. 04688104001)
EGF	Forward Primer Reverse Primer Probe	5'-aagaatgggggtcaaccagt-'3 5'-tgaagttggttgcattgacc-'3 #27 (cat. no. 04687582001)
EPGN	Forward Primer Reverse Primer Probe	5'-tttgggagttccaatatcagc-'3 5'-tgtgattggaggtgttacagtca-'3 #34 (cat. no. 04687671001)
EGFR	Forward Primer Reverse Primer Probe	5'-gccttgactgaggacagca-'3 5'-tttgggaacggactggttta-'3 #69 (cat. no. 04688686001)
ERBB2	Forward Primer Reverse Primer Probe	5'-tgctgtcctgttcaccactc-'3 5'-tcatcctcatcatcttcacattg-'3 #67 (cat. no. 04688660001)
ERBB3	Forward Primer Reverse Primer Probe	5'-ctgatcaccggcctcaat-'3 5'-ggaagacattgagcttctctgg-'3 #37 (cat. no. 04687957001)
ERBB4	Forward Primer Reverse Primer Probe	5'-tctgggtgagccttctcgt-3' 5'-ctccgttcctgcacacact-3' #26 (cat. no. 04687574001)
EREG	Forward Primer Reverse Primer Probe	5'-tggtctcttcactcaggtctca-'3 5'-cgtgagttggcatagggaac-'3 #86 (cat. no. 04689119001)
HBEGF	Forward Primer Reverse Primer Probe	5'-tggggcttctcatgtttagg-'3 5'-catgcccaacttcactttctc-'3 #55 (cat. no. 04688520001)
TGFA	Forward Primer Reverse Primer Probe	5'-ttgctgccactcagaaacag-'3 5'-atctgccacagtccacctg-'3 #63 (cat. no. 04688627001)
H3F3A	Forward Primer Reverse Primer Probe	5'-agtgaggcctatctggttgg-3' 5'-gcacgttctccacgtatgc-3' #42 (cat. no. 04688015001)
PPIA	Forward Primer Reverse Primer Probe	5'-cctaaagcatacgggtcctg-3' 5'-tttcactttgccaaacacca-3' #48 (cat. no. 04688082001)

Table 2-2 Supplementary Table S2.
Antibodies employed for Western blots analysis and their dilution.

Antigen	Antibody	Host	Dilution
EGFR	Santa Cruz, Heidelberg, Germany, #03,	rabbit	1:500
ERBB2	Santa Cruz, #284	rabbit	1:500
ERBB3	Santa Cruz, #285	rabbit	1:500
ERBB4	Santa Cruz, #283	rabbit	1:500
ERBB4	Cell Signaling, Boston, MA, USA, #4795	rabbit	1:1000
ERBB4	Proteintech #19943-1-AP	rabbit	1:1000
Phospho-Tyrosin	Cell Signaling, #9411	mouse	1:2000
p-EGFR (Tyr 1068)	Cell Signaling, #2236	mouse	1:1000
p-EGFR (Tyr 1173)	Santa Cruz, #12351	rabbit	1:500
p-ERBB2 (Tyr 1221/1222)	Cell Signaling, #2243	rabbit	1:1000
p-ERBB2 (Tyr 877)	Cell Signaling, #2242	rabbit	1:1000
p-ERBB3 (Tyr 1289)	Cell Signaling, #4791	rabbit	1:1000
p-ERBB4 (Tyr 1258)	Abcam, Cambridge, UK, #76132	rabbit	1:1000
p-ERBB4 (Tyr 1284)	Cell Signaling, #4757	rabbit	1:1000
p-ERBB4 (Tyr 984)	Cell Signaling, #3790	rabbit	1:1000
p44/42 MAPK	Cell Signaling, #9102	rabbit	1:1000
p-p44/42 MAPK	Cell Signaling, #4370	rabbit	1:1000
AKT	Cell Signaling, #9272	rabbit	1:1000
p-AKT (Ser 473)	Cell Signaling, #4060	rabbit	1:2000
GAPDH	Cell Signaling, #2118	rabbit	1:5000
Donkey α Rabbit	GE Health Care, Munich, Germany, #NA934V	donkey	1:2500
Rabbit α Mouse	Cell Signaling, #7076	rabbit	1:2000
Donkey α Guinea Pig	Fitzgerald, Acton, MA, USA, #43R-ID039HRP	donkey	1:10000

Table 2-3 Supplementary Table S3.
Antibodies employed for immunofluorescence (IF), immunocytochemistry (ICC), and immunohistochemistry (IHC).

Antigen	Antibody	Host	Dilution	Application
EGFR	Cell Signaling, Boston, MA, USA, #4267	rabbit	1:100	ICC
EGFR	Santa Cruz, Heidelberg, Germany, #03,	rabbit	1:200	IF
ERBB2	Cell Signaling, #4290	rabbit	1:800	ICC
ERBB2	Cell Signaling, #2165	rabbit	1:200	IF
ERBB3	Cell Signaling, #12708	rabbit	1:250	ICC
ERBB3	Santa Cruz, #285	rabbit	1:200	IF
ERBB4	Cell Signaling, #4795	rabbit	1:200	ICC
ERBB4	Abcam, Cambridge, UK, #19391	mouse	1:200	IF
ERBB4	Fitzgerald, Acton, MA, USA, #70R-17129	rabbit	1:100	IF
ERBB4	Proteintech, Manchester, UK, #19943-1-AP	rabbit	1:100	IF
ERBB4	Santa Cruz, #8050	mouse	1:100	IF
ERBB4	Santa Cruz, #283	rabbit	1:100	IF
Ki67 (TEC3)	DakoCytomation, Glostrup, Denmark, #M7249	rat	1:200	IHC
anti-rabbit Alexa488	Dianova, Hamburg, Germany, #711-546-152	donkey	1:1000	IF/ICC
anti-rabbit Alexa594	Dianova, # 711-585-152	donkey	1:1000	IF
anti-mouse Alexa488	Thermo Fisher Scientific, Waltham, MA, USA, # A-21202	donkey	1:1000	IF
anti-rat biotinylated	DakoCytomation, #E0468	rabbit	1:200	IHC

2-4 Conclusion and outlook

The present study elucidates a more important function of the RTK receptor ERBB4 than previously assumed. ERBB4 was unambiguously identified in human and murine keratinocytes *in vitro* and *in vivo* and it was shown that EGF can activate ERBB4 *in vitro*. ERBB4 is located in the basal layer of human and murine epidermis and the skin-specific KO of ERBB4 in mice induced the decrease of epidermal thickness and proliferation[161], similar to EGFR KO mice but not as severe[169,265,266]. Although the expression of ERBB4 in the skin has been debated in the literature so far, the epidermal ERBB4 KO phenotype is convincing and indicates an important function of the receptor in the skin. Nevertheless, the molecular mechanisms which influence skin homeostasis and proliferation have to be analyzed in more detail. In contrast, ERBB2 and ERBB3 KO mice showed no epidermal alterations during skin homeostasis, however, the deletion of both non-autonomous receptors influenced tumor progression[154,170]. EGFR also influences skin carcinogenesis[175-178] and ERBB4 is involved in various epithelial cancers[258-262]. In melanoma ERBB4 is often mutated and increases tumor progression[157], dependent on the splice isoform[267]. Also in breast cancer ERBB4 seems to be a two-edged sword, as it can be related to good and poor prognosis depending on the splice isoform [268,269]. Since EGFR, ERBB2 and ERBB3 affect tumorigenesis of the skin, it is reasonable to assume that ERBB4 may also be involved in epidermal carcinogenesis. Therefore, the investigation of the role of ERBB4 during pathological processes in the skin, like wound healing, dermatitis or tumorigenesis would be promising in regard to new treatment strategies in the future.

Chapter 3 Epidermal overexpression of LRIG1 disturbs development and homeostasis in skin by disrupting the ERBB system

3-1 Aim

LRIG1 is an important regulator of SC quiescence in the skin[43,270]. Additionally, the transmembrane protein is involved in the negative feedback loop regulation of ERBB receptor signaling[192,193], which is also indispensable for skin homeostasis and for the control of epidermal SCs[271]. However, the molecular mechanisms of LRIG1 and whether there is an interaction with the ERBB receptor network in the skin are not understood, yet. LRIG1 KO mice develop psoriasis and reveal a similar phenotype to TG mice showing activated ERBB receptor signaling in the skin upon the overexpression of the ligands of EGFR, like TGFA[272] or AREG[221,273]. In addition, LRIG1 was up-regulated in EPGN overexpressing mice, indicating the induction of a feedback mechanism triggered by EGFR activation[274]. These findings point to a correlation of LRIG1 and EGFR also in the skin, as reported in the intestine[219] or in different tumors like glioblastoma[254], bladder cancer[250] or head and neck cancer[251]. ERBB receptors are indispensable for skin development and homeostasis and their dysregulation results in skin pathogenesis like psoriasis[147,148] or NMSC[83,84,154,159,160,170]. An unbalanced epidermal homeostasis can cause more than 3000

skin disorders[275], thus a deeper understanding of the biological processes would be beneficial for better treatment strategies. Therefore, the aim of the following study was to investigate the function of LRIG1 during morphogenesis and homeostasis of the epidermis and of the pilosebaceous unit, in particular with respect to its effect on ERBB receptors, *in vivo*. We generated an inducible, skin-specific gain-of-function mouse model, overexpressing LRIG1 and analyzed the skin morphologically and molecular biologically, with regard to the ERBB signaling network but also to the NOTCH pathway, indispensable for HF development and cell fate specification of adult epidermal SCs[276,277].

3-2 Study

This work is in the process of publication at the Journal of Dermatological Science (submitted July 2019, under review). The following chapters depict the submitted manuscript.

Authors: **C. Hoesl**, J. E. Hundt, C. Rose, R. Wolf, M. R. Schneider, M. Dahlhoff

Author contribution: *Conceptualization:* MD; *Data Curation:* MD; *Formal Analysis:* CH, JEH; *Funding Acquisition:* MD, MRS, RW; *Investigation:* CH, JEH, CR; *Methodology:* CH, JEH; *Project Administration:* MD; *Resources:* MD, MRS; *Supervision:* MD; *Validation:* MD, CH, JEH; *Visualization:* CH; *Writing - Original Draft Preparation:* CH, MD, MRS;

3-2.1 Abstract

Background

More than 3000 skin disorders can develop due to unbalanced epidermal homeostasis. Adult stem cells (SCs), residing in different niches of the skin, are crucial to maintain its structural and functional integrity. The transmembrane protein leucine-rich repeats and immunoglobulin-like domains 1 (LRIG1) is known to promote SC quiescence in the isthmus of the hair follicle and to regulate receptor tyrosine kinases like the ERBB receptor family. ERBBs are pivotal during skin development and homeostasis, regulating proliferation, differentiation or migration, but the interplay of LRIG1 and ERBB receptors in the skin is not fully understood yet.

Objective

The aim of this study was to analyze the impact of LRIG1 on ERBB receptors in the skin during development and homeostasis.

Methods

We generated an inducible, skin-specific LRIG1 transgenic mouse model using the Tet-Off system with the keratin 5 promoter and investigated the impact of LRIG1 on skin development and homeostasis, especially its influence on the ERBB signaling network.

Results

LRIG1 overexpression during embryogenesis led to postnatal lethality accompanied by altered skin differentiation and hair follicle development, influencing the ERBB system. LRIG1 overexpression after birth caused a severe alopecia phenotype and profoundly impaired ERBB signaling. Our results indicated an additional activation of NOTCH signaling and epidermal SCs in LRIG1 transgenic mice.

Conclusion

The present study shows a remarkable effect of LRIG1 on ERBB receptor signaling in the skin, affecting the hair follicle cycle and epidermal SCs.

3-2.2 Introduction

Skin disorders are among the most common causes of human illness[275,278]. The skin is a highly complex organ and proper differentiation during development and homeostasis is indispensable. The continuous self-renewal of the interfollicular epidermis (IFE) and the hair follicles (HFs), and regeneration after wounding, are ensured by adult epidermal stem cells (SCs)[3,279]. SCs reside in distinct niches, each one representing appropriate microenvironments to maintain their function and regulate the balance between SCs, slowly differentiating progenitor cells (PCs) and neighboring cells[49,50]. In the isthmus of HFs, adjacent to the infundibulum and sebaceous gland (SG), a niche, which comprises SCs with multipotent capacity, is located [44,46]. These cells can give rise to the IFE and SG during homeostasis and are characterized by the expression of leucine-rich repeats and immunoglobulin-like domains 1 (LRIG1)[43]. In humans, LRIG1 is expressed in both IFE and HF[210], and promotes SC quiescence[270]. LRIG1-deficient mice developed a psoriatic, hyperplastic phenotype also indicating the important function of LRIG1 in the skin[221].

Furthermore, LRIG1 marks SCs in the intestine[219] and stomach[220]. LRIG1 is one of three members of the transmembrane protein family (LRIG1-3) which has additionally attracted attention due to their impact on receptor tyrosine kinases (RTKs) such as the epidermal growth factor receptor (EGFR, ERBB1, HER1) and the other members of the ERBB receptor family (ERBB2-4, HER2-4)[99,101]. LRIGs are involved in feedback loop regulation of RTKs in different ways[223,224]. While LRIG1 promotes ERBB degradation[188,192,193], LRIG3 stabilizes ERBB receptors[224] and LRIG2 activates EGFR[227]. ERBBs are widely expressed in skin and are involved in crucial processes during development, homeostasis and tumorigenesis[85]. The skin-specific deletion of ERBB2[170] and ERBB3[154] resulted in no obvious phenotype in mice. However, the knockout (KO) of EGFR led to an impaired epithelial development and a shortened lifespan[169,266], and the deletion of ERBB4 caused decreased epidermal thickness and proliferation[161]. Moreover, epidermal overexpression of the EGFR ligand epigen led to receptor activation and increased LRIG1 expression[274], showing the correlation between LRIG1 and EGFR also in the skin. Since EGFR inhibits terminal differentiation and promotes proliferation of epidermal PCs[28], LRIG1 may be an important feedback-regulator of ERBBs in the epidermis, but this has not been shown yet. We addressed this hypothesis by overexpressing LRIG1 skin-specifically in mice using the Tet-Off system with the keratin 5 (KRT5) promoter. This study reveals the effects of LRIG1 excess in skin development and homeostasis in the IFE, HFs and SGs. LRIG1 can be shed and act in an autocrine but also non-cell-autonomous manner[218]. In particular, we focused on the influence on the ERBB system and neurogenic locus notch homolog protein (NOTCH) signaling, both crucial for epidermal and HF cell fate decisions[3,28,277]. Our present data indicate that LRIG1 has crucial impact on epidermal development and homeostasis by regulating ERBB receptors and NOTCH signaling and thereby influencing epidermal SC compartments.

3-2.3 Materials and methods

3-2.3.1 Mice

All mouse experiments were approved by the Committee on Animal Health and Care of the local governmental body of the state of Upper Bavaria (Regierung von Oberbayern), Germany, and were performed in strict compliance with the European Communities Council Directive (86/609/EEC) recommendations for the care and use of laboratory

animals. Mice were maintained under specific-pathogen-free conditions and had access to water and standard rodent diet (V1534; Ssniff, Soest, Germany) *ad libitum*. Pronuclear microinjection into zygotes of C57BL/6N mice was used to generate two independent mouse lines overexpressing LRIG1 skin-specifically. Therefore, *Lrig1* cDNA was cloned into the pTRE-tight vector (Clontech). We used two pTRE-tight-LRIG1-TG mice from two different founders to mate with the previously described keratin 5 (KRT5) promoter driver mouse line (KRT5-tTA), expressing the tetracycline-regulated transcriptional transactivator (tTA) under the control of the KRT5 promoter[280]. Thus, we obtained two independent LRIG1-TG mouse lines expressing exogenous LRIG1 skin-specifically. Both mouse lines showed the same phenotype, all experiments depicted in this manuscript were done with one line, referring to as LRIG1-TG (LRIG1-TG: TRE-LRIG1;KRT5-tTA, Control (Co): wildtype, KRT5-tTA, TRE-LRIG1). All mouse strains were maintained in the C57BL/6N background. Dissection of mice was done at indicated time points and skin samples were snap frozen or embedded in paraffin. Male and female mice were used in this study and did not show sex-bias differences (P0: sex not known; P18,21,28,45: male, P60, six months: female; molecular biological analysis was done with female mice only). To inhibit LRIG1-TG expression during embryogenesis, all pregnant mice received 3 mg/mL doxycycline (Dox) (Beladox 500 mg/g, bela-pharm (Lehnecke 793-588), Schortens, Germany) in the drinking water together with 5% sucrose (Sigma, Taufkirchen, Germany) until they gave birth.

3-2.3.2 Toluidine blue assay

To investigate the outside-in barrier, mice were dissected at indicated times and dehydrated and subsequently rehydrated in 25, 50, 75 and 100% methanol in phosphate-buffered saline (PBS), stained in 0.1% toluidine blue in PBS, and washed with PBS.

3-2.3.3 Histology and immunohistochemistry

Skin samples were either embedded in paraffin or snap frozen on dry ice and embedded in Tissue-Tek® O.C.T.™ Compound (Sakura Finetek, Alphen aan den Rijn, Netherlands). For histological investigations Giemsa or H&E stainings of paraffin sections were used.

Epidermal thickness and sebaceous gland area were measured on 60 visual fields over a length of 39.2 mm, thickness was determined at 180 constantly distributed measuring points. Pictures were taken with a 200x magnification lens using a Leica DFC425C digital camera (Leica Microsystems, Wetzlar, Germany) and the LAS software version 3.8.0 (Leica Microsystems) was used for analysis. HFs of controls and LRIG1-TG mice on indicated days were evaluated according to the HF morphogenesis and cycling stages as described elsewhere[31,281]. The total number (%) of HFs in distinct HF stages was counted. HF density was determined on 19 (HF density at P0) or 37 (HF density at two months) visual fields (12.4 mm or 24.1 mm epidermis). The mean number of HFs per visual field is presented. Only HFs that have contact to the IFE were considered. Paraffin- or cryo-sections were used for immunofluorescence or immunohistochemical stainings as described previously[161]. A 10 mM sodium citrate buffer (pH 6.0) was used as antigen retrieval for all paraffin embedded skin samples. All used primary and secondary antibodies and their dilution are listed in 3-3 Supplementary material, Table 3-1.

3-2.3.4 Western blot analysis

For Western blot analysis Laemmli-extraction-buffer was used to extract proteins from skin samples and a bicinchoninic acid protein assay was used to estimate protein concentrations. 20 µg of total protein were separated by SDS-PAGE, transferred to PVDF membranes (Millipore, Schwalbach, Germany) and immunoblotted against antibodies as indicated. Membranes were stripped with a stripping buffer (2% SDS, 62.5 mM Tris/HCl, pH 6.7 and 100 mM ß-mercaptoethanol) for 40 min at 70 °C to detect reference proteins and to analyze the phosphorylated state as well as the total protein. Densitometrical analysis was done using ImageJ (http://rsb.info.nih.gov/ij). All primary and secondary antibodies and their dilutions are listed in 3-3 Supplementary material, Table 3-1.

3-2.3.5 Quantitative RT-PCR

For RNA analysis, total RNA was isolated from back skin with TRIZOL reagent (Invitrogen, Darmstadt, Germany) and 3 µg RNA were reverse-transcribed in a final volume of 30 µL using RevertAid Reverse Transcriptase (Thermo Scientific, Schwerte, Germany) according to the manufacturer's instructions. The StepOnePlus™ Real-Time PCR System (Applied Biosystems, Waltham, USA) and the PowerUp™ SYBR® Green

Master Mix (Applied Biosystems, Waltham, Massachusetts, USA) were used for quantitative real-time PCR (qPCR) according to the manufacturer's instructions. 2 µL of cDNA in final reaction volume of 10 µl were used and the final primer concentration was 0.5 µM. Cycle conditions were 95 °C for 2 min followed by 40 cycles of 95 °C for 15 s, 60 °C for 15 s, and 72 °C for 1 min. For Quantification the threshold cycle (C_T) number was used. We performed no-template control and no-RT control assays, which produced negligible signals with C_T values that were greater than 35. Experiments were performed in duplicates or triplicates for each sample. Primers used for qPCR are listed in Table S2. Transcript copy numbers were normalized to ribosomal protein L30 (*Rpl30*).

3-2.3.6 Statistical analysis

Quantitative RT-PCR values were related to the mean value of the control group and compared by Student's *t*-test (Prism; GraphPad Software, San Diego, CA), data are presented as box plots with medians. Hair follicle cycle data were analyzed by Mann-Whitney *U*-test and the remaining data were analyzed with Student's *t*-test. Data are presented as means±standard error of the mean (SEM) unless otherwise indicated. Group differences were considered to be statistically significant if $P<0.05$.

3-2.4 Results

3-2.4.1 Prenatal LRIG1 overexpression in the skin results in disturbed differentiation and neonatal lethality

To investigate the function of LRIG1 during skin development and homeostasis we generated a skin-specific inducible, Keratin 5 (KRT5) promoter-driven transgenic (TG) mouse line using the Tet-Off system. Double transgenic KRT5-tTA;LRIG1 mice (LRIG1-TG) skin-specifically overexpress LRIG1 in the basal cells of the interfollicular epidermis and pilosebaceous unit (3-3 Supplementary material, Figure 3-7a,f). LRIG1-TG mice died within one week after birth. At embryonic stages, the distribution of genotypes corresponded to the expected Mendelian ratio (3-3 Supplementary material, Figure 3-7b). Newborn LRIG1-TG mice showed open eyes and short, thick whiskers (Figure 3-1a). Skin

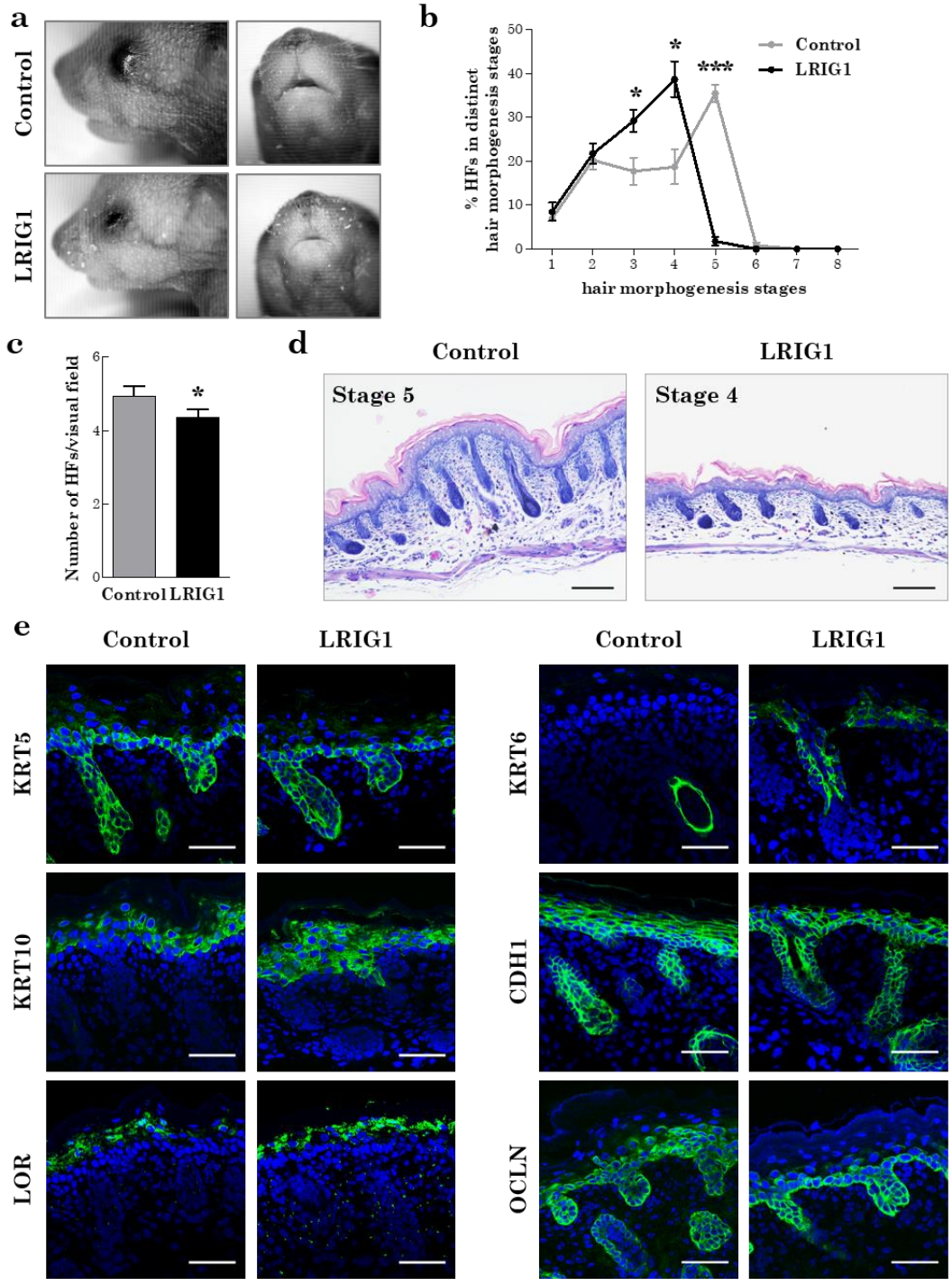

Figure 3-1 LRIG1 overexpression was neonatal lethal and resulted in impaired HF morphogenesis and epidermal differentiation.
(a) Representative pictures of an eye and whiskers of a newborn LRIG1-TG mouse and a control. **(b)** Percentage of HFs found in the different hair morphogenesis stages at P0. **(c)** HF density in LRIG1-TG and control mice. **(d)** Giemsa staining of back skin of LRIG1-TG and control mice at P0 in indicated morphogenesis stages. Scale bars represent 100 µm. **(e)** Immunofluorescence stainings against keratin 5, 10 and 6 (KRT5, KRT10, KRT6), loricrin (LOR), E-Cadherin (CDH1) and occludin (OCLN) (green) on back skin of LRIG1-TG and control mice at P0. Scale bars represent 50 µm. Data in **(b)** and **(c)** are means±SEM and were analyzed by Mann-Whitney *U*-test (n=4). **P*<0.05, ****P*<0.001.

permeability was analyzed by toluidine blue staining. The outside-in barrier was not affected in LRIG1-TG mice at embryonic day E17.5, E18.5 or at birth, additionally we found no alteration in the bodyweight (3-3 Supplementary material, Figure 3-7c,d).

Morphometric studies revealed no differences in epidermal thickness or proliferation of back skin of newborn LRIG1-TG mice and controls (3-3 Supplementary material, Figure 3-7e,f,g). Besides orthologous cornification, the histology of the TG skin appeared normal. However, HF morphogenesis was severely impaired and HF density was significantly reduced in LRIG1-TG mice (Figure 3-1c). While control HFs were mainly in morphogenesis stage 5, TG HFs were still in stage 4 at P0 (Figure 3-1b,d). Additionally, LRIG1-TG mice showed altered differentiation and ectopic expression of keratin 6 (KRT6) in the IFE. Immunofluorescence also revealed an increased expression of keratin 10 (KRT10), with no obvious differences in KRT5, loricrin (LOR) or E-cadherin (CDH1) (Figure 3-1e). However, olccudin (OCLN) was mainly expressed in the basal layer of the IFE in newborn LRIG1-TG mice, while controls revealed OCLN expression also in upper, more differentiated epidermal layers (Figure 3-1e). These findings point to a delayed HF morphogenesis and a disturbed differentiation of the skin due to LRIG1 overexpression, leading probably to postnatal lethality.

3-2.4.2 ERBB2 activation is decreased in newborn LRIG1-TG mice

To determine whether LRIG1 affects ERBB signaling in skin, receptor expression was analyzed by immunofluorescence and Western blots. Regarding ERBB localization, EGFR and ERBB3 were expressed throughout the IFE, whereas ERBB2 expression was present in more differentiated epidermal layers in TG and control animals (Figure 3-2a). Moreover, ERBB2 phosphorylation and ERBB3 expression were decreased upon LRIG1 overexpression, ERBB2 was also less activated, but the EGFR level was unchanged (Figure 3-2b,c). However, Western blot analysis of ERBB downstream targets revealed a decreased activation of RAC-alpha serine/threonine-protein kinase (AKT) but no influence on mitogen-activated protein kinase 1/2 (MAPK1/2) (Figure 3-2b,c). In addition, we investigated the expression of NOTCH1 receptor due to its role in embryonic development, but found no differences (3-3 Supplementary material, Figure 3-7f). In summary, LRIG1 overexpression induces a decrease of ERBB2 activation and ERBB3 expression in neonatal skin, but shows no effect on proliferation or NOTCH1 signaling.

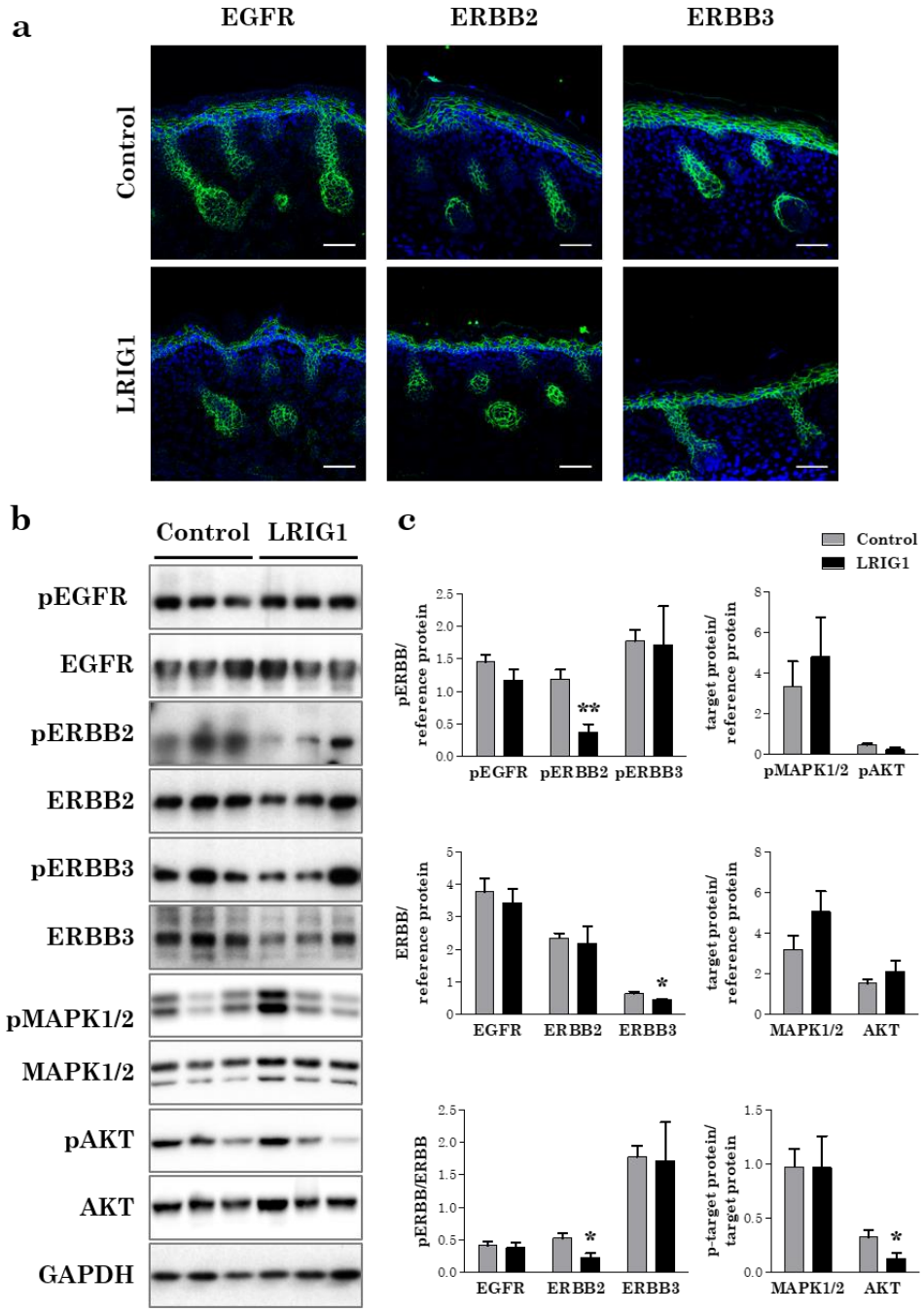

Figure 3-2 ERBB2 activation was decreased in newborn LRIG1-TG mice.
(a) EGFR, ERBB2, and ERBB3 expression (green) by immunofluoresence stainings on back skin of LRIG1-TG and control mice at P0. Scale bars represent 50 μm. **(b)** Western blot and **(c)** densitometrical analysis of phosphorylated and total ERBB receptors (ERBB1-3), MAPK1/2 and AKT. GAPDH was used as reference protein. Data are means+SEM and were analyzed by Student's *t*-test (n=6). **P*<0.05, ***P*<0.01.

3-2.4.3 Postnatal induced LRIG1 overexpression leads to alopecia and hyperproliferation

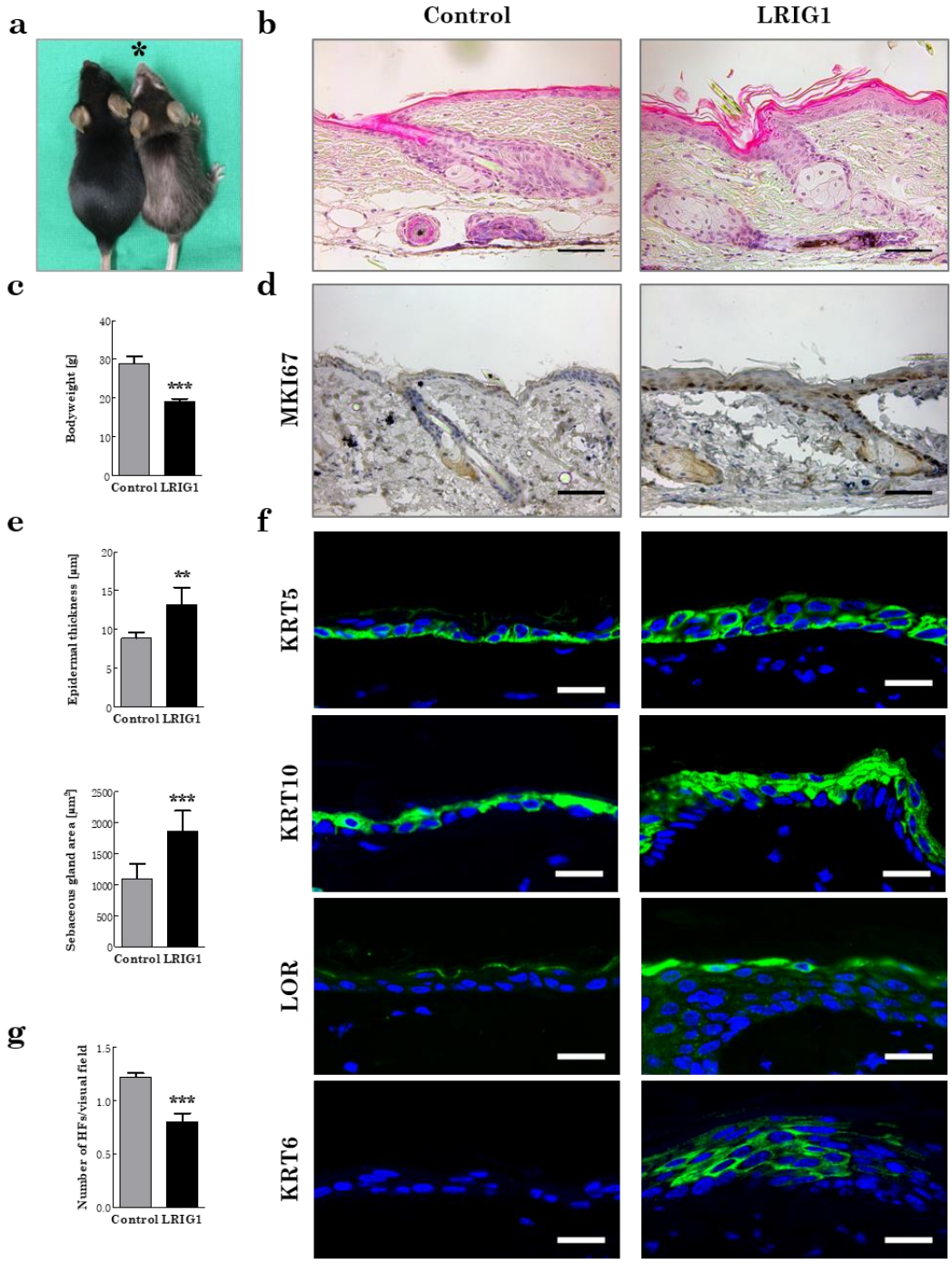

Figure 3-3 Postnatal induced LRIG1 overexpression caused alopecia and hyperplasia.
(a) Picture of a three-month-old LRIG1-TG mouse (*) showing alopecia and a control mouse. **(b)** H&E staining of back skin of six-month-old LRIG1-TG and control mice. **(c)** Body weight of LRIG1-TG mice and controls. **(d)** MKI67-immunohistochemistry on back skin of a six-months-old LRIG1-TG and control mouse. **(e)** Epidermal thickness and area of sebaceous glands (SGs) of six-month-old LRIG1-TG mice. **(f)** Immunofluorescence on back skin of a LRIG1-TG and control mouse for indicated differentiation markers (green). Cell nuclei are stained with DAPI (blue). **(g)** HF density in two-month-old LRIG1-TG and control mice. All data are means+SEM and were analyzed by Student's *t*-test or Mann-Whitney *U*-test (n=4). $^{**}P<0.01$, $^{***}P<0.001$. Scale bars in **(b)** and **(d)** represent 50 µm, **(f)** 20 µm.

To evaluate the impact of LRIG1 in skin homeostasis, we suppressed LRIG1 overexpression until birth by the application of doxycycline to pregnant mice. Accordingly, we obtained postnatal, skin-specifically LRIG1 overexpressing TG mice (3-3 Supplementary material, Figure 3-7h,i) in a Mendelian ratio. Phenotypical studies revealed that LRIG1-TG mice started to lose their hair coat at the age of ten weeks and developed alopecia later on. After six months, TG animals showed a reduced bodyweight and developed hyperkeratosis, malformed HFs, significantly decreased in their density, hyperplasia of SGs and IFE with increased proliferation (Figure 3-3a-e,g). The enlarged SGs resulted in significantly increased sebum secretion in adult mice (data not shown). Regarding epidermal differentiation, LRIG1-TG mice showed an increase in KRT10 and LOR expression (Figure 3-3f). Furthermore, ectopic KRT6 expression occurred in the IFE of TG mice like in newborn animals, showing the disturbed epidermal balance between differentiation and proliferation during homeostasis (Figure 3-3f). These data demonstrate a crucial impact of LRIG1 overexpression on skin homeostasis. LRIG1-TG mice show alopecia and hyperplasia of IFE and SGs, which is consistent with hyperproliferation and altered differentiation.

3-2.4.4 Expression and activation of EGFR is decreased due to epidermal LRIG1 overexpression

As LRIG1 overexpression caused a severe skin phenotype, we investigated the impact on the ERBB network in skin samples of six-month-old mice by Western blot analysis. EGFR, ERBB2 and phosphorylated EGFR were significantly reduced in LRIG1-TG mice, resulting in decreased EGFR activation (Figure 3-4a,b). The decrease of MAPK1/2 and AKT expression and their phosphorylated forms are in accordance with the downregulation of ERBB signaling, but no differences in MAPK1/2 or AKT activation were detected (Figure 3-4a,b). Evaluation of the effect of LRIG1 overexpression on ERBB signaling in adult mice revealed a significant downregulation of the EGFR/ERBB2 pathway.

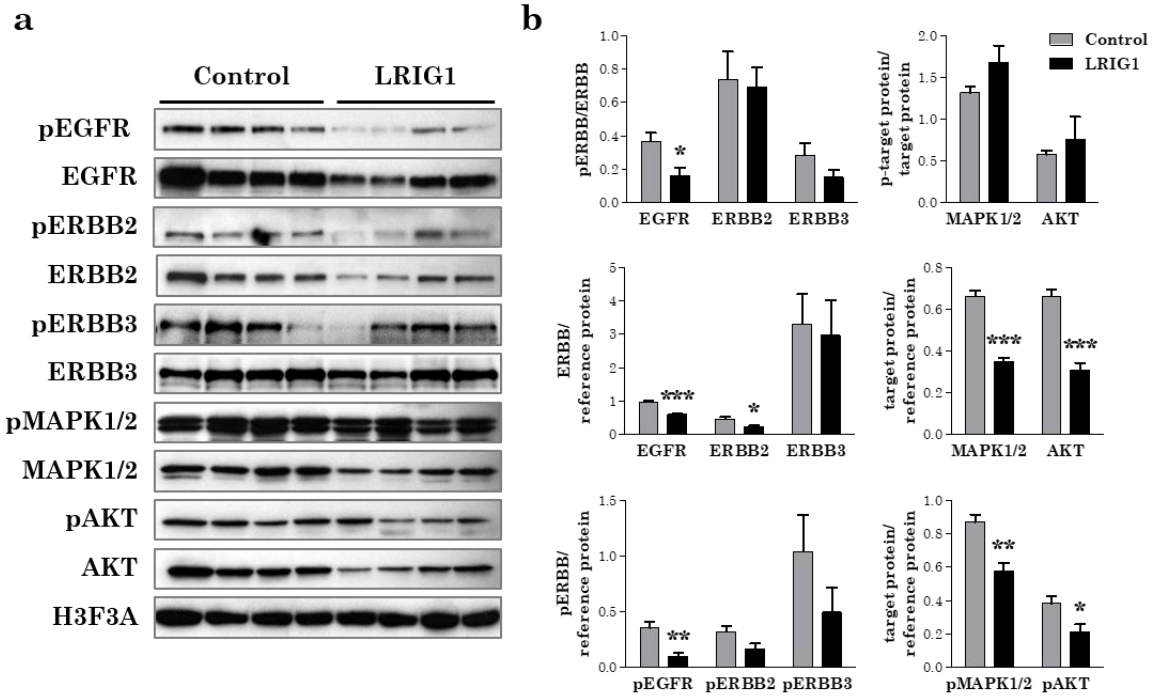

Figure 3-4 EGFR expression and activation were decreased in adult LRIG1-TG skin.
(a) Western blot and **(b)** densitometrical analysis of phosphorylated and total ERBB receptors (ERBB1-3) and their downstream targets MAPK1/2 and AKT in skin samples of six-month-old LRIG1-TG and control mice. H3F3A was used as reference protein. Data are means+SEM and were analyzed by Student's t-test (n=4). **P*<0.05, ***P*<0.01, ****P*<0.001.

3-2.4.5 LRIG1 overexpression disturbs the hair follicle cycle

LRIG1-TG mice showed severe abnormalities in the HF cycle. While the first catagen stage at day P18 seemed to be unaffected, LRIG1-TG mice revealed an accelerated transition to anagen at P21 (Figure 3-5). Control HFs were mainly in telogen phase whereas HFs of LRIG1-TG mice showed predominantly anagen I-II morphology. However, at the end of the first growth phase (P28), HFs of both groups remained in anagen stages V or VI. Nevertheless, TG animals developed strongly malformed HFs. Further, at P45, LRIG1-TG mice revealed a more progressed HF cycle, similar to the first telogen to anagen transition (Figure 3-5). As the HF cycle proceeded, LRIG1-TG mice showed a broad distribution of anagen HFs while control HFs regenerated more slowly. In conclusion, HF cycle analysis revealed a severe impairment of telogen-anagen transition in LRIG1-TG mice compare to controls.

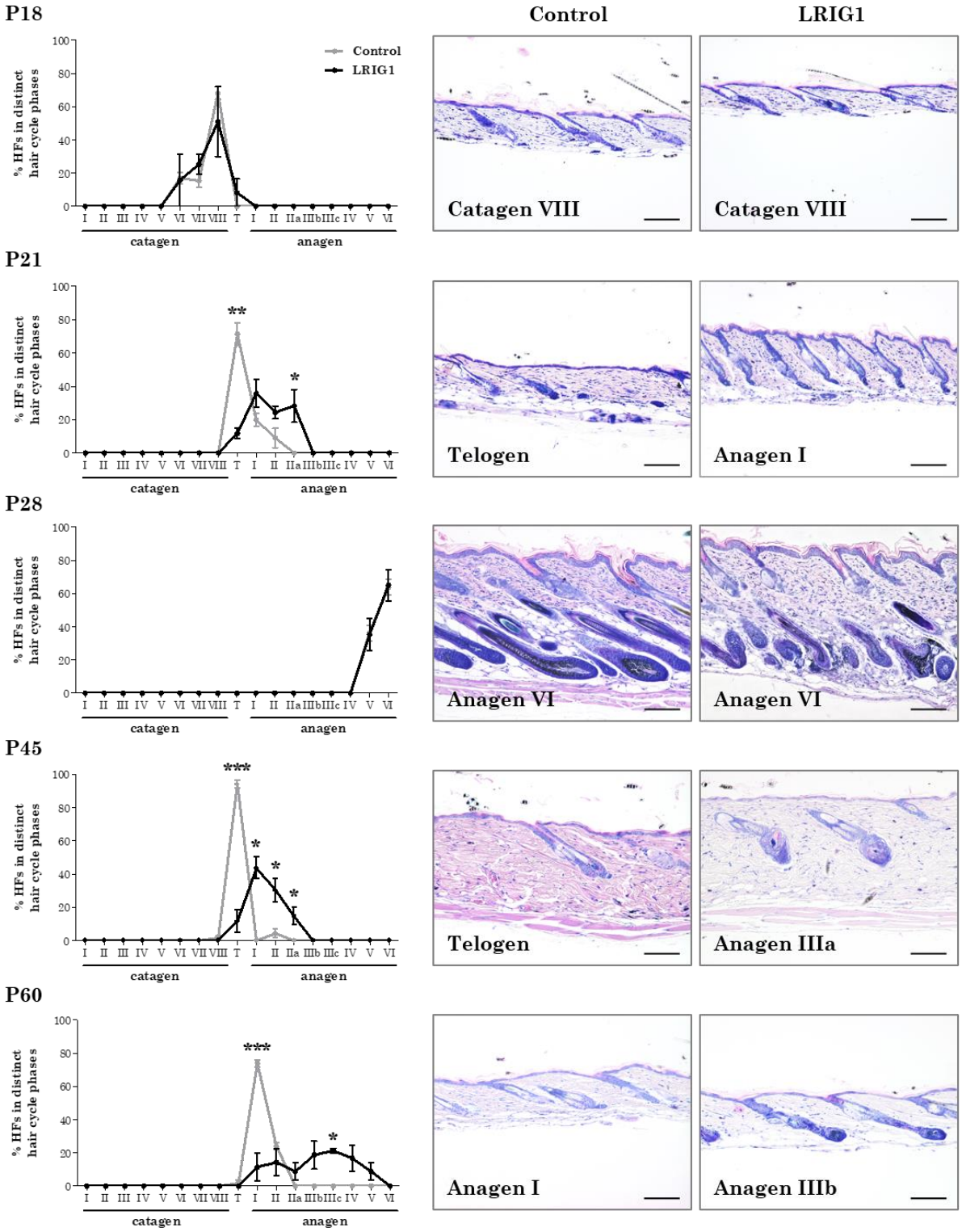

Figure 3-5 The hair follicle cycle of LRIG1-TG mice was severely impaired.
Quantitative histomorphometry of Giemsa-stained back skin of LRIG1-TG and control mice at indicated postnatal days with percentage of HFs found in the different HF stages. Data are means±SEM and were analyzed by Mann-Whitney *U*-test (n=4-6). **P*<0.05, ***P*<0.01, ****P*<0.001. Scale bars represent 100 µm.

3-2.4.6 NOTCH signaling and SC compartments is activated by LRIG1 overexpression at alopecia onset

Ten weeks after birth LRIG1-TG mice start to lose their hair. Therefore, we used skin samples of LRIG1-TG and control animals at P60 to analyze the early phenotypical and cell biological changes and to address the question if LRIG1 also has PC function outside its niche. First, the ERBB system, important for terminal differentiation and proliferation of PCs in the skin[28], and NOTCH1 signaling, crucial in cell fate decision[3,276,277], were studied by Western blot analysis. Contrary to the results of six-month-old animals, the expression of EGFR and ERBB3 was increased but their activation was significantly decreased at P60 (Figure 3-6a,b). Furthermore, activation of ERBB2 and the expression of its phosphorylated form were highly increased in LRIG1-TG mice. Consistent with EGFR/ERBB3 downregulation, MAPK1/2 expression and activation was decreased (Figure 3-6a,b). Investigations of NOTCH1 signaling revealed increase of cleaved NOTCH1 receptor and activation of its downstream targets like recombining binding protein suppressor of hairless (RBPJ), mastermind-like protein 1 (MAML1), Myc proto-oncogene protein (MYC) and transcription factor HES-1 (HES1). A disintegrin and metalloproteinase domain-containing protein 17 (ADAM17), involved in the proteolytic cleavage and activation of NOTCH1[282], and G1/S-specific cyclin-D3 (CCND3), an important regulator of the cell-cycle during G_1/S transition[283], were not affected (Figure 3-6c,d). Additionally, proliferation was highly enhanced in LRIG1-TG animals (Figure 3-6c,d). Further, we used qPCR to investigate epidermal SC marker transcripts in the back skin of LRIG1-TG and control mice at P60 (Figure 3-6e). Our data argue for an increase of SC markers of the bulge and SGs. *Blimp1*, defining a progenitor population in SGs[45], like *Plet1/MTS24*[46], were increased in LRIG1-TG mice compared to control littermates. Transcripts of the bulge SC markers *Cd34*[35] and *Lhx2*[284] were also increased while the transcripts *Lgr6*[285], *Nfatc1*[286] and *Lgr5*[287] revealed no differences (Figure 3-6e). Analysis of the early onset of alopecia in LRIG1-TG mice and controls indicated an influence of LRIG1 on ERBB and NOTCH1 signaling, both involved in PC regulation. In addition, LRIG1 overexpression led to an increase of SG and bulge SC markers pointing to an activation of both SC pools.

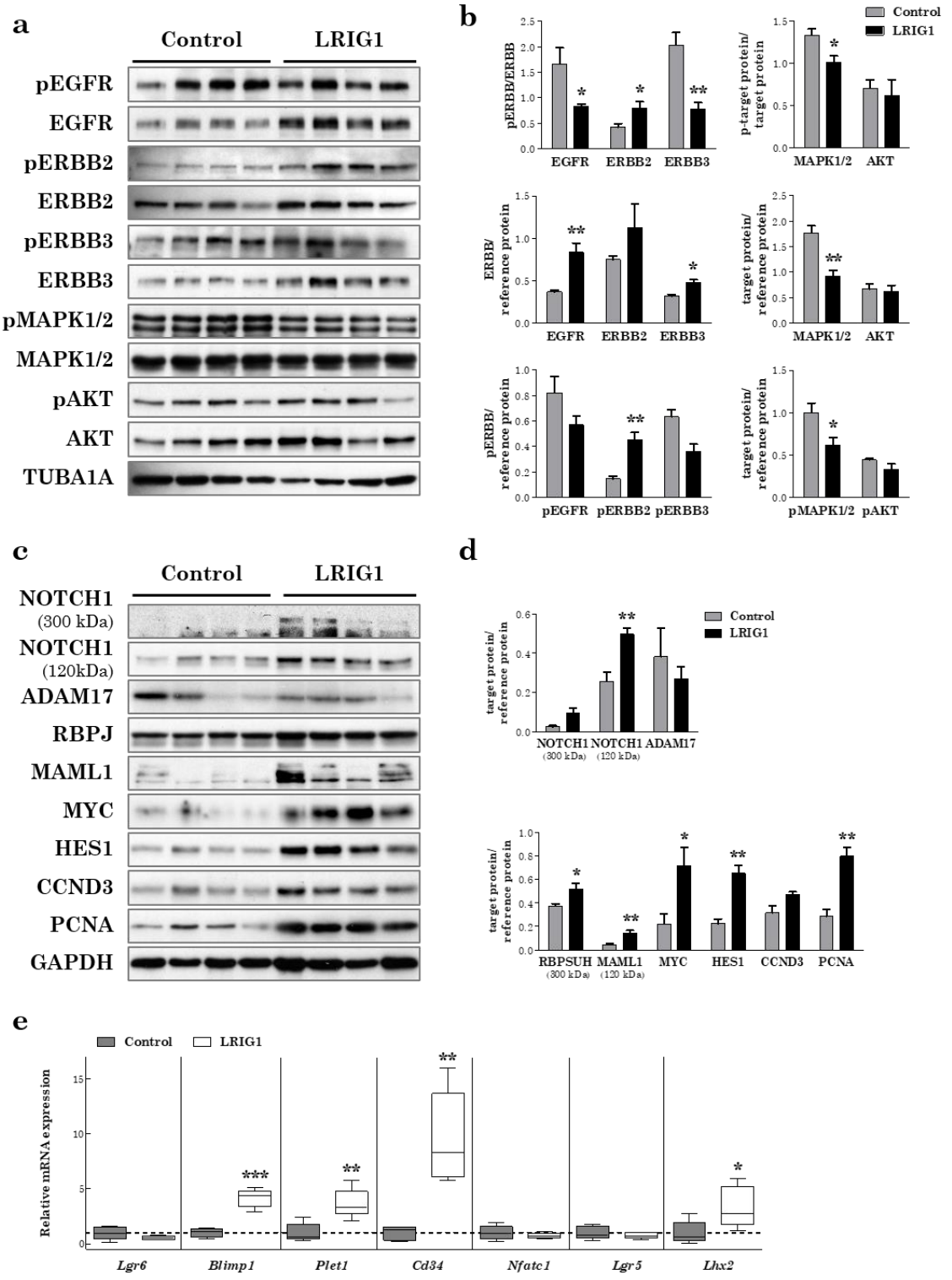

Figure 3-6 LRIG1-TG mice showed altered ERBB and NOTCH signaling at the onset of alopecia. Western blot and densitometrical analysis of **(a,b)** phosphorylated and total ERBB receptors (ERBB1-3), MAPK1/2 and AKT and **(c,d)** NOTCH1 receptor, ADAM17 and activated NOTCH1 targets as indicated in skin samples of LRIG1-TG and control mice at P60. TUBA1A or GAPDH were used as reference protein. Data are means+SEM and were analyzed by Student's *t*-test (n=4). **(e)** Relative expression of indicated skin stem cell marker transcripts in the back skin of LRIG1-TG and control mice at P60. Transcript copy numbers were normalized to *Rpl30*. Data are presented as box plots with medians and were analyzed by Student's *t*-test (n=5). **P*<0.05, ***P*<0.01, ****P*<0.001.

3-2.5 **Discussion**

A balanced proliferation and differentiation are crucial during skin development and homeostasis. The ERBB receptor signaling has important functions in these processes and feedback mechanisms are indispensable for its proper control[184]. LRIG proteins are involved in ERBB feedback loop modulation[192,193,224] and are often dysregulated in various diseases and thus are suitable prognostic markers [209]. Little is known about the function of LRIGs in the skin. LRIG1 expression is located to PCs in the isthmus of HFs[43] and its loss resulted in a psoriasiform epidermal hyperplasia[221]. The underlying molecular mechanisms of LRIG1 activity remain still unclear until today. Therefore, we generated a skin-specific gain-of-function mouse model and investigated the influence of LRIG1 overexpression on skin and the ERBB system during development and homeostasis. Overexpression of LRIG1 during morphogenesis resulted in postnatal lethality. The phenotype of LRIG1-TG mice at P0 was similar to that of EGFR KO mice with open eyes and abnormal whiskers[169]. The delayed HF morphogenesis and the decreased HF density in LRIG1-TG mice together with the orthologue cornification and the altered differentiation suggest mortality due to a disturbed skin barrier[288]. However, the toluidine blue assay revealed no differences in the outside-in barrier, pointing to an effect on the inside-out barrier. In addition, in controls OCLN was expressed in several epidermal layers, whereas in LRIG1-TG mice it was mainly found in the basal layer. These findings indicate failure in the formation of tight junctions during epidermal development, also important for an intact inside-out barrier[289,290]. Newborn LRIG1-TG animals presented changes in ERBB receptor signaling. Although expression of all receptors and their phosphorylated forms tended to be downregulated upon LRIG1 overexpression, only the decrease in ERBB3 and phosphorylated ERBB2 expression were significant. Beside the decreased activation of ERBB2 we found a reduced activation of its downstream target AKT in LRIG1-TG animals. ERBB2 and ERBB3 preferably form heterodimers and induce intracellular signaling which seems to be decreased in the skin of LRIG1-TG mice[291]. Our model suggests an important role of LRIG1 on ERBB signaling during skin development, but ERBB receptors play different roles in epidermal homeostasis and development[169,292,293]. To analyze the function of LRIG1 during homeostasis in more detail we performed a long-term study: we inhibited LRIG1 overexpression until birth by doxycycline treatment und obtained TG animals in a Mendelian ratio. Notably, adult LRIG1-TG mice developed alopecia similar to EGFR KO mice[168], showed hyperplasia of the IFE and SGs and an altered epidermal differentiation resembling newborn TG mice.

Additionally, LRIG1-TG epidermis showed a higher proliferation rate and a decreased activation of EGFR together with decreased expression of EGFR and ERBB2. Inhibition of EGFR or ERBB2 impairs new hair growth[293] and keratinocyte differentiation[294], and both effects were detected in LRIG1-TG mice. Down-regulation of ERBB receptors was in line with the decreased phosphorylation of their main downstream targets MAPK1/2 and AKT. *In vitro* overexpression of LRIG1 seems to induce EGFR downregulation as previously reported[192,193,224]. Otherwise, the loss of LRIG1 *in vivo* in the murine intestine resulted in an upregulation of ERBB1-3[219]. Investigating the skin of LRIG1-TG mice at the early onset of alopecia revealed an even more prominent effect on ERBBs. While the activation of EGFR and ERBB3 was significantly decreased, the activation of ERBB2 was increased, which can contribute to pathological processes[295] and is often involved in cancer[85,170]. The reduced activation of MAPK1/2 supports these results. The altered ERBB signaling due to LRIG1 overexpression can be the reason for the disturbed HF cycle. EGFR deficient mice also showed a disturbed transition from anagen to catagen stage during the HF cycle, causing loss of hair and inflammation[166,168]. Nevertheless, to elucidate this question, further studies of HF stages are necessary. LRIG1 is known to promote quiescence in SCs[43] and NOTCH1, expressed in the IFE and SG (Okuyama et al. 2004, Rangarajan et al. 2001), controls cell fate decision and therefore epidermal SCs by a juxtacrine cellular signaling pathway[3,276,277]. The loss of NOTCH results in disturbed epidermal differentiation (Rangarajan et al. 2001). At the onset of alopecia, LRIG1 overexpression led to an increase of activated NOTCH1 together with several downstream targets like MYC. LRIG1 and MYC act in an autoregulatory loop[296]. MYC activation induces epidermal differentiation[297] and MYC-positive PCs induce hyperplasia of IFE and SG[274,298]. This was also observed in TG mice, confirming the role of LRIG1 in PCs. Analyzing the transcripts of specific SC markers of bulge and SG, *Cd34* and *Lhx2* or *Blimp1* and *Plet1* respectively, revealed an activation of both pools, which may point to a general impact of LRIG1 on SCs outside its original niche in the isthmus. In conclusion, our gain-of-function model revealed a remarkable impact of LRIG1 on epidermal development and homeostasis disrupting ERBB signaling and affecting epidermal SCs. Prenatal overexpression of LRIG1 led to postnatal lethality, probably due to a disturbed epidermal barrier. However, during homeostasis, LRIG1 overexpression decreased EGFR activation and caused alopecia with epidermal hyperplasia and altered the HF cycle.

3-3 Supplementary material

In the following all supplementary figures and tables of the manuscript "Epidermal overexpression of LRIG1 disturbs development and homeostasis in skin by disrupting the ERBB system" are depicted.

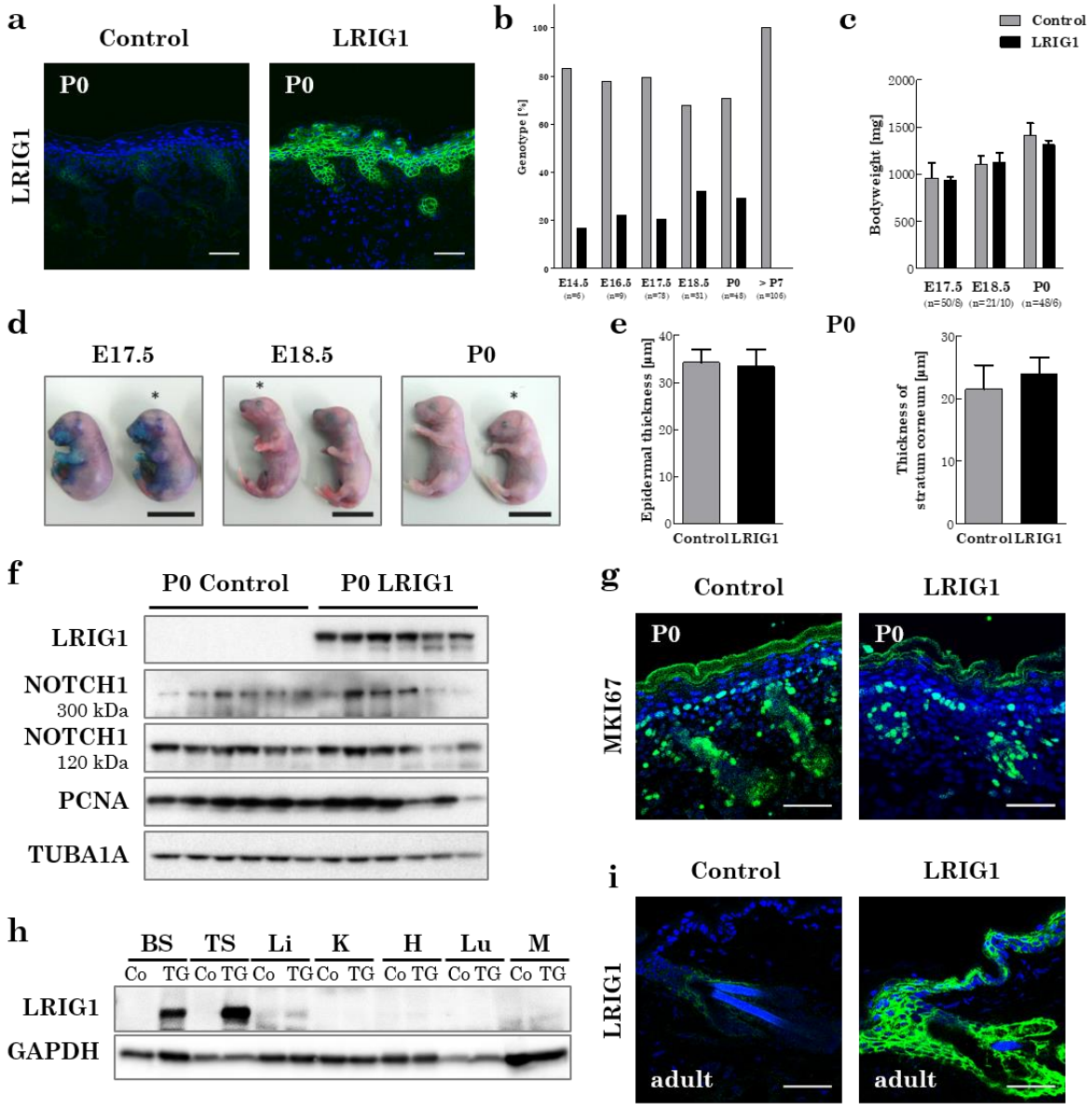

Figure 3-7 Figure S1. The LRIG1-TG mouse model during development and homeostasis. Immunofluorescence staining against **(a), (i)** LRIG1 and **(g)** MKI67 (green) on back skin of LRIG1-TG and control mice at indicated times. Cell nuclei are stained with DAPI (blue). **(b)** Genotype distribution at indicated embryonic stages. Control: wildtype, KRT5-tTA, TRE-LRIG1; LRIG1: TRE-LRIG1;KRT5-tTA. **(c)** Bodyweight of LRIG1-TG and control mice at indicated times. **(d)** Toluidine blue staining of murine embryos at E17.5, 18.5 and P0. Asterisks (*) indicate LRIG1-TG mice. **(e)** Thickness of the epidermis and the *stratum corneum* of LRIG1-TG and control mice at P0. **(f)** Western blot analysis of indicated targets. TUBA1A was used as reference protein. **(h)** Western blot analysis of LRIG1 in different organs of adult LRIG1-TG mice and controls (Co). BS, back skin; TS, tail skin; Li, liver; K, kidney; H, heart; Lu, lung; M, muscle. GAPDH was used as reference protein. Scale bars in **(a)** and **(g)** represent 50 µm, in **(d)** 1 cm, and in **(i)** 20 µm.

Table 3-1 Table S1.
Antibodies employed for Western blot (WB) analysis, immunofluorescence (IF) and immunohistochemistry (IHC) with their dilution.

Antigen	Antibody	App.	Host	Dilution
LRIG1	R&D Systems, Minneapolis, MN, USA, #AF3688	WB/IF	goat	1:1000/1:200
pEGFR (Tyr 1068)	Cell Signaling, Boston, MA, USA, #3777	WB	rabbit	1:1000
EGFR	Santa Cruz, Heidelberg, Germany, #03,	WB	rabbit	1:500
EGFR	R&D Systems, Minneapolis, MN, USA, #AF1280	IF	goat	1:200
pERBB2 (Tyr 877)	Cell Signaling, Boston, MA, USA, #2241	WB	rabbit	1:1000
ERBB2	Cell Signaling, Boston, MA, USA, #4290	WB	rabbit	1:1000
ERBB2	R&D Systems, Minneapolis, MN, USA, #AF5176	IF	sheep	1:200
pERBB3 (Tyr 1289)	Cell Signaling, Boston, MA, USA, #4791	WB	rabbit	1:1000
ERBB3	Cell Signaling, Boston, MA, USA, #12708	WB	rabbit	1:1000
ERBB3	R&D Systems, Minneapolis, MN, USA, #AF4518	IF	sheep	1:1000
pMAPK1/2 (Thr202/Tyr204)	Cell Signaling, Boston, MA, USA, #4370	WB	rabbit	1:1000
MAPK1/2	Cell Signaling, Boston, MA, USA, #9102	WB	rabbit	1:1000
pAKT (Ser 473)	Cell Signaling, Boston, MA, USA, #4060	WB	rabbit	1:2000
AKT	Cell Signaling, Boston, MA, USA, #4691	WB	rabbit	1:1000
PCNA	Cell Signaling, Boston, MA, USA, #13110	WB	rabbit	1:1000
MKI67	Dianova, Hamburg, Germany, #M7249	IF/IHC	rat	1:200
KRT5	BioLegend, San Diego, CA, USA, #905501	IF	rabbit	1:800
KRT6	BioLegend, San Diego, CA, USA, #905701	IF	rabbit	1:800
KRT10	BioLegend, San Diego, CA, USA, #905701	IF	rabbit	1:800
LOR	BioLegend, San Diego, CA, USA, #905101	IF	rabbit	1:800
CDH1	R&D Systems, Minneapolis, MN, USA, #AF748	IF	goat	1:200
OCLN	OriGene Technologies GmbH, Herford, Germany, #AP30626PU-N	IF	rabbit	1:200
NOTCH1	Cell Signaling, Boston, MA, USA, #3608	WB	rabbit	1:1000
ADAM17	BioRad, Hercules, CA, USA, #CD156B	WB	rabbit	1:500
RBPJH	Cell Signaling, Boston, MA, USA, #5313	WB	rabbit	1:1000

MYC	Cell Signaling, Boston, MA, USA, #5605	WB	rabbit	1:1000
MAML1	Cell Signaling, Boston, MA, USA, #12166	WB	rabbit	1:1000
HES1	Cell Signaling, Boston, MA, USA, #1988	WB	rabbit	1:1000
CCND3	Cell Signaling, Boston, MA, USA, #2936	WB	mouse	1:1000
TUBA1A	Cell Signaling, Boston, MA, USA, #2125	WB	rabbit	1:1000
GAPDH	Cell Signaling, Boston, MA, USA, #2118	WB	rabbit	1:5000
H3F3A	Cell Signaling, Boston, MA, USA, #9717	WB	rabbit	1:1000
mouse α rat	Jackson ImmunoResearch, Ely, UK, #212-066-168	IHC	mouse	1:100
donkey α rabbit	Jackson ImmunoResearch, Ely, UK, #711-546-152	IF	donkey	1:1000
donkey α goat	Jackson ImmunoResearch, Ely, UK, #705-545-147	IF	donkey	1:1000
donkey α sheep	Jackson ImmunoResearch, Ely, UK, #713-586-147	IF	donkey	1:1000
rabbit α mouse	Cell Signaling, Boston, MA, USA, #7076	WB	rabbit	1:2500
goat α rabbit	Cell Signaling, Boston, MA, USA, #7074	WB	goat	1:2500
donkey α goat	R&D Systems, Minneapolis, MN, USA, #HAF109	WB	donkey	1:2500

Table 3-2 Table S2.
Primers employed for the quantitative RT-PCR analysis.

Lgr6	Forward Primer Reverse Primer	5′-TGTCAAGTCAGTCCTTCTGGTG-3′ 5′-GGTAGAGCAGTGGGTTGAGG-3′
Blimp1	Forward Primer Reverse Primer	5′-CCACAGTGCCTTCTCCCTTA-3′ 5′-GGGGGACTACTCTCGTCCTT-3′
Plet1	Forward Primer Reverse Primer	5'-GTGCCTGGCTCTGCACTTA-3' 5'-ACCACGCAGGACCCATTAT-3'
Cd34	Forward Primer Reverse Primer	5'-GAACCGTCGCAGTTGGAG-3' 5'-AACAGCCATCAAGGTTCCAG-3'
NfatC1	Forward Primer Reverse Primer	5′-TGTGGCCCTCAAAGTAGAGC-3′ 5′-TCAGAAGTGGGTGGAGTGGT-3′
Lgr5	Forward Primer Reverse Primer	5′-GTGTCTTTTTGCCTTTTGACG-3′ 5′-TGTCAGTCCAAGAAACTGGTGT-3′
Lhx2	Forward Primer Reverse Primer	5′-CAGCTTGCGCAAAAGACC-3′ 5′-CGGGCATTCTGAAACCAG-3′
Rpl30	Forward Primer Reverse Primer	5'-AACAACTGTCCAGCTTTGAGG-'3 5'-GCATACTCTGTAGTATTTTCCACACG-'3

3-4 Conclusion and outlook

Our study revealed a crucial function of LRIG1 during skin development and homeostasis. Prenatal LRIG1 overexpression led to neonatal lethality and caused disturbed epidermal differentiation and HF morphogenesis. Postnatal LRIG1 excess induced the development of alopecia accompanied by hyperplasia of the pilosebaceous unit and the IFE with hyperproliferation and a disturbed HF cycle. Our gain-of-function model revealed a disrupted ERBB receptor network, suggesting involvement of LRIG1 in the negative feedback loop regulation of ERBBs in the skin as reported for the intestine[219]. In contrast, NOTCH signaling was activated at the early onset of alopecia due to LRIG1 overexpression. SC markers of the bulge and SG were increased, indicating LRIG1-dependent activation of both SC pools and control of cell fate and differentiation[3,276,277]. Furthermore, in a loss-of-function mouse model, the deletion of LRIG1 also resulted in a severe epidermal phenotype, showing the development of psoriasis and epidermal hyperplasia[221]. In conclusion, an altered LRIG1 expression in the skin shows a remarkable influence on epidermal morphogenesis and homeostasis. However, mRNA expression of *LRIG1* in the skin is low, whereas *LRIG3* transcripts are most abundantly expressed[203]. Consequently, the question arises as to the function of the other two LRIGs in the skin. The loss of LRIG2 led to increased spontaneous mortality[212] and LRIG3 is also involved in crucial developmental processes[211,235], but nothing is known about their function in the skin. LRIG1 and LRIG3 show a very similar expression pattern during development and are rather homologous to each other than to LRIG2[235,238]. In contrast to LRIG1 though, LRIG3 increased ERBB receptor levels in HEK293T cells[238], suggesting opposing functions of LRIG1 and LRIG3. Therefore, we hypothesize that LRIG3 induces ERBB up-regulation in the skin and that LRIG1 expression increases due to the negative ERBB feedback mechanism. In turn, LRIG1 initiates receptor degradation as well as a decrease of LRIG3[224]. We generated a LRIG3-TG mouse model, similar to LRIG1-TG mice, which will shed light on the underlying mechanism in future studies. However, investigation of LRIG3 expression in LRIG1-TG mice may also provide evidence for this theory. In addition, the function of LRIG2 seems also to differ from that of the other LRIG family members, although, currently there is no literature available on LRIG2 function in the skin. Especially with regard to carcinogenesis, LRIG2 acts as an oncoprotein in various tumors[225,227], whereas LRIG1 and LRIG3 show tumor suppressive functions[207,209]. Even though LRIG2 enhances EGFR/PI3K/AKT signaling[227], it appears to have no major impact on ERBB expression levels[224]. In the context of this thesis, the function of LRIG2 in the

skin during homeostasis and tumorigenesis and its influence on the ERBB network was investigated (see Chapter 4). In conclusion, the function of LRIG proteins in the skin might be very distinct and their impact on skin diseases, as well as on their role as prognostic factors for tumor therapy has to be examined very carefully. The identification of LRIG interaction partners and especially the influence of LRIGs on the ERBB system in the skin is highly important with respect to prospective therapy approaches of NMSC.

Chapter 4 The transmembrane protein LRIG2 increases tumor progression in skin carcinogenesis

4-1 Aim

High cumulative sun exposure and a history of sunburns are the causes of 90% of NMSC incidences, and numbers are remarkably increasing in recent years, especially in younger people[75]. Particularly cSCC occurrence correlates directly with the number of hours patients spent in the sun[79]. UV radiation results in the upregulation of EGFR[87] and ERBB2[88], which is in accordance with an altered ERBB receptor expression in NMSC[160]. ERBB inhibitors are commonly used in cancer therapy[299]. However, their side effects are undesirable, and novel, more specific therapeutic targets could improve treatment strategies. Therefore, LRIG proteins arose our attention. As feedback loop regulators of the ERBB network[193,227,238] and potential prognostic factors in different types of cancer[207], LRIG proteins are promising targets in NMSC treatment. We found increased LRIG2 expression in the cSCC cell line A431 compared to healthy keratinocytes and also an altered expression of LRIG2 in tissue samples of cSCC patients. Therefore, we proposed a tumorigenic impact of LRIG2 on cSCC. To analyze the impact of LRIG2 on skin homeostasis and tumorigenesis, in particular on NMSC, we developed a skin-specific TG mouse model, overexpressing LRIG2. 10% of SCC incidences show RAS activation[300], and

cSCC arises from precursor lesions in a multi-stage model[69], prompting our decision to apply a two-stage chemical carcinogenesis protocol to LRIG2-TG mice and control (Co) littermates. The model consists of an initiation and a promotion phase[301]. The initially required *Ras* mutation, predominantly *HRas1*, is induced by the application of the tumor initiating agent DMBA[302], and the repeated administration of the chemical agent TPA triggers sustained epidermal hyperplasia and promotes tumor growth[301]. Papillomata arise due to the treatment, which may progress into invasive SCC and spindle cell carcinoma, dependent on the genetic background[301]. The following study focused on the impact of LRIG2 on the skin and skin carcinogenesis. We analyzed the influence of LRIG2 excess on tumor initiation and progression in the skin, especially with regard to the ERBB system. Additionally, we used a TPA-induced epidermal dysplasia model to investigate the effect of LRIG2 during early hyperproliferative stages of tumor development.

4-2 Study

This work is in the process of publication at Molecular Oncology (revision submitted July 2019, under review). The following chapters depict the submitted manuscript.

Authors: **C. Hoesl**, T. Fröhlich, J.E. Hundt, H. Kneitz, M. Goebeler, R. Wolf, M.R. Schneider, M. Dahlhoff

Author contribution: *Conception and design:* MD, CH, MRS; *Development of methodology:* MD, CH, MRS; *Acquisition of data (provided animals, acquired and managed patients provided facilities, etc.):* MD, RW, MG, JEH; *Analysis and interpretation of data:* MD, CH, HK, TF, JEH; *Writing, review, and/or revision of the manuscript:* MD, CH; *Study supervision:* MD; *Discussion of the experiments at planning stage and discussions of the results:* MD, CH, MRS, MG, HK, TF, JEH;

4-2.1 Abstract

In the last decades, non-melanoma skin cancer (NMSC) became more significant with over three million cases every year worldwide. The members of the ERBB receptor family are important regulators of skin development and homeostasis and, when dysregulated, contribute to skin pathogenesis. In this study, we investigated leucine-rich repeats and

immunoglobulin-like domains 2 (LRIG2), a transmembrane protein involved in feedback loop regulation of the ERBB receptor family, during NMSC. LRIG2 was identified to be up-regulated in various types of squamous cell carcinoma (SCC), but only little is known about LRIG2 in cutaneous SCC (cSCC). To investigate the function of LRIG2 in cSCC in vivo, we generated a skin-specific LRIG2 overexpressing transgenic mouse line (LRIG2-TG) using the Tet-Off system. We employed the 7,12-dimethylbenz(a)anthracene/12-O-tetra-decanoylphorbol-13-acetate (DMBA/TPA) two-stage chemical carcinogenesis model and analyzed the skin during homeostasis and tumorigenesis. LRIG2-TG mice revealed no alterations in skin development and homeostasis but showed interaction between LRIG2 and thrombospondin-1, often involved in angiogenesis and tumorigenesis. However, during carcinogenesis, transgenic animals showed significantly increased tumor progression and a more rapid development of cSCC. This was accompanied by changes in the ERBB system. After a single TPA application, inflammation of the epidermis was also impaired under LRIG2 overexpression. In human skin samples, LRIG2 expression was identified in the basal layer of the epidermis and in hair follicles of normal skin, but also in cSCC samples. In conclusion, epidermal LRIG2 excess is associated with accelerated tumor progression in NMSC and activated EGFR/ERBB4-MAPK signaling, making LRIG2 a potential oncoprotein in skin.

4-2.2 **Introduction**

Excessive exposure to the sun and a history of sunburns are often linked to an increased incidence of malignant skin lesions[75,79]. Every third cancer diagnosis is skin cancer, the most common type of cancer amongst Caucasians, with up to 3 million new non-melanoma skin cancer (NMSC) cases per year worldwide[63]. Increasing NMSC incidences claim for the development of new therapies and prophylactic measures as well as for the optimization of screenings. NMSC arises from keratinocytes, and can be divided into basal cell carcinoma (BCC) or cutaneous squamous cell carcinoma (cSCC) depending on the cell type from which tumors develop[64-66]. Dysregulated growth factors and their receptors have a deep impact on tumor initiation and progression[303]. The epidermal growth factor receptor (EGFR, ERBB1, HER1) plays a crucial role in human cSCC[84]. The EGFR and the other members of the ERBB receptor family (ERBB2-4, HER2-4) are widely expressed in human epidermis[161] and regulate key processes of epidermal homeostasis, including proliferation, differentiation, and cell death[101]. The deletion of ERBB4 in murine skin results in decreased epidermal thickness and keratinocyte proliferation[161]. Skin-specific ERBB2[170]

and ERBB3[154] knockout mice revealed a major role of both receptors in NMSC promotion, and also EGFR plays a crucial role in skin carcinogenesis[177,178,304]. Signaling of the ERBB receptors is controlled by negative or positive feedback loops[184]. During pathogenic processes, the dysregulation of those pathways can also influence ERBB signaling in a tumorigenic manner[177]. The leucine-rich repeats and immunoglobulin-like domains (LRIG) family comprises three transmembrane proteins (LRIG1-3)[200-203] involved in the regulation of receptor tyrosine kinases (RTKs) such as the ERBB receptors[203,224]. LRIG proteins attracted attention especially due to their potential as prognostic markers in different cancer types[209]. In the skin, LRIG1 is predominantly expressed in a stem cell pool of the hair follicle (HF)[43], similarly to its expression in the intestine[219] or stomach[220], while LRIG2 and LRIG3 are expressed throughout the epidermis[210]. LRIG1 knockout mice develop psoriasis-like skin lesions[221]. It was shown that LRIG1 promotes EGFR, ERBB2, and ERBB3 degradation from the cell surface in a negative feedback loop[188,192,193] and that the extracellular domain of LRIG1 decreases EGFR signaling in a paracrine manner[218]. LRIG3 opposes the function of LRIG1 and stabilizes the ERBB receptors at the cell surface of HEK293 cells[224]. While tumor suppressive functions of LRIG1[252] and LRIG3[255] were reported in malignant glioma, LRIG2 seems to act more as an oncoprotein[212,225,227]. LRIG2 expression correlates with poor prognosis in SCC of the cervix and uterus, which show increased *LRIG2* RNA levels[242]. However, although it is known that LRIG proteins can promote and suppress tumor growth in a tissue-specific manner[208], the molecular mechanisms and their impact on tumorigenesis in the skin are mostly unknown. The aim of this study was to investigate the function of LRIG2 in the skin during development, homeostasis and tumorigenesis, and in particular its impact on the ERBB system. Therefore, we generated a skin-specific transgenic (TG) mouse line overexpressing LRIG2 using the Tet-Off system. LRIG2-TG mice were viable and showed no major phenotype during development and homeostasis. However, when homeostasis was disrupted, overexpression of LRIG2 resulted in increased inflammation, angiogenesis and tumor progression along with an early onset of cSCC, affecting ERBB signaling and components of the extracellular matrix (ECM).

4-2.3 Materials and methods

4-2.3.1 Cell culture

HaCaT keratinocytes, A431 and A375 cells were purchased from CLS (Cell lines service, Eppelheim, Germany) four months before the experiments were performed. All human permanent cell lines in the CLS cell bank have been authenticated by using the STR DNA profiling analysis. Mycoplasma testing will be done every 6 months for all cultured cells using a mycoplasma detection kit (PlasmoTest, InvivoGen, Toulouse, France). Cells were cultured in DMEM® medium (Biochrom, Berlin, Germany) supplemented with 10% fetal calf serum (FCS, Biochrom) and 1% penicillin/streptomycin (Biochrom) in a humidified incubator with 5% CO_2 at 37 ˚C.

4-2.3.2 Human samples

Biopsy samples of cSCC were obtained from 10 patients between 71 and 92 years of age. They were obtained at the Department of Dermatology, University Hospital Würzburg, Germany, and taken from the following anatomical sites: cheeks (3 patients), forehead (3 patients), nose, ear, dorsum of the hand and lower leg (1 patient each). Eight of these patients were diagnosed at stage I (pT1G1: 6 patients, pT1G2: 2 patients) and two at stage II (pT2G2 and pT2G3: one patient each) as classified according to the 8th Edition of the staging manual of the American Joint Committee on Cancer (AJCC-8)[305]. Skin samples from non-diseased skin of 10 individuals served as controls. Analysis of human tissue samples was approved by the Ethics Committee of the Medical Faculty, University of Würzburg, Germany (reference number #169/12).

4-2.3.3 Mice

Mice were maintained under specific-pathogen-free conditions and had access to water and standard rodent diet (V1534; Ssniff, Soest, Germany) *ad libitum*. C57BL/6N mice expressing the tetracycline-regulated transcriptional transactivator (tTA) under the keratin 5 (KRT5) promoter have been originally described previously[280]. We cloned murine *Lrig2* cDNA into the pTRE-tight vector (Clontech) (pTRE-tight-LRIG2-TG mouse line) or

fused *Lrig2* cDNA with a sequence encoding the human influenza hemagglutinin (HA)-epitope C-terminally (pTRE-tight-HA-LRIG2-TG mouse line), and used these constructs to generate two independent TG mouse lines by pronuclear microinjection into zygotes of C57BL/6N mice. To obtain two independent TG KRT5-LRIG2 mouse lines expressing transgenic LRIG2 skin-specifically, the KRT5-tTA mouse line was mated with either the pTRE-tight-LRIG2- or the pTRE-tight-HA-LRIG2-TG mouse line. Mouse strains were maintained in the C57BL/6N background. For further studies we used the HA-tagged TG mouse line, referring to as LRIG2-TG.

To study proliferation rates of twelve-month-old mice, 10 mM bromodeoxyuridine (BrdU, Roche, Mannheim, Germany) dissolved in PBS were injected intraperitoneal to the mice (30 mg/kg body weight) three hours before dissection.

To inhibit LRIG2-TG expression, 3 mg/mL doxycycline (Dox) (Beladox 500 mg/g, bela-pharm (Lehnecke 793-588), Schortens, Germany) was added to the drinking water together with 5% sucrose (Sigma, Taufkirchen, Germany) for two weeks.

LRIG2-TG mice and controls (Co) were dissected at indicated time points, skin samples were fixed in 4% paraformaldehyde (PFA, Sigma, Taufkirchen, Germany), dehydrated, and embedded in paraffin or snap-frozen and stored at -80 °C until use. All murine experiments were approved by the Committee on Animal Health and Care of the local governmental body of the state of Upper Bavaria (Regierung von Oberbayern), Germany, and were performed in strict compliance with the European Communities Council Directive (86/609/EEC) recommendations for the care and use of laboratory animals.

4-2.3.4 Chemical skin carcinogenesis and TPA-induced epidermal dysplasia

Chemical carcinogenesis was carried out as described elsewhere, according to internationally accepted standards[301]. For tumor initiation, the carcinogen 7,12-dimethylbenz(a)anthracene (100 µL DMBA dissolved in acetone, 400 nmol, Sigma-Aldrich) was applied once to the shaved back skin of seven-week-old, female LRIG2-TG mice and controls. Tumor promotion was achieved by repeated application of the tumor promoting agent 12-O-tetra-decanoylphorbol-13-acetate (50 µL TPA dissolved in ethanol, 10 nmol, Sigma Aldrich) twice a week for 24 weeks. Tumor development was assessed weekly.

To investigate the effect of LRIG2 during early hyperproliferative stages, shaved back skin of nine-week-old LRIG2-TG mice and controls were exposed to a single dose of TPA (50 µL

TPA dissolved in ethanol, 10 nmol, Sigma Aldrich). Mice were euthanized 48 h after TPA application. Skin samples were processed as described before.

4-2.3.5 Co-immunoprecipitation and Western blot analysis

Protein was extracted by using Laemmli extraction buffer for skin samples or protein lysis buffer (0.05 M Hepes pH 7.5, 10% glycerol, 0.15 M NaCl, 1% Triton X-100, 0.5 M EDTA, 0.5 M EGTA, 0.01 M NaF, 0.025 M ß-glycerol phosphate, 0.01 M Na_3Vo_4, Phosphatase inhibitor cocktail (Roche)) for cell lysates or skin samples used for co-immunoprecipitation (IP) experiments. Protein concentration was estimated by bicinchoninic acid protein assay. 300 µg of total protein were used for co-immunoprecipitation with 1.8 µg HA-Tag antibody and Dynabeads® Protein G (Invitrogen, Carlsbad, CA, United States). Protein lysates were pre-cleared with Dynabeads® Protein G for 60 min at 4 °C and immunoprecipitated with the HA-Tag antibody conjugated to the beads for 2 h at 4 °C. Samples were washed and elution was done with 2x Laemmli extraction buffer by heating at 95 °C for 5 min. For Western blot analysis half of the co-IP eluate or 5-20 µg of total protein were separated by SDS-PAGE, transferred to PVDF membranes (Millipore, Schwalbach, Germany) and immunoblotted (IB) against antibodies as indicated. For reference proteins and to analyze the phosphorylated state as well as the total protein, we stripped the membranes by incubating them with a stripping buffer (2% SDS, 62.5 mM Tris/HCl, pH 6.7 and 100 mM ß-mercaptoethanol (BME)) for 40 min at 70 °C. Afterwards membranes where washed, blocked and incubated with the second primary antibody. All primary and secondary antibodies and their dilutions are provided in 4-3 Supplementary material, Table 4-1. Densitometrical analysis was done using ImageJ (http://rsb.info.nih.gov/ij).

4-2.3.6 Histology, immunohistochemistry, and morphometric analysis

Skin samples were either embedded in paraffin or snap frozen on dry ice and embedded in Tissue-Tek® O.C.T.™ Compound (Sakura Finetek, Alphen aan den Rijn, Netherlands). Giemsa or hematoxylin and eosin (H&E)-staining, immunofluorescence, and immunohistochemistry were performed as described previously[161]. Giemsa and H&E-stained sections were employed for histological analysis. For analysis of LRIG2 expression in human tissue samples and the detection of proliferating cells (MKI67 or BrdU positive), immunohistochemical staining were performed. Briefly, sections were boiled in 10 mM sodium citrate buffer (pH 6.0) for antigen retrieval, and the endogenous peroxidase was

blocked with 3% H_2O_2 for 15 min. Slides were blocked with 5% serum from the secondary antibody host and incubated overnight at 4 °C with indicated antibodies. After being washed in Tris-buffered saline solution, the slides were incubated for 1 h with appropriate secondary biotin-conjugated antibodies followed by 30 min incubation with streptavidin-biotin complex (Vector Laboratories, Burlingame, USA). ImmPACT® AMEC Red or DAB Peroxidase (HRP) substrate (Vector Laboratories) were used as chromogen. Counterstaining was performed with hematoxylin. Immunofluorescence stainings were performed accordingly without blocking endogenous peroxidase and incubation with the streptavidin-biotin complex. Additionally, the M.O.M. Immunodetection Basic kit (Vector Laboratories) was applied to murine sections if primary antibodies were raised in mice. All primary and secondary antibodies and their dilution are listed in 4-3 Supplementary material, Table 4-1. For morphometric investigations, three different H&E- or Giemsa-stained back skin sections were analyzed. Per animal, 60 pictures covering a total length of 39.2 mm of back skin epidermis were taken with a 200x magnification lens using a Leica DFC425C digital camera (Leica Microsystems, Wetzlar, Germany). The area of all visible SGs was recorded with LAS software version 3.8.0 (Leica Microsystems) and employed to calculate the mean gland area. Epidermal thickness was investigated on the same sections on three constantly distributed measuring points per picture, resulting in a total of 180 measuring points per animal. To analyze the epidermal proliferation rate, BrdU- or MKI67-stained sections were evaluated and the total number of epidermal nuclei and the total number of BrdU or MKI67 positive nuclei were determined similarly on 60 images covering a length of 39.2 mm.

4-2.3.7 Gelatin zymography

Gelatin zymography was performed as described previously[306]. Briefly, protein samples (50 µg) lysed in protein lysis buffer were separated on an 8% acrylamide gel with 1% gelatin. Gels were incubated in a renaturation-buffer (2.5% Triton X-100 in H_2O), followed by a 20 h developing step in the incubation buffer (500 mM TRIS, 2 M NaCl, 50 mM $CaCl_2$, 50 µM $ZnCl_2$) at 37 °C, stained with Coomassie Brilliant Blue R and washed with decolorizing solution (5% methanol, 7% acetic acid). Proteinase-activities were determined by densitometrical analysis of the inverse band intensities using ImageJ.

4-2.3.8 Mass-spectrometry analysis

For mass spectrometry analysis reduced (8% BME) and non-reduced protein samples of LRIG2-TG back skin and controls were separated by SDS-PAGE. Gels were stained with Coomassie Brilliant Blue R, and protein bands above 300 kDa were excised. To reduce disulfide bonds, the gel slices were incubated in 45 mM dithioerythritol / 50 mM NH_4HCO_3 for 30 min at 55 °C. Free sulfhydryl groups were blocked using 0.1 M iodoacetamide in 50 mM NH_4HCO_3 at room temperature for 2 x 15 min. For digestion, gel pieces were minced and covered with 100 ng porcine trypsin in 50 mM NH_4HCO_3 (Promega, Madison, WI, USA). Peptides were separated on a C18 column (PepMap RSLC, C18, 2 µm, 100A, 75 µm x 50 cm, Thermo Scientific, Rockford, IL, USA) at a flow rate of 200 nL/min using an EASY-nLC 1000 system (Thermo Scientific, Rockford, IL, USA). The gradients consisted of a 120 min ramp from 2% to 25% B (100% acetonitrile, 0.1% formic acid) and a consecutive ramp to 50% B within 10 min. Mass spectra were acquired using a top 5 data-dependent method on an online coupled LTQ Orbitrap XL instrument (Thermo Scientific, Rockford, IL, USA). Spectra were searched using MASCOT V2.4 (Matrix Science Ltd, London, UK) and the murine subset of the UniProt database. For evaluation of the data, Scaffold V 4.1 (Proteome Software, Inc, Portland, OR, USA) was used.

4-2.3.9 RNA expression analysis

Organs were homogenized in TRIzol reagent (Invitrogen, Darmstadt, Germany) for RNA isolation. 3 µg RNA were reverse-transcribed in a final volume of 30 µL using RevertAid Reverse Transcriptase (Thermo Scientific, Schwerte, Germany) according to the manufacturer's instructions. For qualitative analysis of mRNA expression of *HA-Lrig2*, reverse transcription-PCR (RT-PCR) using reagents from Qiagen (Hilden, Germany) was performed. The final reaction volume was 20 µl, and cycle conditions were 94 °C for 5 min followed by 35 cycles of 94 °C for 1 min, 60 °C for 1 min, and 72 °C for 1 min. Following primers were employed: *HA-Lrig2* forward primer 5′-GAGGCAGGCAGCCATCAGC-3′ and reverse primer 5′-TCAAGCGTAGTCTGGGACG-3′ and *Gapdh* forward primer 5′-TCATCAACGGGAAGCCCATCAC-3′ and reverse primer 5′-AGACTCCACGACATACTCAGCACCG-3′.

Quantitative mRNA expression analysis was performed by quantitative real-time PCR (qPCR) using the StepOnePlus™ Real-Time PCR System (Applied Biosystems, Waltham, USA) and the PowerUp™ SYBR® Green Master Mix (Applied Biosystems) according to

the manufacturer's instructions. The final primer concentration was 0.5 µM, and the final reaction volume was 20 µl, and cycle conditions were 95 °C for 2 min followed by 40 cycles of 95 °C for 15 s, 60 °C for 15 s, and 72 °C for 1 min. Quantitative values were obtained from the threshold cycle (C_T) number, at which the increase in the signal associated with the exponential growth of PCR products begins to be detected. Absolute mRNA quantification was performed by using standard curves generated with a plasmid containing the murine *Lrig2* cDNA. We performed no-template control and no-RT control assays, which produced negligible signals with C_T values that were greater than 35. Experiments were performed in duplicates. The following primers were used:
Lrig2-Fw: 5'-CACTGAAATACCTGAATTTGAGC-'3,
Lrig2-Rev: 5'-TCAGTTCCAAGAACTGGAGATG-'3.

4-2.3.10 Statistical analysis

Data are presented as mean±SEM and compared by Student's *t*-test (GraphPad Prism version 5.0 for Windows, GraphPad Software, San Diego, CA, USA), and in the case of more than two groups by analysis of variance (ANOVA) and Tukey's multiple comparison test. Incidence, papilloma burden, and size were analyzed by 2-way ANOVA. Group differences were considered to be statistically significant if $P<0.05$.

4-2.4 Results

4-2.4.1 LRIG2 is expressed in human skin cancer

To evaluate the significance of LRIG2 in human skin homeostasis and tumorigenesis, we investigated LRIG2 expression in different human skin cell lines and tissue samples of healthy individuals and patients with cSCC. Western blot analysis revealed that LRIG2 expression was significantly increased in human cSCC (A431) and melanoma (A375) cell lines compared to human keratinocytes (HaCaT) (Figure 4-1a). In normal human skin LRIG2 is predominantly expressed in the basal and lower spinous layer of the epidermis and in HFs with a mainly cytoplasmatic pattern. In upper spinous layers LRIG2 is also located in nuclei. cSCC samples revealed prominent LRIG2 expression in tumor cells with a predominantly nuclear staining pattern (Figure 4-1b). These data indicate a role of LRIG2 during the pathogenesis of cSCC in humans.

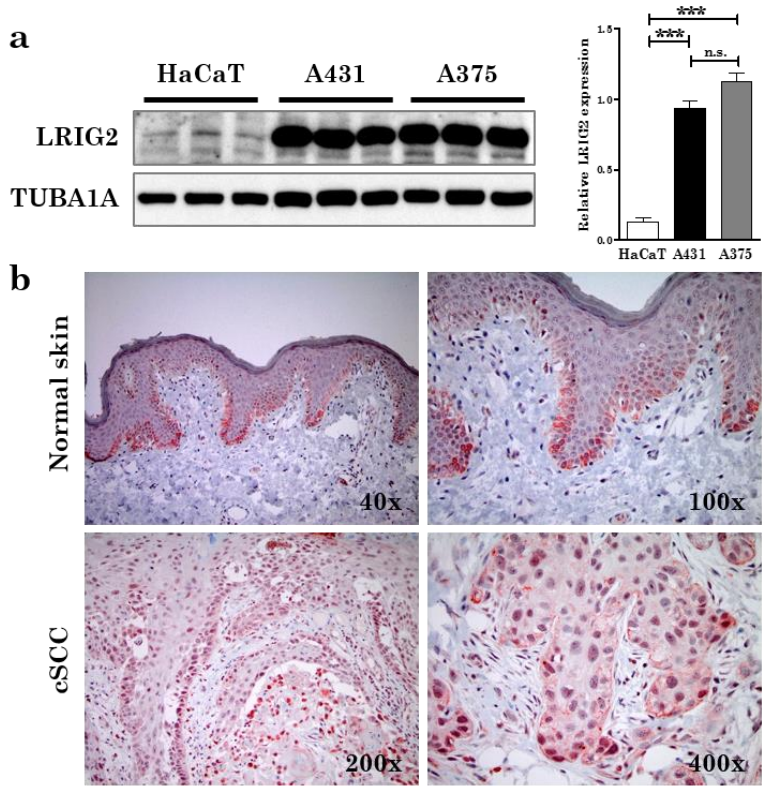

Figure 4-1 LRIG2 is expressed in human skin, cSCC, and human skin cell lines.
(a) Western blot analysis of LRIG2 expression in HaCaT, A431, and A375 cells. TUBA1A was used as reference protein. Densitometrical analysis of LRIG2 in relation to TUBA1A reveals that LRIG2 is significantly higher expressed in both tumor cell lines compared to HaCaT keratinocytes. Data were analyzed by ANOVA and Tukey's multiple comparison test. ***P<0.001. **(b)** Immunohistochemical visualization of LRIG2 expression (in red) in normal human skin and cSCC. Micrographs are representative for 10 cSCCs (8 patients with stage I and 2 patients with stage II according to AJCC-8[305], see Materials and Methods for details) and 10 normal skin samples. Magnification as indicated in the micrographs.

4-2.4.2 Overexpression of LRIG2 has no influence on skin development and homeostasis

To investigate the function of LRIG2 in the skin we generated two independent skin-specific inducible transgenic mouse lines using the Tet-Off system. Both lines were mated with a keratin 5 promoter (KRT5-tTA) driver mouse line. As both mouse lines showed no phenotype, in spite of an overexpression of LRIG2 on RNA level (data not shown), the LRIG2 transgenic mouse line (LRIG2-TG) with a c-terminal HA-tag was used for all experiments descripted in this manuscript. LRIG2-TG mice were viable, showed no macroscopic phenotype, and bred in a Mendelian ratio (4-3 Supplementary material, Figure 4-7a). RT-PCR (4-3 Supplementary material, Figure 4-7b), qPCR (4-3 Supplementary material, Figure 4-7d) and Western blot analysis (4-3 Supplementary material, Figure 4-7c) confirmed skin-specific overexpression of the transgene. Western blots revealed that LRIG2-TG animals treated for two weeks with doxycycline (Dox+)

showed no transgene expression but endogenous LRIG2 levels comparable to those of control mice (4-3 Supplementary material, Figure 4-7e). LRIG2-TG mice showed no altered expression of the other LRIG family members LRIG1 and LRIG3 (4-3 Supplementary material, Figure 4-7e). Immunofluorescence staining against the HA-tag revealed expression of LRIG2 in the epidermis and HFs of transgenic animals (Figure 4-2a). Histologically, LRIG2 overexpression had no effect on skin at any time under homeostatic conditions (Figure 4-2b), not even in a long-term study (up to 12 months). While the HF cycle was not impaired in LRIG2-TG mice, they showed

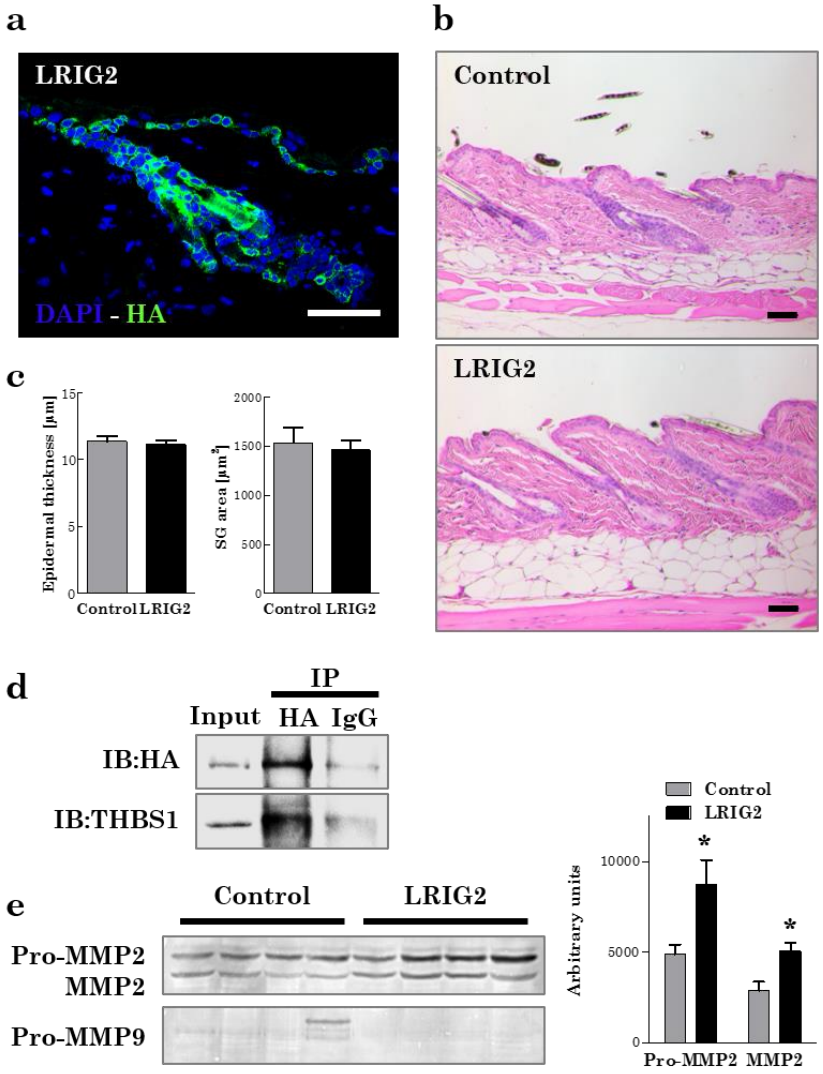

Figure 4-2 Skin-specific overexpression of LRIG2 causes no phenotypical alterations.
(a) Immunofluorescence staining against HA-tag in the skin of a twelve-month-old LRIG2-TG animal demonstrates a strong expression of LRIG2 in epidermis, hair follicles, and sebaceous glands. HA-tag in green and cell nuclei are stained with DAPI (blue). Scale bar represents 50 µm. **(b)** H&E staining of the skin of a twelve-month-old LRIG2-TG mouse and a control littermate. Scale bars represent 50 µm. **(c)** Morphometric analysis of the epidermal thickness and sebaceous gland area revealed no alterations (n=4). Data were analyzed by Student's *t*-test. **(d)** Co-immunoprecipitation (IP) of HA-tag in a LRIG2-TG skin sample of a twelve-month-old mouse. Immunoblotting (IB) revealed precipitation of LRIG2 and binding of THBS1. **(e)** Gelatin zymography of skin samples of twelve-month-old LRIG2-TG mice and controls (n=4). Densitometrical analysis of gelatin zymography revealed increased expression and activity of MMP2. Data were analyzed by Student's *t*-test. **P*<0.01.

significantly more HFs in the late catagen phase VIII compared to controls on day P18 (4-3 Supplementary material, Figure 4-10). However, these changes seem to be transient, as such a finding could not be confirmed at any other time point. Epidermal thickness and sebaceous gland size showed no differences (Figure 4-2c) between LRIG2-TG animals and control littermates. In addition, epidermal differentiation and proliferation rate were unchanged in LRIG2-TG mice (4-3 Supplementary material, Figure 4-8). Since LRIG proteins are feedback loop regulators of the ERBB receptor family, we analyzed ERBB expression and activation in the skin of LRIG2-TG and control mice as well as their main target kinases mitogen-activated protein kinase 1/2 (MAPK1/2) and RAC-alpha serine/threonine-protein kinase (AKT), but no differences became apparent (4-3 Supplementary material, Figure 4-9). Thus, we can conclude that LRIG2 overexpression does not influence epidermis and HF development and homeostasis.

4-2.4.3 LRIG2 binds thrombospondin-1

To identify potential interacting partners of the transmembrane protein LRIG2, we performed mass spectrometry analysis and co-IPs. Investigation of LRIG2 expression in adult LRIG2-TG and control mice under reducing and non-reducing conditions by Western blot, revealed transgenic LRIG2 at a size of 120 kDa. Additionally, we detected a positive signal at 300 kDa but only in non-reduced LRIG2-TG protein samples (4-3 Supplementary material, Figure 4-11a), indicating the presence of proteins interacting with LRIG2. Corresponding bands of transgenic and control animals were analyzed by mass spectrometry to detect potential binding partners. Besides LRIG2, 40 further proteins were exclusively identified in transgenic animals and were sorted by total spectral counts of the non-reduced LRIG2-TG protein fraction. A table of the top 20 proteins is shown in Figure 4-11b (4-3 Supplementary material). We identified several keratins but also two glycoproteins, laminin subunit beta-1 (LAMB1) and thrombospondin-1 (THBS1), both containing EGF-like motifs that possibly interact with LRIG2. In contrast to LAMB1, THBS1 has been shown previously to play a role in SCC and other cancers[307]. Therefore, we focused on THBS1 for further studies. THBS1 was exclusively identified in LRIG2-TG samples by four individual peptides. Corresponding MS spectra as well as probability scores are shown in Figure 4-11c,d (4-3 Supplementary material). THBS1 has an important role in tyrosine kinase-dependent signaling, is involved in angiogenesis and tumorigenesis and mediates cell-to-cell and cell-to-matrix interactions. Immunoprecipitation revealed that THBS1 binds LRIG2, suggesting that it could be an

important interaction partner of LRIG2 (Figure 4-2d). However, although its expression was not increased in LRIG2-TG animals, THBS1 may be stabilized by LRIG2 binding (4-3 Supplementary material, Figure 4-9). THBS1 regulates the matrix-metalloproteinases (MMPs) 2 and 9[308], which could be essential for tumor progression. Therefore, we analyzed MMP2 and MMP9 activity by zymography. LRIG2-TG mice showed significantly increased levels of pro-MMP2 and active MMP2 whereas no changes of MMP9 levels were detected (Figure 4-2e). In summary, we identified THBS1 as a binding partner of LRIG2 and observed increased levels of pro- and active MMP2, an important modulator of the ECM, in the skin of LRIG2-TG mice.

4-2.4.4 LRIG2 has a significant impact on progression of skin carcinogenesis

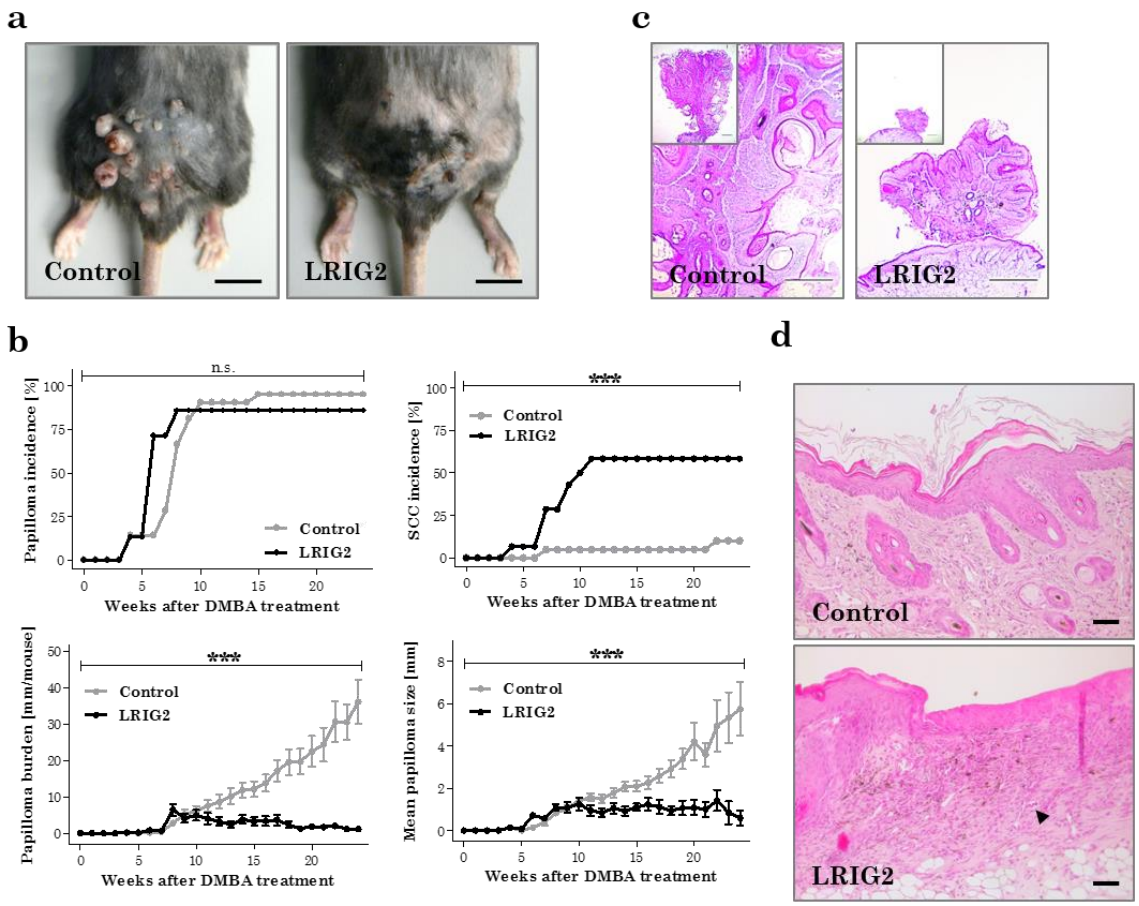

Figure 4-3 Accelerated development of cSCCs in LRIG2-TG mice in a chemically induced two-step model of skin tumorigenesis.
(a) Macroscopic pictures of the lower back skin of a representative LRIG2-TG animal and a control littermate at the final stage. Scale bars represent 1 cm. **(b)** Papilloma incidence, cSCC incidence, papilloma burden, and papilloma size of LRIG2-TG animals compared to control littermates (n= 21 Co/ 15 TG). Data were analyzed by 2-way ANOVA. Interaction: ***P<0.001. n.s.: not significant. **(c)** H&E staining of a papilloma of a LRIG2-TG mouse and a control littermate. Scale bars represent 500 µm. **(d)** H&E staining of cSCC of a LRIG2-TG mouse and back skin of a control littermate. Arrow points to tissue vascularization, indicating angiogenesis in LRIG2-TG mice. Scale bars represent 50 µm.

To determine whether LRIG2 affects skin tumorigenesis, we performed a two-stage chemical skin carcinogenesis model with onetime application of DMBA on the back skin of LRIG2-TG mice and control littermates causing tumor initiation followed by TPA treatment twice a week. In both groups, the first papillomata arose four weeks after DMBA treatment, without differences in tumor incidence, papilloma burden or size at this time. However, 10 weeks after tumor initiation we noticed a less pronounced increase of papilloma burden and papilloma size in LRIG2-TG animals as compared to controls (Figure 4-3b,c). Instead of papillomata, LRIG2-TG mice developed a cSCC-like phenotype at their backs starting six weeks after tumor initiation (Figure 4-3b). 58% of the transgenic animals, but only 10% of control littermates were affected (Figure 4-3a,b). Histological and

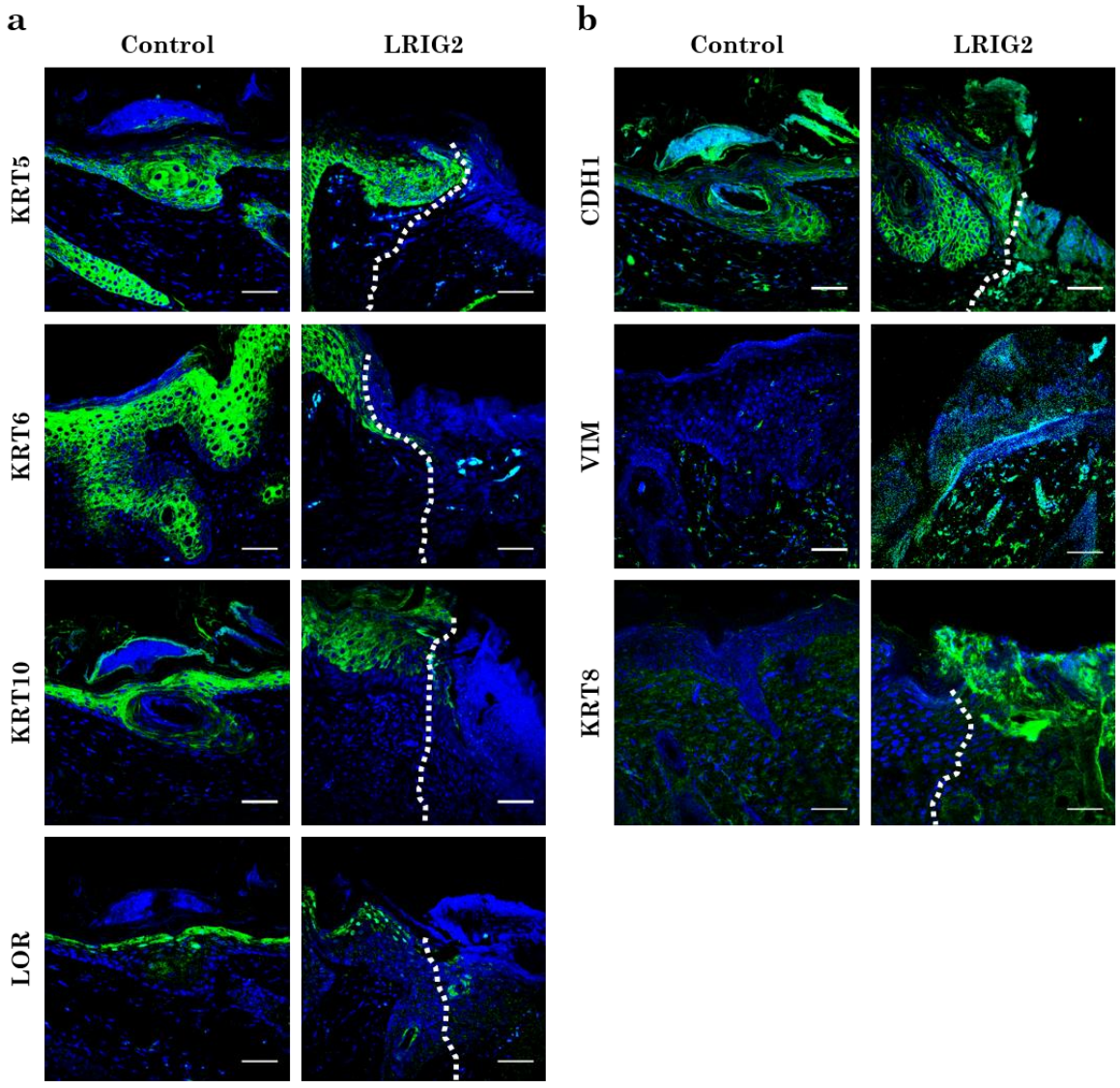

Figure 4-4 Epidermial differentiation during chemically induced skin tumorigenesis.
(a) Immunofluorescence stainings against epidermal differentiation markers KRT5, KRT6, KRT10, and LOR (in green). **(b)** Immunofluorescence staining against CDH1, VIM, and KRT8 (in green). Cell nuclei are stained with DAPI (blue). Skin was obtained 24 weeks after initiation of chemically induced tumorigenesis. Shown are representative pictures of control skin including papillomata or close to papillomata and of LRIG2-TG skin at the transition from epidermis to cSCC (white dashed line). Scale bars represent 50 µm.

immunofluorescence analysis of the skin lesions revealed a phenotype resembling human cSCC. Atypical spindle-like tumor cells arising from the epidermis protruded into the dermis and were accompanied by an inflammatory infiltrate (Figure 4-3d). Moreover, vascularization appeared to be increased indicating angiogenesis (arrow, Figure 4-3d). Tumors were stained for keratin 8 (KRT8), an established marker for cSCC in mice [309], which was highly expressed in the cSCC-like lesions of LRIG2-TG mice but not in controls (Figure 4-4b). Additionally, cSCC-like lesions of transgenic mice were poorly differentiated. In transgenic animals, the expression of epidermal differentiation markers (keratin 5 (KRT5), keratin 6 (KRT6), keratin 10 (KRT10), and loricrin (LOR), see Figure 4-4a) in the cSCC-like lesions decreased significantly in comparison to the adjacent epidermis, whereas the epidermis around the papillomata of controls were still differentiated. Moreover, epithelial polarity was lost. A decrease of epidermal CDH1 and a concomitant increase of vimentin (VIM) expression in the dermis indicate an enhanced tumor invasiveness, which might refer to epithelial–mesenchymal transition (EMT) (Figure 4-4b). Altogether, our data argue for a tumor promoting function of LRIG2 in murine skin resulting in an accelerated onset of cSCC development.

4-2.4.5 LRIG2 overexpression affects EGFR and ERBB4 expression during tumor progression

To investigate whether the tumor promoting activity of LRIG2 is ERBB-receptor-dependent, we analyzed the expression of the latter and respective downstream targets in transgenic and control skin during two-stage skin carcinogenesis. Immunofluorescence and Western blot analyses revealed an increased expression of EGFR and ERBB4 in the cSCC-like lesions of LRIG2-TG mice (Figure 4-5a,b). Concomitantly, the intracellular domain (ICD) of ERBB4 was significantly increased in LRIG2-TG mice (Figure 4-5a), indicating that the receptor undergoes regulated intramembrane proteolysis, thus the ICD can translocate to the nucleus and act as transcription factor. Additionally, phosphorylated ERBB4 and phospho-EGFR were significantly increased upon LRIG2 overexpression as compared to control littermates. We identified increased levels of AKT and phosphorylated AKT, a typical downstream target of the ERBB receptors and phosphorylation of MAPK1/2 was significantly increased in transgenic animals compared to controls (Figure 4-5c). Other downstream targets such as SHC-transforming protein 1 (SHC1), signal transducer and activator of transcription 3 (STAT3), STAT5, and GTPase Ras proteins (RAS) were unchanged in their activity (data not shown). Phosphorylation of

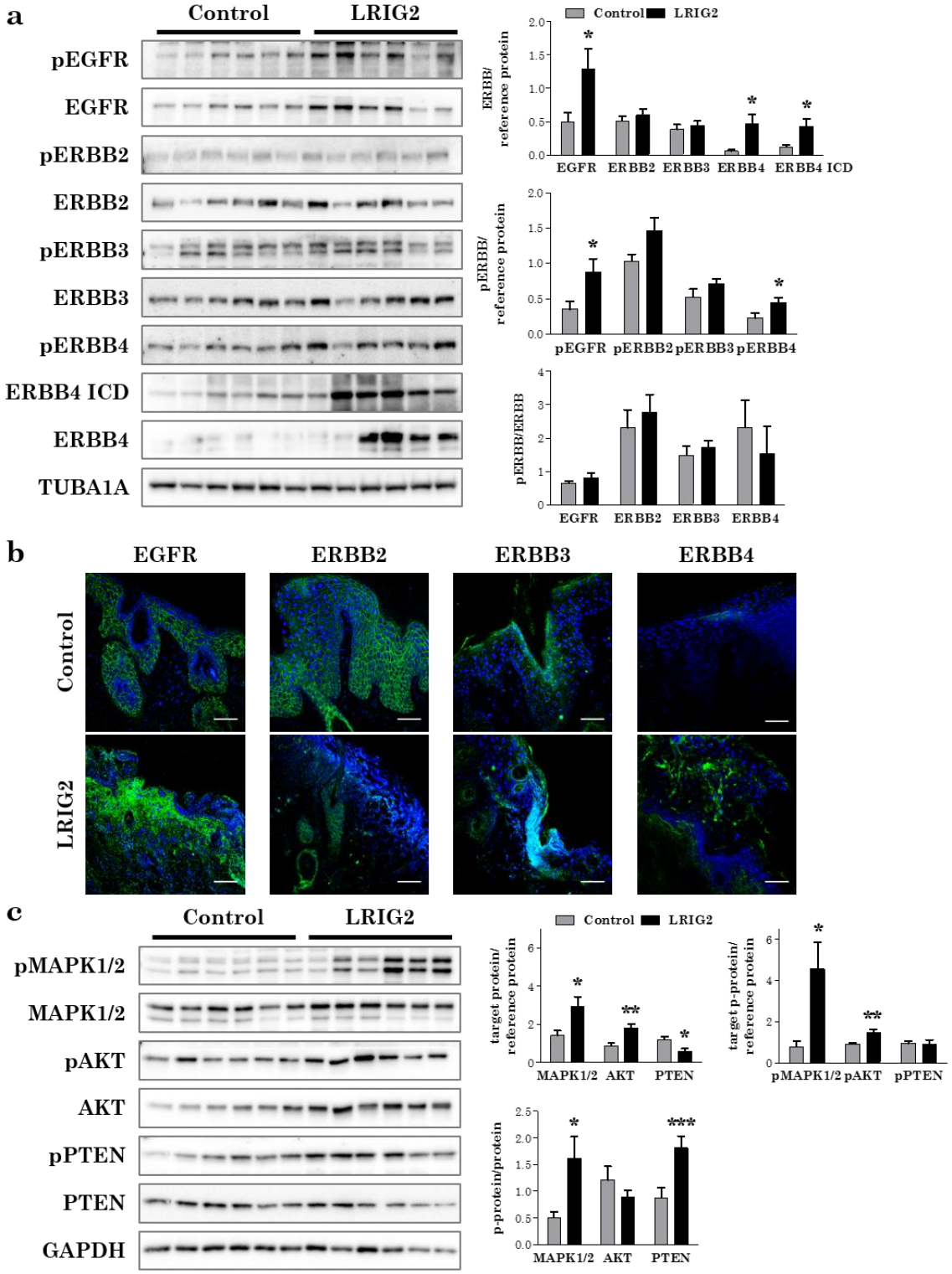

Figure 4-5 ERBB receptor expression during chemically induced skin tumorigenesis.
(a) Western blot and densitometrical analysis of phosphorylated ERBB receptors and ERBB receptors in skin samples obtained 24 weeks after initiation of chemically induced tumorigenesis. TUBA1A was used as reference protein. **(b)** Immunofluorescence staining against ERBB1-4 receptors (in green) using back skin sections from the carcinogenesis experiment of control and LRIG2-TG mice. Scale bars represent 50 µm. **(c)** Western blot and densitometrical analysis of phosphorylated and total downstream targets of ERBB receptors (MAPK1/2, AKT, and PTEN). GAPDH was used as reference protein. (n=6). Data were analyzed by Student's *t*-test. **P*<0.05, ***P*<0.01, ****P*<0.001.

phosphatidylinositol 3,4,5-triphosphate 3-phosphatase and dual specificity protein phosphatase PTEN (PTEN) was significantly increased while total PTEN was decreased, implying loss of the tumor suppressive function of PTEN (Figure 4-5c). Western blot analysis of THBS1 and zymography analysis for MMP2 and MMP9 revealed no differences between LRIG2-TG and control animals (data not shown). In summary, these data indicate that during tumorigenesis LRIG2 increases skin tumor progression, associated with activation of EGFR/ERBB4-MAPK signaling.

4-2.4.6 LRIG2 impairs TPA-induced epidermal hyperplasia

Our data suggest that LRIG2 is involved in tumor progression and accelerates tumorigenesis. To investigate an early point of time we induced epidermal hyperplasia by application of a single dose of TPA. In comparison to control mice the increase of epidermal thickness upon TPA treatment was less pronounced in LRIG2-TG animals (Figure 4-6a,b). These, however, developed a more prominent neutrophil-dominated inflammation (Figure 4-6a). Western blot analysis revealed that the proinflammatory cytokine interleukin-1-alpha (IL1A) was significantly increased in LRIG2-TG mice while interleukin-6 (IL6) was unchanged (Figure 4-6c,i). As previously observed in our carcinogenesis model, ERBB4 was up-regulated in the back skin of LRIG2-TG mice 48 h after TPA treatment, but the fraction of phosphorylated ERBB4 was reduced. The other ERBB receptors were unchanged except for ERBB2, which was higher expressed in LRIG2-TG mice compared to control littermates after TPA treatment (Figure 4-6c,f). Additionally, we found increased activation of MAPK1 in LRIG2-TG, TPA treated skin, while MAPK2 was not affected (Figure 4-6c,h). Importantly, PTEN expression levels were increased in LRIG2-TG mice, but appeared to be phosphorylated and therefore inactivated (Figure 4-6c,g). In accordance with a less prominent increase of epidermal thickness we found significantly increased levels of cleaved caspase-3 (CASP3) in the skin of TPA treated LRIG2-TG mice as compared to controls (Figure 4-6c,g), while the proliferation rate was unchanged (Figure 4-6c,d,g). Moreover, LRIG2-TG mice revealed a significant increase in THBS1 expression (Figure 4-6c,g) and a significant upregulation of pro-MMP9 (Figure 4-6e). However, unlike the findings under homeostatic conditions, MMP2 activity was not affected by LRIG2 overexpression due to TPA treatment (Figure 4-6e). In summary, LRIG2 overexpression leads to an increased inflammatory response after TPA treatment, which might contribute to tumorigenesis.

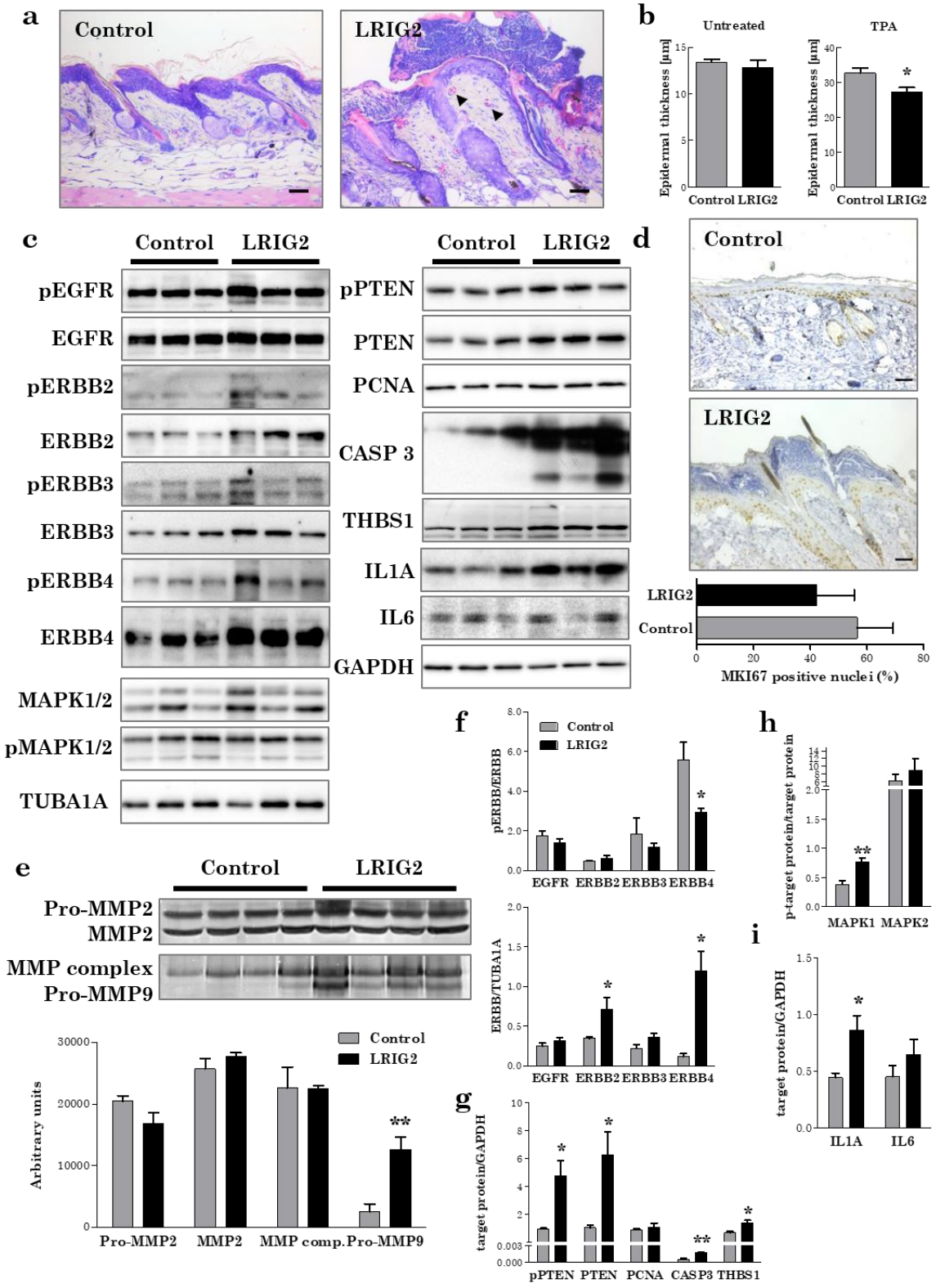

Figure 4-6 TPA induces an increased inflammation of the skin of LRIG2-TG mice.
(a) Giemsa staining reveals huge inflammation spots and blood vessels (arrows) in the skin of LRIG2-TG mice 48 hours after a single application of TPA. Scale bars represent 50 µm. **(b)** Morphometric measurements of the epidermal thickness showed less pronounced increase of epidermal thickness in LRIG2-TG mice compared to controls after TPA treatment (n=4). **(c)** Western blot of phosphorylated and total ERBB receptors, MAPK1/2, PTEN, PCNA, CASP3, THBS1, and the inflammation markers: IL1A and IL6. GAPDH or TUBA1A were used as reference protein. **(d)** The proliferation index is not altered in LRIG2-TG mice compared to controls (n=4). MKI67 staining of back skin of a TPA treated TG and control mouse. Scale bars represent 50 µm. **(e)** Gelatin zymography with densitometrical analysis of skin samples of TPA treated LRIG2-TG mice and controls (n=4) revealed increased expression of pro-MMP9. **(f-i)** Densitometrical analysis of Western blots in **(c)**. Data were analyzed by Student's *t*-test. **P*<0.05; ***P*<0.01.

4-2.5 Discussion

LRIG proteins are important regulators of different RTKs and are involved in negative and positive feedback loops of the ERBB receptor family[184]. LRIG1 and LRIG3 show mostly tumor-suppressive function, while LRIG2 seems to frequently act as an oncoprotein[209]. Increased LRIG2 expression correlates with a poorer prognosis in patients with oligodendroglioma[225], cervical SCC[242], non-small cell lung cancer[230] and glioblastoma[226]. Ubiquitous LRIG2 knockout mice were protected against glioblastoma, demonstrating that LRIG2 plays a crucial role in glioblastoma initiation and progression[212]. It was shown that the extracellular domain of the transmembrane LRIG2 protein is the part of the protein that is required to mediate the proliferative effect during glioblastoma progression[227]. This is an important finding as the extracellular domain of a protein is usually a more amenable drug target. Nevertheless, tumorigenic activity of LRIG proteins is often tissue-specific[209,225,242] and nothing is known about the function of LRIG2 in the skin and skin tumorigenesis. We identified LRIG2 expression in a human keratinocyte cell line (HaCaT), in an epidermal tumor cell line (A431), in a human melanoma cell line (A375), and in human tissue samples of cSCC patients and normal skin. Our study revealed increased LRIG2 expression in cancer cells *in vitro*, indicating a tumorigenic function of LRIG2. Interestingly, LRIG2 expression is mostly cytoplasmic in normal, basal epidermis, but nuclear in more differentiated epidermal layers and in cancer cells. LRIG proteins show an altered localization in psoriasis[210]. The nuclear localization of LRIG2 in our cSCC tissue samples can also indicate proliferative and pathogenic function.

To investigate the impact of LRIG2 during skin development, homeostasis, and tumorigenesis *in vivo*, we generated a skin-specific LRIG2-TG mouse model. Long-term studies of the mouse line revealed no major phenotypical changes under homeostatic conditions. LRIG2 has no impact on epidermal thickness, sebaceous gland size, epidermal differentiation or proliferation. By employing proteomic analysis, we identified THBS1 as a potential binding-partner of LRIG2. THBS1 attracted our attention because of its EGF-like motifs[310], its function in the modulation of the ECM, angiogenesis and its implication in SCC and other types of cancer[307,308,311,312]. The binding of THBS1 could be related to an increase of pro-MMP2 and active MMP2, which is essential for tumor cell invasion, inflammation or neovascularization[313]. While these effects of LRIG2 have no obvious impact on skin homeostasis, LRIG2-TG mice showed an increased tumor progression compared to control littermates during two-stage chemical skin carcinogenesis. Animals showed no differences in tumor initiation, but at the end of the experiment, 58% of all

LRIG2-TG mice, but only 10% of all controls developed skin tumors resembling human cSCCs. LRIG2-TG mice showed downward invasion of atypical cells, neovascularization, and inflammation, accompanied by KRT8 expression and the loss of epidermal differentiation markers. Additionally, the decreased expression of CDH1 and concomitant increase of VIM suggest an epithelial-mesenchymal transition[314,315] in LRIG2-TG animals, a process essential for cell-cell interaction and cSCC progression. Analysis of ERBB receptor expression revealed an increase of EGFR and ERBB4 and their downstream targets MAPK and AKT. The autonomous EGFR and ERBB4 receptors are important for tissue development and homeostasis, but they also play a major role in tumorigenesis and particularly during skin cancer[99,101,109]. Additionally, we found the ICD of ERBB4 increased in cSCC tissue samples of LRIG2-TG mice, which may act as a transcription factor and have an important impact on tumorigenesis[136,316]. Increased levels of phosphorylated MAPK and AKT and the concomitant loss of PTEN phosphatase activity are often observed in rapid and aggressive tumorigenesis[317,318]. LRIG2 overexpression seems to influence tumor suppressor PTEN activity, which may explain the dramatic phenotype during skin carcinogenesis and the absence of effects in skin homeostasis. Phosphorylation and thus inactivation of PTEN at residues Ser380/Thr382/383 is significantly increased in LRIG2-TG mice 24 weeks after initiation of chemically induced tumorigenesis[318]. However, as the altered molecular signaling may reflect the differences between papillomata and cSCC tissue, we additionally analyzed tumor initiation in the transgenic LRIG2 model. To investigate the very early tumor initiation in more detail, we performed an epidermal hyperplasia experiment by a single TPA application. LRIG2-TG mice showed increased inflammatory cell infiltration and neovascularization, which can be an indication for tumor promotion and progression. These findings were additionally confirmed by an increase of IL1A expression[319], as well as by up-regulation of ERBB2 and ERBB4, in the skin of LRIG2-TG mice. However, EGFR was not increasingly expressed or phosphorylated at this early stage, but the increased expressed PTEN amount seems to be phosphorylated and thus inactivated. Inactivation of PTEN plays an important role in human cSCC development[320,321], consequently the loss of PTEN's tumor suppressive function might be an important element of LRIG2-mediated tumor progression during skin cancer. Furthermore, it was shown that THBS1 up-regulates MMP9 expression in endothelial cells and promotes tumor cell invasion[311]. We found THBS1 and concomitant MMP9 increase in LRIG2-TG mice 48 h after TPA application, indicating a correlation between THBS1 expression and LRIG2-mediated tumor initiation and progression[312]. THBS1 may induce angiogenesis in tumors, influence tumor cell adhesion, migration, invasion, and metastasis both *in vitro* and *in vivo*[322]. Additionally, THBS1 is expressed in

tumor cells, showing tumor progressive function and THBS1 also induce auto-phosphorylation of EGFR in A431 cells[323], supporting a relationship to the ERBB receptor system. However, the increase of inflammatory cells like macrophages and monocytes may also have led to the increase of THBS1[324]. Our findings during early hyperproliferative stages point to a tumor promoting influence of LRIG2 excess. Contradictory, we found no alterations in THBS1 or MMP levels during skin carcinogenesis. The upregulation of pro-MMP9 during TPA approach and the increase of pro- and active MMP2 may be overlaid by a general increase of MMP2 and MMP9 in cSCC as previously described[325].

4-2.6 **Conclusions**

In conclusion, our study reveals an important function of LRIG2 during skin carcinogenesis. In human skin, LRIG2 is expressed in the HF and in the basal layer of the epidermis, and our preliminary data indicates that its expression is increased in skin cancer cell lines as well as in human cSCC samples. Even though LRIG2 overexpression has no obvious major impact on skin development and homeostasis, LRIG2 may promote tumor growth and induces a more severe carcinogenic phenotype, possibly by inactivating the tumor suppressor PTEN. Our results show an early onset of cSCC in LRIG2-TG mice during two-stage chemical skin carcinogenesis accompanied by altered ERBB signaling.

4-3 Supplementary material

In the following all supplementary figures and tables of the manuscript "The transmembrane protein LRIG2 increases tumor progression in skin carcinogenesis" are depicted.

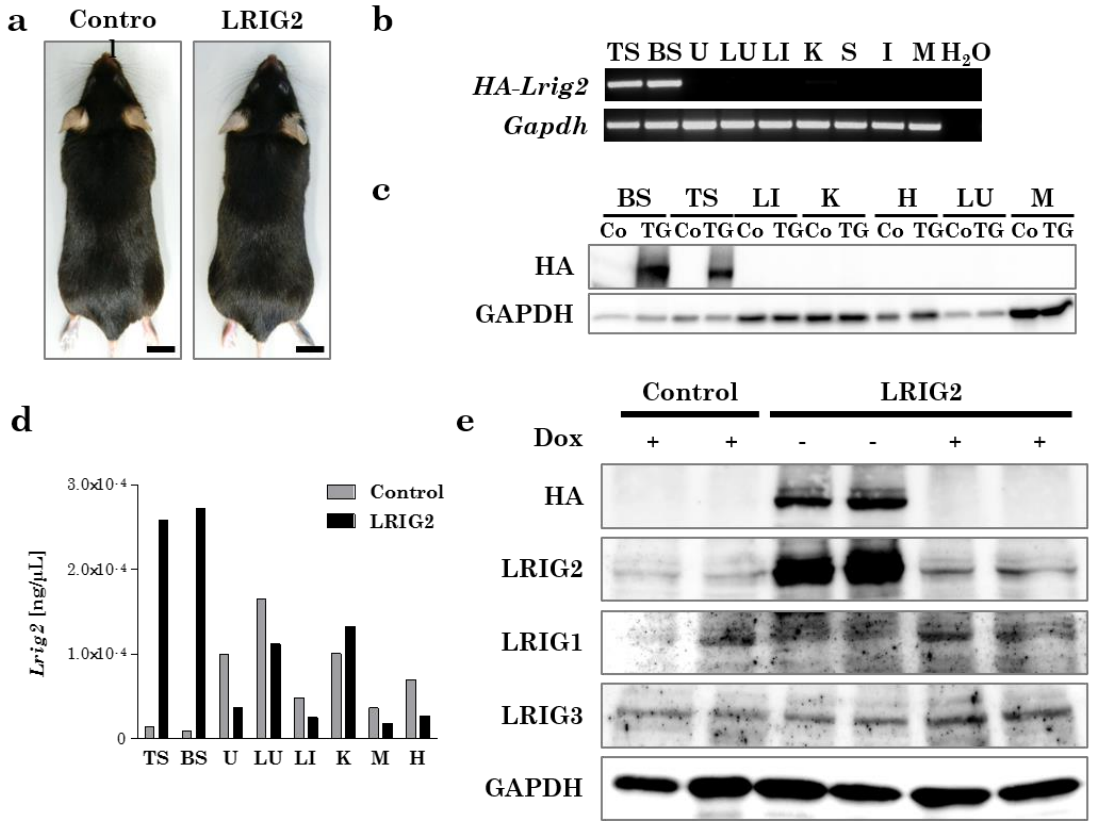

Figure 4-7 Figure S1.
(a) Macroscopic appearance of a representative LRIG2-TG animal and a control littermate. Scale bars represent 1 cm. **(b)** Reverse transcription PCR shows transgene expression only in tail and back skin. *Gapdh* was used as reference gene. **(c)** Western blot analysis revealed the expression of a HA-tag only in the skin of TG mice. GAPDH was used as reference protein. **(d)** Quantification of *Lrig2* mRNA in indicated organs by quantitative real-time PCR. **(e)** Western blot analysis of HA-tag and LRIG proteins of the back skin of LRIG2-TG mice and control littermates. To inhibit LRIG2-TG overexpression doxycycline (3 mg/mL) was added to the drinking water for two weeks. GAPDH was used as reference protein. All mice were female and six months old when they were dissected. TS: tail skin, BS: back skin, U: uterus, LU: lung, LI: liver, K: kidney, S: spleen, I: intestine, M: muscle, H: heart, Dox: doxycycline, +: mice received 3 mg/ml Dox in the drinking water for two weeks, -: mice received no Dox.

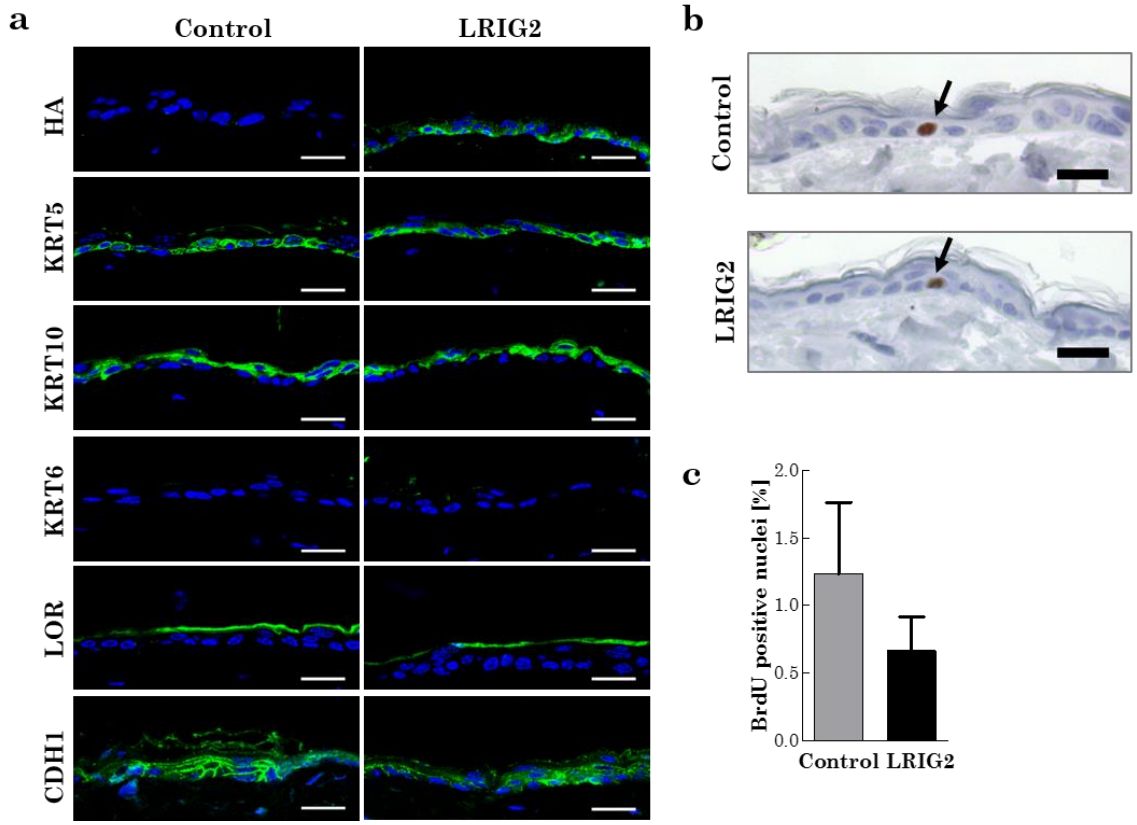

Figure 4-8 Figure S2.
(a) Immunofluorescence staining against the differentiation markers KRT5, KRT10, KRT6, LOR, CDH1 and the HA-tag (all in green) using back skin sections of six-month-old control and LRIG2-TG mice. Cell nuclei are stained with DAPI (blue). **(b)** BrdU staining of back skin of a twelve-month-old TG and control mouse. Arrows indicate BrdU positive, proliferating cells. **(c)** Proliferation index is not altered in LRIG2-TG mice compared to controls. Data are presented as mean+SD and were analyzed by Student's *t*-test. Scale bars in **(a)** and **(b)** represent 20 µm.

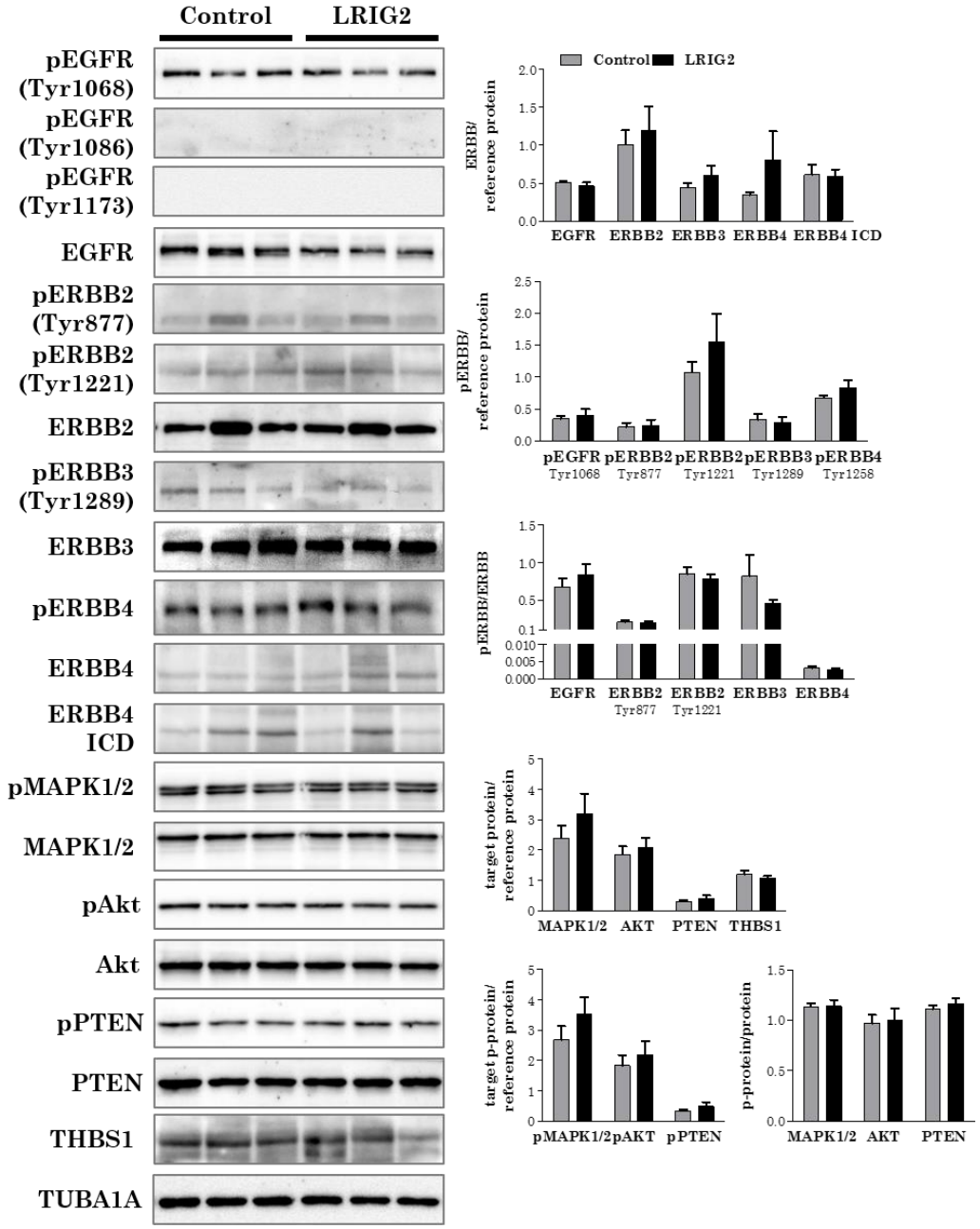

Figure 4-9 Figure S3.
Western blot and densitometrical analysis of phosphorylated and non-phosphorylated ERBB receptors, MAPK1/2, AKT and PTEN and THBS1 of the back skin of twelve-month-old LRIG2-TG mice and control littermates. TUBA1A was used as reference protein. Data are presented as mean+SEM and were analyzed by Student's *t*-test.

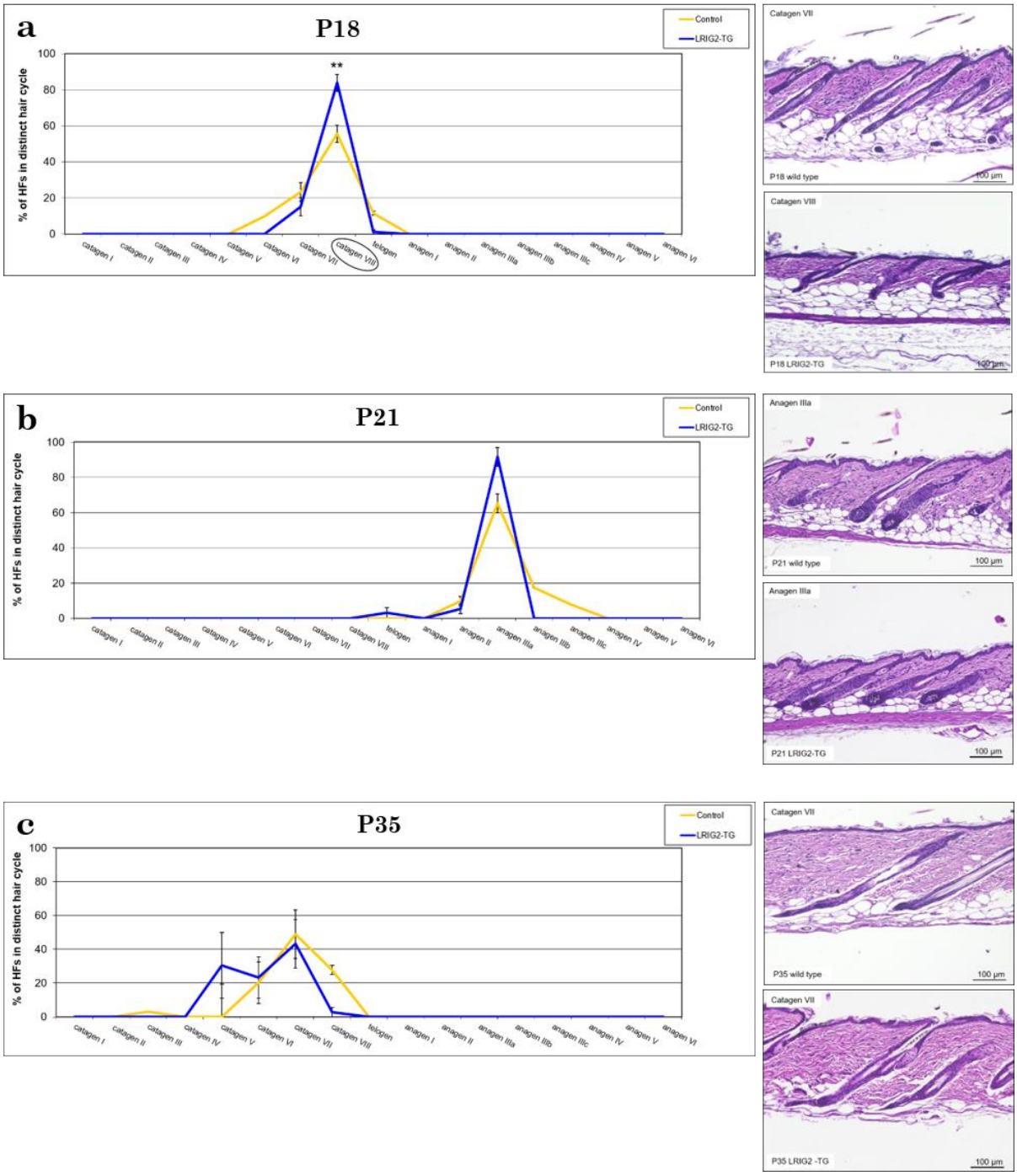

Figure 4-10 Figure S4.
The hair follicle cycle in LRIG2-TG mice. Hair follicles (HFs) of controls and LRIG2-TG mice on days post partum (P) 18, 21 and 35 were evaluated according to the HF cycling phases as described elsewhere[31]. The total number (%) of HFs in distinct HF cycle phases was counted in LRIG2-TG and wild type mice; mean ± SEM, using Mann-Whitney *U*-test, $^{**}P \leq 0.01$, n= 3-5, representative H&E stainings of a LRIG2-TG and a control mouse are shown for each P. Scale bars represent 100 µm. **(a)** LRIG2-TG mice on P18 show significantly more HFs in the late catagen phase VIII compared to controls. **(b)** There are no differences in HF cycle phases on P21 between control and LRIG2-TG mice. **(c)** No remarkable differences in the HF cycle phases on P35 can be found between control and LRIG2-TG mice.

a

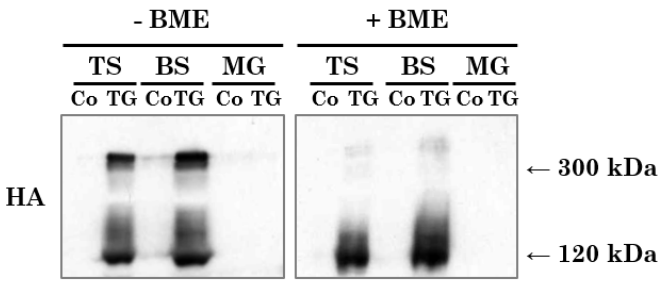

b

	Protein	Molecular Weight		Protein	Molecular Weight
1	KRT71	57 kDa	11	ATP1B3	56 kDa
2	KRT31	47 kDa	12	HSPA1A	70 kDa
3	KRT27	49 kDa	13	ACTN3	103 kDa
4	LAMB1	197 kDa	14	ACTN2	104 kDa
5	KRT83	55 kDa	15	UBA1	118 kDa
6	KRT75	60 kDa	16	LRIG2	118 kDa
7	**THSB1**	**130 kDa**	17	LAMA2	343 kDa
8	TPM2	33 kDa	18	MDH2	36 kDa
9	PYGM	97 kDa	19	ANXA2	39 kDa
10	SLC4A1	103 kDa	20	PADI2	76 kDa

c

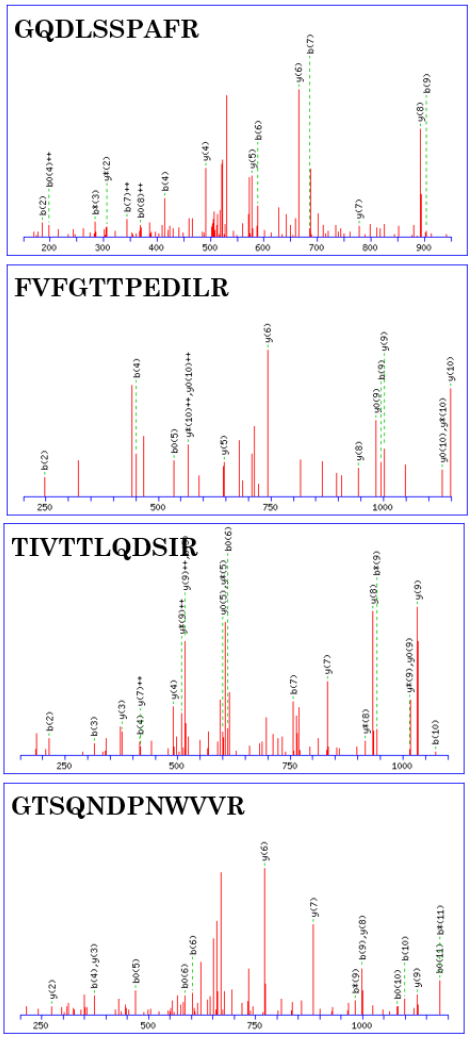

d

Sequence	Prob	Mascot Ion score	Observed	Actual Mass	Charge	Delta Da	Delta PPM	Start - End
(K)GQDLSSPAFR(I)	100%	26.29	539.2702	1,076.53	2	0.0006781	0.6293	51 - 60
(R)FVFGTTPEDILR(N)	100%	27.49	697.87	1,393.73	2	0.001078	0.7729	217 - 228
(R)FVFGTTPEDILR(N)	100%	28.29	697.8701	1,393.73	2	0.001278	0.9163	217 - 228
(R)TIVTTLQDSIR(K)	100%	37.36	623.8544	1,245.69	2	0.001178	0.9449	289 - 299
(R)TIVTTLQDSIR(K)	100%	25.02	623.8541	1,245.69	2	0.0005781	0.4637	289 - 299
(K)GTSQNDPNWVVR(H)	100%	30.49	686.8333	1,371.65	2	-0.001122	-0.8173	969 - 980

Figure 4-11 Figure S5.
(a) Western blot analysis reveals an additional signal for LRIG2 at 300 kDa under non-reducing conditions. Co: control, TG: transgen, TS: tail skin, BS: back skin, MG: mammary gland, +/-BME: with/without beta-Mercaptoethanol. **(b)** List of top 20 proteins which were exclusively identified around 300 kDa in LRIG2-TG samples and not in controls sorted by total spectral counts of the non-reduced LRIG2-TG protein fraction. **(c)** Spectra of four individual TSP1 peptides. **(d)** Identified TSP1 peptides with probability and MASCOT scores.

Table 4-1 Table S1.
Antibodies employed for Western blot (WB) analysis, immunoprecipitation (IP), immunohistochemistry (IHC), and immunofluorescence(IF).

Antigen	**Antibody**	**App.**	**Host**	**Dilution**
LRIG2	GeneTex, Alton Pkwy Irvine, CA, USA, #37384	WB	rabbit	1:500
LRIG2	LSBio, Seattle, WA, USA, #C165865	IHC	rabbit	1:100
LRIG2	Abcam, Cambridge, UK, #121472	WB	rabbit	1:500
HA-tag	Cell Signaling, Boston, MA, USA, #3724	WB/IF	rabbit	1:1000/1:200
HA-tag	Abcam, Cambridge, UK, #9110	WB/IP	rabbit	1:5000
LRIG1	R&D Systems, Minneapolis, MN, USA, #AF3688	WB	goat	1:2500
LRIG3	R&D Systems, Minneapolis, MN, USA, #MAB3495	WB	mouse	1:1000
p-EGFR (Tyr 1068)	Cell Signaling, Boston, MA, USA, #3777	WB	rabbit	1:1000
p-EGFR (Tyr 1086)	Cell Signaling, Boston, MA, USA, #2220	WB	rabbit	1:1000
p-EGFR (Tyr 1173)	Santa Cruz, Heidelberg, Germany, #12351,	WB	rabbit	1:500
EGFR	Santa Cruz, Heidelberg, Germany, #03,	WB	rabbit	1:500
EGFR	R&D Systems, Minneapolis, MN, USA, #AF1280	IF	goat	1:200
p-ERBB2 (Tyr 877)	Cell Signaling, Boston, MA, USA, #2241	WB	rabbit	1:1000
p-ERBB2 (Tyr 1221)	Cell Signaling, Boston, MA, USA, #2243	WB	rabbit	1:1000
ERBB2	Cell Signaling, Boston, MA, USA, #4290	WB	rabbit	1:1000
ERBB2	R&D Systems, Minneapolis, MN, USA, #AF5176	IF	sheep	1:200
p-ERBB3 (Tyr 1289)	Cell Signaling, Boston, MA, USA, #4791	WB	rabbit	1:1000
ERBB3	Cell Signaling, Boston, MA, USA, #12708	WB	rabbit	1:1000
ERBB3	R&D Systems, Minneapolis, MN, USA, #AF4518	IF	sheep	1:1000
p-ERBB4 (Tyr 1258)	Abcam, Cambridge, UK, #76132	WB	rabbit	1:1000

ERBB4	Santa Cruz, Heidelberg, Germany, #283	WB	rabbit	1:500
ERBB4	Santa Cruz, Heidelberg, Germany, #8050	WB/IF	mouse	1:500/1:50
THBS1	Cell Signaling, Boston, MA, USA, #37879	WB	rabbit	1:1000
p-MAPK1/2 (Thr202/Tyr204)	Cell Signaling, Boston, MA, USA, #4370	WB	rabbit	1:1000
MAPK1/2	Cell Signaling, Boston, MA, USA, #9102	WB	rabbit	1:1000
p-AKT (Ser 473)	Cell Signaling, Boston, MA, USA, #4060	WB	rabbit	1:2000
AKT	Cell Signaling, Boston, MA, USA, #4691	WB	rabbit	1:1000
p-PTEN (Ser380/Thr382/383)	Cell Signaling, Boston, MA, USA, #9554	WB	rabbit	1:1000
PTEN	Cell Signaling, Boston, MA, USA, #9552	WB	rabbit	1:1000
PCNA	Cell Signaling, Boston, MA, USA, #13110	WB	rabbit	1:1000
CASP3	Cell Signaling, Boston, MA, USA, #9662	WB	rabbit	1:1000
IL1A	R&D Systems, Minneapolis, MN, USA, #AF400NA	WB	goat	1:2000
IL6	Cell Signaling, Boston, MA, USA, #12912	WB	rabbit	1:1000
MKI67	Dianova, Hamburg, Germany, #M7249	IHC	Rat	1:200
KRT5	BioLegend, San Diego, CA, USA, #905501	IF	rabbit	1:800
KRT6	BioLegend, San Diego, CA, USA, #905701	IF	rabbit	1:800
KRT8	BioLegend, San Diego, CA, USA, #904801	IF	mouse	1:200
KRT10	BioLegend, San Diego, CA, USA, #905701	IF	rabbit	1:800
LOR	BioLegend, San Diego, CA, USA, #905101	IF	rabbit	1:800
CDH1	R&D Systems, Minneapolis, MN, USA, #AF748	IF	goat	1:200
VIM	Cell Signaling, Boston, MA, USA, #5741	IF	rabbit	1:200
TUBA1A	Cell Signaling, Boston, MA, USA, #2125	WB	rabbit	1:1000

GAPDH	Cell Signaling, Boston, MA, USA, #2118	WB	rabbit	1:5000
BrdU	AbDSeroTec, Puchheim, Germany, #OBT0030	IHC	rat	1:100
donkey α rabbit	Jackson ImmunoResearch, Ely, UK, #711-546-152	IF	donkey	1:1000
donkey α goat	Jackson ImmunoResearch, Ely, UK, #705-545-147	IF	donkey	1:1000
donkey α sheep	Jackson ImmunoResearch, Ely, UK, #713-586-147	IF	donkey	1:1000
donkey α mouse	Jackson ImmunoResearch, Ely, UK, #715-585-140	IF	donkey	1:1000
mouse α rat	Jackson ImmunoResearch, Ely, UK, #212-066-168	IHC	mouse	1:100
rabbit α rat	AbDSeroTec, Puchheim, Germany, #STAR21B	ICH	rabbit	1:100
rabbit α mouse	Cell Signaling, Boston, MA, USA, #7076	WB	rabbit	1:2500
goat α rabbit	Cell Signaling, Boston, MA, USA, #7074	WB	goat	1:2500
goat α rat	Cell Signaling, Boston, MA, USA, #7077	WB	Goat	1:2500
donkey α goat	R&D Systems, Minneapolis, MN, USA, #HAF109	WB	donkey	1:2500

4-4 Conclusion and outlook

LRIG2 excess in the epidermis showed no impact on skin homeostasis. However, the TG mouse model revealed THBS1 as binding partner of LRIG2, indicating a role for LRIG2 in tumor progression, modulation of the ECM or angiogenesis[308,311,312]. After challenging the skin with a single application of TPA, thereby inducing epidermal hyperplasia and inflammation, or in the two-stage chemical carcinogenesis experiment, LRIG2 overexpression caused increased inflammation and accelerated tumor progression. The early onset of cSCC in TG mice may has been triggered by inactivation of the tumor suppressor PTEN and is accompanied by an altered ERBB signaling network. Even though we cannot exclude, that the effect on EGFR and ERBB4 expression reflects the difference between severely and benignly affected tumor tissue, the mouse model clearly revealed a tumor progressive function of LRIG2 in cSCC as previously reported for other cancers[226,227,230,242]. Therefore, LRIG2 might be a promising target for cSCC treatment. The inhibition of LRIG2 is possibly a suitable alternative for surgery or conventional radio- or chemotherapy and probably more specific than anti-EGFR targeted therapy to overcome severe side effects[71,91]. However, the molecular mechanism of LRIG2 in the skin has to be analyzed in more detail to confirm this hypothesis. In contrast, LRIG1 and LRIG3 act as tumor suppressors in duodenal adenomas[219], prostate cancer[241] or glioblastoma[240,252,255] and are related to good prognoses in various tumors[229,245,246]. Consequently, both LRIGs may also be potential prognostic factors in the skin and promising molecules to develop novel strategies for tumor therapy. Recent studies revealed, that LRIG1 expression significantly correlated with the sensitivity to conventional chemotherapeutics, most likely due to altered EGFR signaling[231]. The internalization of EGFR is a common repair mechanism upon DNA damage and often the reason for insensitivity to chemotherapy[326]. LRIG1 might influence this process and thus reduce nuclear EGFR activity, thereby increasing apoptosis, as it has been shown in bladder cancer[327]. In Chapter 3 it was shown that epidermal EGFR expression is decreased due to LRIG1 overexpression during skin homeostasis. According to this, a tumor suppressive function of LRIG1 in the skin is very likely and the transmembrane protein may represent an auspicious protein for novel therapies and prophylactic measures. The two-stage chemical carcinogenesis in LRIG1-TG mice allows the study of LRIG1 function during skin tumorigenesis, similar to the experiments with LRIG2-TG mice, shown in this chapter. However, our preliminary data suggest the opposite of this hypothesis. LRIG1-TG mice revealed an increased papillomata incidence in the DMBA/TPA mouse model. TG animals developed melanocytic nevi, which

often transform into invasive melanoma in humans, possibly due to an effect of shed LRIG1 on melanocytes. These results demonstrate the importance of investigating the molecular mechanisms of LRIG proteins tissue-specifically.

In conclusion, LRIG function in the skin seems to be very distinct. While LRIG1-TG mice show a severe phenotype during homeostasis (see Chapter 3), LRIG2 overexpression revealed no major phenotype. However, during carcinogenesis, the excess of both LRIGs in the epidermis triggers tumorigenesis, although in a different manner. The LRIGs represent a very versatile protein family with intriguing functions in the skin. Future studies on their molecular mechanisms and interaction partners in the skin are needed to elucidate their precise role in cSCC and their potential as prognostic factors or drug targets for tumor therapy.

References

1 Kolarsick, P. A. J., Kolarsick, M. A. & Goodwin, C. Anatomy and Physiology of the Skin. *Journal of the Dermatology Nurses' Association* **3**, 203-213, (2011).

2 Gallo, R. L. Human Skin Is the Largest Epithelial Surface for Interaction with Microbes. *J. Invest. Dermatol.* **137**, 1213-1214, (2017).

3 Blanpain, C. & Fuchs, E. Epidermal stem cells of the skin. *Annu. Rev. Cell Dev. Biol.* **22**, 339-373, (2006).

4 Fuchs, E. Skin stem cells: rising to the surface. *J. Cell Biol.* **180**, 273-284, (2008).

5 Fuchs, E. Keratins and the skin. *Annu. Rev. Cell Dev. Biol.* **11**, 123-153, (1995).

6 Casey, G. Physiology of the skin. *Nurs Stand* **16**, 47-51; quiz 53, 55, (2002).

7 Losquadro, W. D. Anatomy of the Skin and the Pathogenesis of Nonmelanoma Skin Cancer. *Facial Plast. Surg. Clin. North Am.* **25**, 283-289, (2017).

8 Wong, R., Geyer, S., Weninger, W., Guimberteau, J. C. & Wong, J. K. The dynamic anatomy and patterning of skin. *Exp. Dermatol.* **25**, 92-98, (2016).

9 Kretzschmar, K. & Watt, F. M. Markers of epidermal stem cell subpopulations in adult mammalian skin. *Cold Spring Harbor Perspect. Med.* **4**, (2014).

10 Cichorek, M., Wachulska, M., Stasiewicz, A. & Tymińska, A. Skin melanocytes: biology and development. *Postepy Dermatol. Alergol.* **30**, 30-41, (2013).

11 Brenner, M. & Hearing, V. J. The protective role of melanin against UV damage in human skin. *Photochem. Photobiol.* **84**, 539-549, (2008).

12 Rajesh, A., Wise, L. & Hibma, M. The role of Langerhans cells in pathologies of the skin. *Immunol. Cell Biol.*, (2019).

13 Van Keymeulen, A. *et al.* Epidermal progenitors give rise to Merkel cells during embryonic development and adult homeostasis. *J. Cell Biol.* **187**, 91-100, (2009).

14 Moll, I. *et al.* Human Merkel cells – aspects of cell biology, distribution and functions. *Eur. J. Cell Biol.* **84**, 259-271, (2005).

15 Lucarz, A. & Brand, G. Current considerations about Merkel cells. *Eur. J. Cell Biol.* **86**, 243-251, (2007).

16 Alam, H., Sehgal, L., Kundu, S. T., Dalal, S. N. & Vaidya, M. M. Novel function of keratins 5 and 14 in proliferation and differentiation of stratified epithelial cells. *Mol. Biol. Cell* **22**, 4068-4078, (2011).
17 Albers, K. M. Keratin biochemistry. *Clin Dermatol.* **14**, 309-320, (1996).
18 Vaezi, A., Bauer, C., Vasioukhin, V. & Fuchs, E. Actin cable dynamics and Rho/Rock orchestrate a polarized cytoskeletal architecture in the early steps of assembling a stratified epithelium. *Dev. Cell* **3**, 367-381, (2002).
19 Nithya, S., Radhika, T. & Jeddy, N. Loricrin - an overview. *J. Oral Maxillofac. Pathol.* **19**, 64-68, (2015).
20 Watt, F. M. Involucrin and Other Markers of Keratinocyte Terminal Differentiation. *J. Invest. Dermatol.* **81**, S100-S103, (1983).
21 Kezic, S. & Jakasa, I. Filaggrin and Skin Barrier Function. *Curr. Probl. Dermatol.* **49**, 1-7, (2016).
22 Candi, E., Schmidt, R. & Melino, G. The cornified envelope: a model of cell death in the skin. *Nat. Rev. Mol. Cell Biol.* **6**, 328-340, (2005).
23 Gurtner, G. C., Werner, S., Barrandon, Y. & Longaker, M. T. Wound repair and regeneration. *Nature* **453**, 314-321, (2008).
24 Mesa, K. R. *et al.* Homeostatic Epidermal Stem Cell Self-Renewal Is Driven by Local Differentiation. *Cell Stem Cell* **23**, 677-686.e674, (2018).
25 Alcolea, M. P. & Jones, P. H. Lineage analysis of epidermal stem cells. *Cold Spring Harbor Perspect. Med.* **4**, a015206, (2014).
26 Mackenzie, I. C. Retroviral transduction of murine epidermal stem cells demonstrates clonal units of epidermal structure. *J. Invest. Dermatol.* **109**, 377-383, (1997).
27 Ghazizadeh, S. & Taichman, L. B. Multiple classes of stem cells in cutaneous epithelium: a lineage analysis of adult mouse skin. *EMBO J.* **20**, 1215-1222, (2001).
28 Schneider, M. R. & Yarden, Y. The EGFR-HER2 module: a stem cell approach to understanding a prime target and driver of solid tumors. *Oncogene* **35**, 2949-2960, (2016).
29 Watt, F. M., Estrach, S. & Ambler, C. A. Epidermal Notch signalling: differentiation, cancer and adhesion. *Curr. Opin. Cell Biol.* **20**, 171-179, (2008).
30 Nakatsuji, T. *et al.* The microbiome extends to subepidermal compartments of normal skin. *Nat. Commun.* **4**, 1431, (2013).
31 Muller-Rover, S. *et al.* A comprehensive guide for the accurate classification of murine hair follicles in distinct hair cycle stages. *J. Invest. Dermatol.* **117**, 3-15, (2001).
32 Kaufman, C. K. *et al.* GATA-3: an unexpected regulator of cell lineage determination in skin. *Genes Dev.* **17**, 2108-2122, (2003).
33 Matsuo, K., Mori, O. & Hashimoto, T. J. A. o. D. R. Apoptosis in murine hair follicles during catagen regression. *Arch. Dermatol. Res.* **290**, 133-136, (1998).
34 Lindner, G. *et al.* Analysis of apoptosis during hair follicle regression (catagen). *Am. J. Pathol.* **151**, 1601-1617, (1997).
35 Trempus, C. S. *et al.* Enrichment for living murine keratinocytes from the hair follicle bulge with the cell surface marker CD34. *J. Invest. Dermatol.* **120**, 501-511, (2003).
36 Cotsarelis, G., Sun, T. T. & Lavker, R. M. Label-retaining cells reside in the bulge area of pilosebaceous unit: implications for follicular stem cells, hair cycle, and skin carcinogenesis. *Cell* **61**, 1329-1337, (1990).
37 Blanpain, C., Lowry, W. E., Geoghegan, A., Polak, L. & Fuchs, E. Self-renewal, multipotency, and the existence of two cell populations within an epithelial stem cell niche. *Cell* **118**, 635-648, (2004).
38 Morris, R. J. *et al.* Capturing and profiling adult hair follicle stem cells. *Nat. Biotechnol.* **22**, 411-417, (2004).

39 Oshima, H., Rochat, A., Kedzia, C., Kobayashi, K. & Barrandon, Y. Morphogenesis and renewal of hair follicles from adult multipotent stem cells. *Cell* **104**, 233-245, (2001).

40 Oliver, R. F. & Jahoda, C. A. B. Dermal-epidermal interactions. *Clin Dermatol.* **6**, 74-82, (1988).

41 Schneider, M. R., Schmidt-Ullrich, R. & Paus, R. The Hair Follicle as a Dynamic Miniorgan. *Curr. Biol.* **19**, R132-R142, (2009).

42 Millar, S. E. Molecular mechanisms regulating hair follicle development. *J. Invest. Dermatol.* **118**, 216-225, (2002).

43 Jensen, K. B. *et al.* Lrig1 expression defines a distinct multipotent stem cell population in mammalian epidermis. *Cell Stem Cell* **4**, 427-439, (2009).

44 Jensen, U. B. *et al.* A distinct population of clonogenic and multipotent murine follicular keratinocytes residing in the upper isthmus. *J. Cell Sci.* **121**, 609-617, (2008).

45 Horsley, V. *et al.* Blimp1 defines a progenitor population that governs cellular input to the sebaceous gland. *Cell* **126**, 597-609, (2006).

46 Nijhof, J. G. *et al.* The cell-surface marker MTS24 identifies a novel population of follicular keratinocytes with characteristics of progenitor cells. *Development* **133**, 3027-3037, (2006).

47 Watt, F. M. The stem cell compartment in human interfollicular epidermis. *J. Dermatol. Sci.* **28**, 173-180, (2002).

48 Frances, D. & Niemann, C. Stem cell dynamics in sebaceous gland morphogenesis in mouse skin. *Dev. Biol.* **363**, 138-146, (2012).

49 Hall, P. A. & Watt, F. M. Stem cells: the generation and maintenance of cellular diversity. *Development* **106**, 619-633, (1989).

50 Spradling, A., Drummond-Barbosa, D. & Kai, T. Stem cells find their niche. *Nature* **414**, 98-104, (2001).

51 Watt, F. M. & Jensen, K. B. Epidermal stem cell diversity and quiescence. *EMBO Mol. Med.* **1**, 260-267, (2009).

52 Watt, F. M. & Hogan, B. L. Out of Eden: stem cells and their niches. *Science* **287**, 1427-1430, (2000).

53 Lin, H. The stem-cell niche theory: lessons from flies. *Nat. Rev. Cancer* **3**, 931-940, (2002).

54 Dry, F. W. The coat of the mouse (Mus musculus). *J. Genet.*, 287-340 (1926).

55 Geyfman, M., Plikus, M. V., Treffeisen, E., Andersen, B. & Paus, R. Resting no more: re-defining telogen, the maintenance stage of the hair growth cycle. *Biol. Rev. Cambridge Philos. Soc.* **90**, 1179-1196, (2015).

56 Ito, M. *et al.* Stem cells in the hair follicle bulge contribute to wound repair but not to homeostasis of the epidermis. *Nat. Med.* **11**, 1351-1354, (2005).

57 Koch, P. J. *et al.* Desmoglein 3 anchors telogen hair in the follicle. *J. Cell Sci.* **111 (Pt 17)**, 2529-2537, (1998).

58 Stenn, K. S. & Paus, R. Controls of hair follicle cycling. *Physiol. Rev.* **81**, 449-494, (2001).

59 Lim, H. W. *et al.* The burden of skin disease in the United States. *J. Am. Acad. Dermatol.* **76**, 958-972.e952, (2017).

60 Leiter, U., Eigentler, T. & Garbe, C. Epidemiology of skin cancer. *Adv. Exp. Med. Biol.* **810**, 120-140, (2014).

61 Perera, E. & Sinclair, R. An estimation of the prevalence of nonmelanoma skin cancer in the U.S. *F1000Res* **2**, 107, (2013).

62 Lomas, A., Leonardi-Bee, J. & Bath-Hextall, F. A systematic review of worldwide incidence of nonmelanoma skin cancer. *Br. J. Dermatol.* **166**, 1069-1080, (2012).

63 WHO. http://www.who.int/uv/faq/skincancer/en/index1.html, 2019).

64 Tan, S. T., Ghaznawie, M., Heenan, P. J. & Dosan, R. Basal Cell Carcinoma Arises from Interfollicular Layer of Epidermis. *J. Oncol.* **2018**, 3098940, (2018).

65 Lapouge, G. *et al.* Identifying the cellular origin of squamous skin tumors. *Proc. Natl. Acad. Sci. U. S. A.* **108**, 7431-7436, (2011).

66 Sanchez-Danes, A. & Blanpain, C. Deciphering the cells of origin of squamous cell carcinomas. *Nat. Rev. Cancer* **18**, 549-561, (2018).

67 Apalla, Z., Nashan, D., Weller, R. B., Castellsagué, X. J. D. & Therapy. Skin Cancer: Epidemiology, Disease Burden, Pathophysiology, Diagnosis, and Therapeutic Approaches. *Dermatol. Ther.* **7**, 5-19, (2017).

68 Didona, D., Paolino, G., Bottoni, U. & Cantisani, C. Non Melanoma Skin Cancer Pathogenesis Overview. *Biomedicines* **6**, (2018).

69 Boukamp, P. Non-melanoma skin cancer: what drives tumor development and progression? *Carcinogenesis* **26**, 1657-1667, (2005).

70 Erb, P., Ji, J., Kump, E., Mielgo, A. & Wernli, M. Apoptosis and pathogenesis of melanoma and nonmelanoma skin cancer. *Adv. Exp. Med. Biol.* **624**, 283-295, (2008).

71 Griffin, L. L., Ali, F. R. & Lear, J. T. Non-melanoma skin cancer. *Clin. Med. (Lond)* **16**, 62-65, (2016).

72 Odenbro, A., Bellocco, R., Boffetta, P., Lindelöf, B. & Adami, J. Tobacco smoking, snuff dipping and the risk of cutaneous squamous cell carcinoma: a nationwide cohort study in Sweden. *Br. J. Cancer* **92**, 1326-1328, (2005).

73 Silverberg, M. J. *et al.* HIV infection status, immunodeficiency, and the incidence of non-melanoma skin cancer. *J. Natl. Cancer Inst.* **105**, 350-360, (2013).

74 Herman, S., Rogers, H. D. & Ratner, D. Immunosuppression and squamous cell carcinoma: a focus on solid organ transplant recipients. *Skinmed* **6**, 234-238, (2007).

75 Kim, Y. & He, Y. Y. Ultraviolet radiation-induced non-melanoma skin cancer: Regulation of DNA damage repair and inflammation. *Genes Dis.* **1**, 188-198, (2014).

76 Calzavara-Pinton, P., Ortel, B. & Venturini, M. Non-melanoma skin cancer, sun exposure and sun protection. *G. Ital. Dermatol. Venereol.* **150**, 369-378, (2015).

77 Brash, D. E. *et al.* A role for sunlight in skin cancer: UV-induced p53 mutations in squamous cell carcinoma. *Proc. Natl. Acad. Sci. U. S. A.* **88**, 10124-10128, (1991).

78 Black, A. P. & Ogg, G. S. The role of p53 in the immunobiology of cutaneous squamous cell carcinoma. *Clin. Exp. Immunol.* **132**, 379-384, (2003).

79 Rosso, S. *et al.* The multicentre south European study 'Helios'. II: Different sun exposure patterns in the aetiology of basal cell and squamous cell carcinomas of the skin. *Br. J. Cancer* **73**, 1447-1454, (1996).

80 Tojo, M. *et al.* Expression of sonic hedgehog signal transducers, patched and smoothened, in human basal cell carcinoma. *Pathol. Int.* **49**, 687-694, (1999).

81 Epstein, E. H. Basal cell carcinomas: attack of the hedgehog. *Nat. Rev. Cancer* **8**, 743-754, (2008).

82 T. Lopez, A., Liu, L. & Geskin, L. (2018).

83 Yamamoto, T. *et al.* High incidence of amplification of the epidermal growth factor receptor gene in human squamous carcinoma cell lines. *Cancer Res.* **46**, 414-416, (1986).

84 Rittie, L. *et al.* Differential ErbB1 signaling in squamous cell versus basal cell carcinoma of the skin. *Am. J. Pathol.* **170**, 2089-2099, (2007).

85 Schneider, M. R., Werner, S., Paus, R. & Wolf, E. Beyond wavy hairs: the epidermal growth factor receptor and its ligands in skin biology and pathology. *Am. J. Pathol.* **173**, 14-24, (2008).

86 Nazmi, M. N., Dykes, P. J. & Marks, R. Epidermal growth factor receptors in human epidermal tumours. *Br. J. Dermatol.* **123**, 153-161, (1990).

87 El Abaseri, T. B., Putta, S. & Hansen, L. A. Ultraviolet irradiation induces keratinocyte proliferation and epidermal hyperplasia through the activation of the epidermal growth factor receptor. *Carcinogenesis* **27**, 225-231, (2006).

88 Madson, J. G., Lynch, D. T., Tinkum, K. L., Putta, S. K. & Hansen, L. A. Erbb2 regulates inflammation and proliferation in the skin after ultraviolet irradiation. *Am. J. Pathol.* **169**, 1402-1414, (2006).
89 El Abaseri, T. B. *et al.* Chemoprevention of UV light-induced skin tumorigenesis by inhibition of the epidermal growth factor receptor. *Cancer Res.* **65**, 3958-3965, (2005).
90 Soyer H., A. G., Hofmann-Wellenhof R., Johr R. in *Color Atlas of Melanocytic Lesions of the Skin.* Ch. Chapter V.4, 295-302 (Springer, Berlin, Heidelberg, 2007).
91 Gaffney, D. C., Soyer, H. P. & Simpson, F. The epidermal growth factor receptor in squamous cell carcinoma: An emerging drug target. *Australas. J. Dermatol.* **55**, 24-34, (2014).
92 Scaltriti, M. & Baselga, J. The Epidermal Growth Factor Receptor Pathway: A Model for Targeted Therapy. *Clin. Cancer Res.* **12**, 5268-5272, (2006).
93 Li, T. & Perez-Soler, R. Skin toxicities associated with epidermal growth factor receptor inhibitors. *Target. Oncol.* **4**, 107-119, (2009).
94 Segaert, S. *et al.* Skin toxicities of targeted therapies. *Eur. J. Cancer* **45 Suppl 1**, 295-308, (2009).
95 Ullrich, A. *et al.* Human epidermal growth factor receptor cDNA sequence and aberrant expression of the amplified gene in A431 epidermoid carcinoma cells. *Nature* **309**, 418-425, (1984).
96 Coussens, L. *et al.* Tyrosine kinase receptor with extensive homology to EGF receptor shares chromosomal location with neu oncogene. *Science* **230**, 1132-1139, (1985).
97 Plowman, G. D. *et al.* Molecular cloning and expression of an additional epidermal growth factor receptor-related gene. *Proc. Natl. Acad. Sci. U. S. A.* **87**, 4905-4909, (1990).
98 Plowman, G. D. *et al.* Ligand-specific activation of HER4/p180erbB4, a fourth member of the epidermal growth factor receptor family. *Proc. Natl. Acad. Sci. U. S. A.* **90**, 1746-1750, (1993).
99 Citri, A. & Yarden, Y. EGF-ERBB signalling: towards the systems level. *Nat. Rev. Mol. Cell Biol.* **7**, 505-516, (2006).
100 Roskoski, R., Jr. The ErbB/HER family of protein-tyrosine kinases and cancer. *Pharmacol. Res.* **79**, 34-74, (2014).
101 Yarden, Y. & Sliwkowski, M. X. Untangling the ErbB signalling network. *Nat. Rev. Mol. Cell Biol.* **2**, 127-137, (2001).
102 Schneider, M. R. & Wolf, E. The epidermal growth factor receptor ligands at a glance. *J. Cell. Physiol.* **218**, 460-466, (2009).
103 Riese, D. J. & Stern, D. F. Specificity within the EGF family/ErbB receptor family signaling network. *Bioessays* **20**, 41-48, (1998).
104 Falls, D. L. Neuregulins: functions, forms, and signaling strategies. *Exp. Cell Res.* **284**, 14-30, (2003).
105 Massague, J. & Pandiella, A. Membrane-anchored growth factors. *Annu. Rev. Biochem.* **62**, 515-541, (1993).
106 Harris, R. C., Chung, E. & Coffey, R. J. EGF receptor ligands. *Exp. Cell Res.* **284**, 2-13, (2003).
107 Rio, C., Buxbaum, J. D., Peschon, J. J. & Corfas, G. Tumor necrosis factor-alpha-converting enzyme is required for cleavage of erbB4/HER4. *J. Biol. Chem.* **275**, 10379-10387, (2000).
108 Singh, A. B. & Harris, R. C. Autocrine, paracrine and juxtacrine signaling by EGFR ligands. *Cell. Signalling* **17**, 1183-1193, (2005).
109 Holbro, T. & Hynes, N. E. ErbB receptors: directing key signaling networks throughout life. *Annu. Rev. Pharmacol. Toxicol.* **44**, 195-217, (2004).

110 Kovacs, E., Zorn, J. A., Huang, Y., Barros, T. & Kuriyan, J. A structural perspective on the regulation of the epidermal growth factor receptor. *Annu. Rev. Biochem.* **84**, 739-764, (2015).

111 Ferguson, K. M. *et al.* EGF Activates Its Receptor by Removing Interactions that Autoinhibit Ectodomain Dimerization. *Mol. Cell* **11**, 507-517, (2003).

112 Klapper, L. N. *et al.* The ErbB-2/HER2 oncoprotein of human carcinomas may function solely as a shared coreceptor for multiple stroma-derived growth factors. *Proc. Natl. Acad. Sci. U. S. A.* **96**, 4995-5000, (1999).

113 Garrett, T. P. *et al.* The crystal structure of a truncated ErbB2 ectodomain reveals an active conformation, poised to interact with other ErbB receptors. *Mol. Cell* **11**, 495-505, (2003).

114 Pinkas-Kramarski, R. *et al.* Diversification of Neu differentiation factor and epidermal growth factor signaling by combinatorial receptor interactions. *EMBO J.* **15**, 2452-2467, (1996).

115 Tzahar, E. *et al.* A hierarchical network of interreceptor interactions determines signal transduction by Neu differentiation factor/neuregulin and epidermal growth factor. *Mol. Cell. Biol.* **16**, 5276-5287, (1996).

116 Guy, P. M., Platko, J. V., Cantley, L. C., Cerione, R. A. & Carraway, K. L., III. Insect cell-expressed p180erbB3 possesses an impaired tyrosine kinase activity. *Proc. Natl. Acad. Sci. U. S. A.* **91**, 8132-8136, (1994).

117 Steinkamp, M. P. *et al.* erbB3 is an active tyrosine kinase capable of homo- and heterointeractions. *Mol. Cell. Biol.* **34**, 965-977, (2014).

118 Schulze, W. X., Deng, L. & Mann, M. Phosphotyrosine interactome of the ErbB-receptor kinase family. *Mol. Syst. Biol.* **1**, 2005.0008, (2005).

119 Pastore, S., Mascia, F., Mariani, V. & Girolomoni, G. The Epidermal Growth Factor Receptor System in Skin Repair and Inflammation. *J. Invest. Dermatol.*, (2007).

120 Herbst, J. J., Opresko, L. K., Walsh, B. J., Lauffenburger, D. A. & Wiley, H. S. Regulation of postendocytic trafficking of the epidermal growth factor receptor through endosomal retention. *J. Biol. Chem.* **269**, 12865-12873, (1994).

121 Sorkin, A. & Carpenter, G. Interaction of activated EGF receptors with coated pit adaptins. *Science* **261**, 612-615, (1993).

122 Baulida, J., Kraus, M. H., Alimandi, M., Di Fiore, P. P. & Carpenter, G. All ErbB receptors other than the epidermal growth factor receptor are endocytosis impaired. *J. Biol. Chem.* **271**, 5251-5257, (1996).

123 Wiley, H. S. Trafficking of the ErbB receptors and its influence on signaling. *Exp. Cell Res.* **284**, 78-88, (2003).

124 Lenferink, A. E. *et al.* Differential endocytic routing of homo- and hetero-dimeric ErbB tyrosine kinases confers signaling superiority to receptor heterodimers. *EMBO J.* **17**, 3385-3397, (1998).

125 Waterman, H., Alroy, I., Strano, S., Seger, R. & Yarden, Y. The C-terminus of the kinase-defective neuregulin receptor ErbB-3 confers mitogenic superiority and dictates endocytic routing. *EMBO J.* **18**, 3348-3358, (1999).

126 Levkowitz, G. *et al.* Ubiquitin ligase activity and tyrosine phosphorylation underlie suppression of growth factor signaling by c-Cbl/Sli-1. *Mol. Cell* **4**, 1029-1040, (1999).

127 Marmor, M. D. & Yarden, Y. Role of protein ubiquitylation in regulating endocytosis of receptor tyrosine kinases. *Oncogene* **23**, 2057-2070, (2004).

128 Hsu, S. C. & Hung, M. C. Characterization of a novel tripartite nuclear localization sequence in the EGFR family. *J. Biol. Chem.* **282**, 10432-10440, (2007).

129 Lin, S.-Y. *et al.* Nuclear localization of EGF receptor and its potential new role as a transcription factor. *Nat. Cell Biol.* **3**, 802, (2001).

130 Giri, D. K. *et al.* Endosomal transport of ErbB-2: mechanism for nuclear entry of the cell surface receptor. *Mol. Cell. Biol.* **25**, 11005-11018, (2005).

131 Offterdinger, M., Schofer, C., Weipoltshammer, K. & Grunt, T. W. c-erbB-3: a nuclear protein in mammary epithelial cells. *J. Cell Biol.* **157**, 929-939, (2002).

132 Elenius, K. *et al.* A novel juxtamembrane domain isoform of HER4/ErbB4. Isoform-specific tissue distribution and differential processing in response to phorbol ester. *J. Biol. Chem.* **272**, 26761-26768, (1997).

133 Lo, H. W. *et al.* Nuclear interaction of EGFR and STAT3 in the activation of the iNOS/NO pathway. *Cancer Cell* **7**, 575-589, (2005).

134 Wang, S. C. *et al.* Binding at and transactivation of the COX-2 promoter by nuclear tyrosine kinase receptor ErbB-2. *Cancer Cell* **6**, 251-261, (2004).

135 Reif, R. *et al.* Activated ErbB3 Translocates to the Nucleus via Clathrin-independent Endocytosis, Which Is Associated with Proliferating Cells. *J. Biol. Chem.* **291**, 3837-3847, (2016).

136 Maatta, J. A. *et al.* Proteolytic cleavage and phosphorylation of a tumor-associated ErbB4 isoform promote ligand-independent survival and cancer cell growth. *Mol. Biol. Cell* **17**, 67-79, (2006).

137 Tovey, S. M., Dunne, B., Witton, C. J., Cooke, T. G. & Bartlett, J. M. HER4 in breast cancer: comparison of antibodies against intra- and extra-cellular domains of HER4. *Breast Cancer Res.* **8**, R19, (2006).

138 Ni, C. Y., Murphy, M. P., Golde, T. E. & Carpenter, G. gamma -Secretase cleavage and nuclear localization of ErbB-4 receptor tyrosine kinase. *Science* **294**, 2179-2181, (2001).

139 Williams, C. C. *et al.* The ERBB4/HER4 receptor tyrosine kinase regulates gene expression by functioning as a STAT5A nuclear chaperone. *J. Cell Biol.* **167**, 469-478, (2004).

140 Komuro, A., Nagai, M., Navin, N. E. & Sudol, M. WW domain-containing protein YAP associates with ErbB-4 and acts as a co-transcriptional activator for the carboxyl-terminal fragment of ErbB-4 that translocates to the nucleus. *J. Biol. Chem.* **278**, 33334-33341, (2003).

141 Aqeilan, R. I. *et al.* WW domain-containing proteins, WWOX and YAP, compete for interaction with ErbB-4 and modulate its transcriptional function. *Cancer Res.* **65**, 6764-6772, (2005).

142 Gilbertson, R. *et al.* Novel ERBB4 juxtamembrane splice variants are frequently expressed in childhood medulloblastoma. *Genes, Chromosomes Cancer* **31**, 288-294, (2001).

143 Veikkolainen, V. *et al.* Function of ERBB4 is determined by alternative splicing. *Cell Cycle* **10**, 2647-2657, (2011).

144 Vecchi, M., Baulida, J. & Carpenter, G. Selective cleavage of the heregulin receptor ErbB-4 by protein kinase C activation. *J. Biol. Chem.* **271**, 18989-18995, (1996).

145 Vecchi, M. & Carpenter, G. Constitutive proteolysis of the ErbB-4 receptor tyrosine kinase by a unique, sequential mechanism. *J. Cell Biol.* **139**, 995-1003, (1997).

146 Elenius, K. *et al.* Characterization of a naturally occurring ErbB4 isoform that does not bind or activate phosphatidyl inositol 3-kinase. *Oncogene* **18**, 2607-2615, (1999).

147 Ben-Bassat, H. & Klein, B. Y. Inhibitors of tyrosine kinases in the treatment of psoriasis. *Curr. Pharm. Des.* **6**, 933-942, (2000).

148 Nanney, L. B., Stoscheck, C. M., Magid, M. & King, L. E., Jr. Altered [125I]epidermal growth factor binding and receptor distribution in psoriasis. *J. Invest. Dermatol.* **86**, 260-265, (1986).

149 Cook, P. W. *et al.* Amphiregulin messenger RNA is elevated in psoriatic epidermis and gastrointestinal carcinomas. *Cancer Res.* **52**, 3224-3227, (1992).

150 Piepkorn, M. Overexpression of amphiregulin, a major autocrine growth factor for cultured human keratinocytes, in hyperproliferative skin diseases. *Am. J. Dermatopathol.* **18**, 165-171, (1996).

151 Elder, J. T. *et al.* Overexpression of transforming growth factor alpha in psoriatic epidermis. *Science* **243**, 811-814, (1989).

152 Stoll, S. W. & Elder, J. T. Retinoid regulation of heparin-binding EGF-like growth factor gene expression in human keratinocytes and skin. *Exp. Dermatol.* **7**, 391-397, (1998).

153 Stoscheck, C. M., Nanney, L. B. & King, L. E., Jr. Quantitative determination of EGF-R during epidermal wound healing. *J. Invest. Dermatol.* **99**, 645-649, (1992).

154 Dahlhoff, M., Schafer, M., Muzumdar, S., Rose, C. & Schneider, M. R. ERBB3 is required for tumor promotion in a mouse model of skin carcinogenesis. *Mol. Oncol.* **9**, 1825-1833, (2015).

155 Forsberg, S. & Rollman, O. Re-epithelialization from human skin explant cultures is promoted by ligand-activated HER3 receptor. *J. Dermatol. Sci.* **59**, 7-15, (2010).

156 Rudloff, U. & Samuels, Y. A growing family: adding mutated Erbb4 as a novel cancer target. *Cell Cycle* **9**, 1487-1503, (2010).

157 Prickett, T. D. *et al.* Analysis of the tyrosine kinome in melanoma reveals recurrent mutations in ERBB4. *Nat. Genet.* **41**, 1127-1132, (2009).

158 Gordon-Thomson, C., Jones, J., Mason, R. S. & Moore, G. P. ErbB receptors mediate both migratory and proliferative activities in human melanocytes and melanoma cells. *Melanoma Res.* **15**, 21-28, (2005).

159 Ben-Yosef, R. *et al.* ErbB4 expression in squamous cell carcinoma of the head and neck. *Target. Oncol.* **1**, 181-185, (2006).

160 Krahn, G. *et al.* Coexpression patterns of EGFR, HER2, HER3 and HER4 in non-melanoma skin cancer. *Eur. J. Cancer* **37**, 251-259, (2001).

161 Hoesl, C., Rohrl, J. M., Schneider, M. R. & Dahlhoff, M. The receptor tyrosine kinase ERBB4 is expressed in skin keratinocytes and influences epidermal proliferation. *Biochim. Biophys. Acta, Gen. Subj.* **1862**, 958-966, (2018).

162 Nanney, L. B., Magid, M., Stoscheck, C. M. & King, L. E., Jr. Comparison of epidermal growth factor binding and receptor distribution in normal human epidermis and epidermal appendages. *J. Invest. Dermatol.* **83**, 385-393, (1984).

163 Piepkorn, M., Predd, H., Underwood, R. & Cook, P. Proliferation-differentiation relationships in the expression of heparin-binding epidermal growth factor-related factors and erbB receptors by normal and psoriatic human keratinocytes. *Arch. Dermatol. Res.* **295**, 93-101, (2003).

164 Maguire, H. C., Jr. *et al.* Distribution of neu (c-erbB-2) protein in human skin. *J. Invest. Dermatol.* **92**, 786-790, (1989).

165 Srinivasan, R., Poulsom, R., Hurst, H. C. & Gullick, W. J. Expression of the c-erbB-4/HER4 protein and mRNA in normal human fetal and adult tissues and in a survey of nine solid tumour types. *J. Pathol.* **185**, 236-245, (1998).

166 Hansen, L. A. *et al.* Genetically null mice reveal a central role for epidermal growth factor receptor in the differentiation of the hair follicle and normal hair development. *Am. J. Pathol.* **150**, 1959-1975, (1997).

167 Hansen, L. A. *et al.* in *Hair research for the next millenium* (eds D.J.J. Van Neste & V.A. Randall) 425-431 (Elsevier, 1996).

168 Murillas, R. *et al.* Expression of a dominant negative mutant of epidermal growth factor receptor in the epidermis of transgenic mice elicits striking alterations in hair follicle development and skin structure. *EMBO J.* **14**, 5216-5223, (1995).

169 Miettinen, P. J. *et al.* Epithelial immaturity and multiorgan failure in mice lacking epidermal growth factor receptor. *Nature* **376**, 337-341, (1995).

170 Dahlhoff, M., Muzumdar, S., Schafer, M. & Schneider, M. R. ERBB2 Is Essential for the Growth of Chemically Induced Skin Tumors in Mice. *J. Invest. Dermatol.* **137**, 921-930, (2017).

171 Bol, D. *et al.* Severe follicular hyperplasia and spontaneous papilloma formation in transgenic mice expressing the neu oncogene under the control of the bovine keratin 5 promoter. *Mol. Carcinog.* **21**, 2-12, (1998).

172 Kiguchi, K. *et al.* Constitutive expression of erbB2 in epidermis of transgenic mice results in epidermal hyperproliferation and spontaneous skin tumor development. *Oncogene* **19**, 4243-4254, (2000).
173 Xie, W., Chow, L. T., Paterson, A. J., Chin, E. & Kudlow, J. E. Conditional expression of the ErbB2 oncogene elicits reversible hyperplasia in stratified epithelia and up-regulation of TGFalpha expression in transgenic mice. *Oncogene* **18**, 3593-3607, (1999).
174 Xie, W. *et al.* Targeted expression of activated erbB-2 to the epidermis of transgenic mice elicits striking developmental abnormalities in the epidermis and hair follicles. *Cell Growth Differ.* **9**, 313-325, (1998).
175 Hansen, L. A. *et al.* The epidermal growth factor receptor is required to maintain the proliferative population in the basal compartment of epidermal tumors. *Cancer Res.* **60**, 3328-3332, (2000).
176 Dlugosz, A. A. *et al.* Targeted disruption of the epidermal growth factor receptor impairs growth of squamous papillomas expressing the v-ras(Ha) oncogene but does not block in vitro keratinocyte responses to oncogenic ras. *Cancer Res.* **57**, 3180-3188, (1997).
177 Dahlhoff, M., Rose, C., de Angelis, M. H., Wolf, E. & Schneider, M. R. Negative feedback mechanisms surpass the effect of intrinsic EGFR activation during skin chemical carcinogenesis. *Am. J. Pathol.* **180**, 1378-1385, (2012).
178 Dahlhoff, M., Rose, C., Wolf, E. & Schneider, M. R. Decreased incidence of papillomas in mice with impaired EGFR function during multi-stage skin carcinogenesis. *Exp. Dermatol.* **20**, 290-293, (2011).
179 Nicholson, R. I., Gee, J. M. & Harper, M. E. EGFR and cancer prognosis. *Eur. J. Cancer* **37 Suppl 4**, S9-15, (2001).
180 Wang, Z. ErbB Receptors and Cancer. *Methods Mol. Biol.* **1652**, 3-35, (2017).
181 Zimmermann, S. & Moelling, K. Phosphorylation and regulation of Raf by Akt (protein kinase B). *Science* **286**, 1741-1744, (1999).
182 Biscardi, J. S. *et al.* c-Src-mediated phosphorylation of the epidermal growth factor receptor on Tyr845 and Tyr1101 is associated with modulation of receptor function. *J. Biol. Chem.* **274**, 8335-8343, (1999).
183 Caldieri, G., Malabarba, M. G., Di Fiore, P. P. & Sigismund, S. EGFR Trafficking in Physiology and Cancer. *Prog. Mol. Subcell. Biol.* **57**, 235-272, (2018).
184 Avraham, R. & Yarden, Y. Feedback regulation of EGFR signalling: decision making by early and delayed loops. *Nat. Rev. Mol. Cell Biol.* **12**, 104-117, (2011).
185 Prenzel, N. *et al.* EGF receptor transactivation by G-protein-coupled receptors requires metalloproteinase cleavage of proHB-EGF. *Nature* **402**, 884-888, (1999).
186 Berset, T. A., Hoier, E. F. & Hajnal, A. The C. elegans homolog of the mammalian tumor suppressor Dep-1/Scc1 inhibits EGFR signaling to regulate binary cell fate decisions. *Genes Dev.* **19**, 1328-1340, (2005).
187 Haj, F. G., Verveer, P. J., Squire, A., Neel, B. G. & Bastiaens, P. I. Imaging sites of receptor dephosphorylation by PTP1B on the surface of the endoplasmic reticulum. *Science* **295**, 1708-1711, (2002).
188 Rubin, C., Gur, G. & Yarden, Y. Negative regulation of receptor tyrosine kinases: unexpected links to c-Cbl and receptor ubiquitylation. *Cell Res.* **15**, 66-71, (2005).
189 Rubin, C. *et al.* Sprouty fine-tunes EGF signaling through interlinked positive and negative feedback loops. *Curr. Biol.* **13**, 297-307, (2003).
190 Reich, A., Sapir, A. & Shilo, B. Sprouty is a general inhibitor of receptor tyrosine kinase signaling. *Development* **126**, 4139-4147, (1999).
191 Egan, J. E., Hall, A. B., Yatsula, B. A. & Bar-Sagi, D. The bimodal regulation of epidermal growth factor signaling by human Sprouty proteins. *Proc. Natl. Acad. Sci. U. S. A.* **99**, 6041-6046, (2002).

192 Laederich, M. B. *et al.* The leucine-rich repeat protein LRIG1 is a negative regulator of ErbB family receptor tyrosine kinases. *J. Biol. Chem.* **279**, 47050-47056, (2004).
193 Gur, G. *et al.* LRIG1 restricts growth factor signaling by enhancing receptor ubiquitylation and degradation. *EMBO J.* **23**, 3270-3281, (2004).
194 Yarden, Y. & Pines, G. The ERBB network: at last, cancer therapy meets systems biology. *Nat. Rev. Cancer* **12**, 553, (2012).
195 Shtiegman, K. *et al.* Defective ubiquitinylation of EGFR mutants of lung cancer confers prolonged signaling. *Oncogene* **26**, 6968-6978, (2007).
196 Cloughesy, T. F. *et al.* Antitumor activity of rapamycin in a Phase I trial for patients with recurrent PTEN-deficient glioblastoma. *PLoS Med.* **5**, e8, (2008).
197 Yi, W. *et al.* Expression of leucine-rich repeats and immunoglobulin-like domains (LRIG) proteins in human ependymoma relates to tumor location, WHO grade, and patient age. *Clin Neuropathol.* **28**, 21-27, (2009).
198 Amit, I. *et al.* A module of negative feedback regulators defines growth factor signaling. *Nat. Genet.* **39**, 503-512, (2007).
199 Musacchio, M. & Perrimon, N. The Drosophila kekkon genes: novel members of both the leucine-rich repeat and immunoglobulin superfamilies expressed in the CNS. *Dev. Biol.* **178**, 63-76, (1996).
200 Suzuki, Y., Sato, N., Tohyama, M., Wanaka, A. & Takagi, T. cDNA cloning of a novel membrane glycoprotein that is expressed specifically in glial cells in the mouse brain. LIG-1, a protein with leucine-rich repeats and immunoglobulin-like domains. *J. Biol. Chem.* **271**, 22522-22527, (1996).
201 Nilsson, J. *et al.* Cloning, characterization, and expression of human LIG1. *Biochem. Biophys. Res. Commun.* **284**, 1155-1161, (2001).
202 Holmlund, C. *et al.* Characterization and tissue-specific expression of human LRIG2. *Gene* **332**, 35-43, (2004).
203 Guo, D., Holmlund, C., Henriksson, R. & Hedman, H. The LRIG gene family has three vertebrate paralogs widely expressed in human and mouse tissues and a homolog in Ascidiacea. *Genomics* **84**, 157-165, (2004).
204 Simion, C., Cedano-Prieto, M. E. & Sweeney, C. The LRIG family: enigmatic regulators of growth factor receptor signaling. *Endocr.-Relat. Cancer* **21**, R431-443, (2014).
205 Williams, A. F. & Barclay, A. N. The immunoglobulin superfamily--domains for cell surface recognition. *Annu. Rev. Immunol.* **6**, 381-405, (1988).
206 Kobe, B. & Kajava, A. V. The leucine-rich repeat as a protein recognition motif. *Curr. Opin. Struct. Biol.* **11**, 725-732, (2001).
207 Malik, U. & Javed, A. LRIGs: A Prognostically Significant Family with Emerging Therapeutic Competence against Cancers. *Curr. Cancer Drug Targets* **17**, 3-16, (2017).
208 Hedman, H. & Henriksson, R. LRIG inhibitors of growth factor signalling - double-edged swords in human cancer? *Eur. J. Cancer* **43**, 676-682, (2007).
209 Lindquist, D., Kvarnbrink, S., Henriksson, R. & Hedman, H. LRIG and cancer prognosis. *Acta Oncol.* **53**, 1135-1142, (2014).
210 Karlsson, T., Mark, E. B., Henriksson, R. & Hedman, H. Redistribution of LRIG proteins in psoriasis. *J. Invest. Dermatol.* **128**, 1192-1195, (2008).
211 Zhao, H., Tanegashima, K., Ro, H. & Dawid, I. B. Lrig3 regulates neural crest formation in Xenopus by modulating Fgf and Wnt signaling pathways. *Development* **135**, 1283-1293, (2008).
212 Rondahl, V. *et al.* Lrig2-deficient mice are protected against PDGFB-induced glioma. *PLoS One* **8**, e73635, (2013).
213 Knuutila, S. *et al.* DNA copy number losses in human neoplasms. *Am. J. Pathol.* **155**, 683-694, (1999).

214 Miller, J. K. *et al.* Suppression of the negative regulator LRIG1 contributes to ErbB2 overexpression in breast cancer. *Cancer Res.* **68**, 8286-8294, (2008).
215 Shattuck, D. L. *et al.* LRIG1 is a novel negative regulator of the Met receptor and opposes Met and Her2 synergy. *Mol. Cell. Biol.* **27**, 1934-1946, (2007).
216 Ledda, F., Bieraugel, O., Fard, S. S., Vilar, M. & Paratcha, G. Lrig1 is an endogenous inhibitor of Ret receptor tyrosine kinase activation, downstream signaling, and biological responses to GDNF. *J. Neurosci.* **28**, 39-49, (2008).
217 Goldoni, S. *et al.* A soluble ectodomain of LRIG1 inhibits cancer cell growth by attenuating basal and ligand-dependent EGFR activity. *Oncogene* **26**, 368-381, (2007).
218 Yi, W. *et al.* Paracrine regulation of growth factor signaling by shed leucine-rich repeats and immunoglobulin-like domains 1. *Exp. Cell Res.* **317**, 504-512, (2011).
219 Powell, A. E. *et al.* The Pan-ErbB Negative Regulator Lrig1 Is an Intestinal Stem Cell Marker that Functions as a Tumor Suppressor. *Cell* **149**, 146-158, (2012).
220 Choi, E. *et al.* Lrig1+ gastric isthmal progenitor cells restore normal gastric lineage cells during damage recovery in adult mouse stomach. *Gut* **67**, 1595-1605, (2018).
221 Suzuki, Y. *et al.* Targeted disruption of LIG-1 gene results in psoriasiform epidermal hyperplasia. *FEBS Lett.* **521**, 67-71, (2002).
222 Jensen, K. B., Jones, J. & Watt, F. M. A stem cell gene expression profile of human squamous cell carcinomas. *Cancer Lett.* **272**, 23-31, (2008).
223 Neirinckx, V., Hedman, H. & Niclou, S. P. Harnessing LRIG1-mediated inhibition of receptor tyrosine kinases for cancer therapy. *Biochim. Biophys. Acta* **1868**, 109-116, (2017).
224 Rafidi, H. *et al.* Leucine-rich repeat and immunoglobulin domain-containing protein-1 (Lrig1) negative regulatory action toward ErbB receptor tyrosine kinases is opposed by leucine-rich repeat and immunoglobulin domain-containing protein 3 (Lrig3). *J. Biol. Chem.* **288**, 21593-21605, (2013).
225 Holmlund, C. *et al.* Cytoplasmic LRIG2 expression is associated with poor oligodendroglioma patient survival. *Neuropathology* **29**, 242-247, (2009).
226 Wang, B. *et al.* Downregulation of LRIG2 expression by RNA interference inhibits glioblastoma cell (GL15) growth, causes cell cycle redistribution, increases cell apoptosis and enhances cell adhesion and invasion in vitro. *Cancer Biol. Ther.* **8**, 1018-1023, (2009).
227 Xiao, Q. *et al.* Soluble LRIG2 ectodomain is released from glioblastoma cells and promotes the proliferation and inhibits the apoptosis of glioblastoma cells in vitro and in vivo in a similar manner to the full-length LRIG2. *PLoS One* **9**, e111419, (2014).
228 Stuart, H. M. *et al.* LRIG2 mutations cause urofacial syndrome. *Am J Hum Genet* **92**, 259-264, (2013).
229 Lindstrom, A. K. *et al.* LRIG1 and squamous epithelial uterine cervical cancer: correlation to prognosis, other tumor markers, sex steroid hormones, and smoking. *Int. J. Gynecol. Cancer* **18**, 312-317, (2008).
230 Wang, G., Wu, J. & Song, H. LRIG2 expression and prognosis in non-small cell lung cancer. *Oncol. Lett.* **8**, 667-672, (2014).
231 Wu, X. *et al.* Expression of EGFR and LRIG proteins in oesophageal carcinoma with emphasis on patient survival and cellular chemosensitivity. *Acta Oncol.* **51**, 69-76, (2012).
232 Mischel, P. S. *et al.* Identification of molecular subtypes of glioblastoma by gene expression profiling. *Oncogene* **22**, 2361-2373, (2003).
233 Reifenberger, G. *et al.* Refined mapping of 12q13-q15 amplicons in human malignant gliomas suggests CDK4/SAS and MDM2 as independent amplification targets. *Cancer Res.* **56**, 5141-5145, (1996).
234 Zhou, Y. *et al.* Genome-wide identification of chromosomal regions of increased tumor expression by transcriptome analysis. *Cancer Res.* **63**, 5781-5784, (2003).

235 Abraira, V. E. *et al.* Cross-repressive interactions between Lrig3 and netrin 1 shape the architecture of the inner ear. *Development* **135**, 4091-4099, (2008).

236 Smith, N. L. *et al.* Association of genome-wide variation with the risk of incident heart failure in adults of European and African ancestry: a prospective meta-analysis from the cohorts for heart and aging research in genomic epidemiology (CHARGE) consortium. *Circ Cardiovasc Genet* **3**, 256-266, (2010).

237 Ma, L. *et al.* Genome-wide association analysis of total cholesterol and high-density lipoprotein cholesterol levels using the Framingham heart study data. *BMC Med Genet* **11**, 55, (2010).

238 Abraira, V. E., Satoh, T., Fekete, D. M. & Goodrich, L. V. Vertebrate Lrig3-ErbB interactions occur in vitro but are unlikely to play a role in Lrig3-dependent inner ear morphogenesis. *PLoS. One* **5**, e8981, (2010).

239 Guo, L. *et al.* Expression and significance of LRIG3 in human cervical squamous cell carcinoma. *Eur. J. Gynaecol. Oncol.* **36**, 414-419, (2015).

240 Cai, M. *et al.* Inhibition of LRIG3 gene expression via RNA interference modulates the proliferation, cell cycle, cell apoptosis, adhesion and invasion of glioblastoma cell (GL15). *Cancer Lett.* **278**, 104-112, (2009).

241 Chen, Y., Wang, Q., Wang, M. & Li, M. Overexpressed LRIG3 gene ameliorates prostate cancer through suppression of cell invasion and migration. *Int. J. Biol. Macromol.* **124**, 1-9, (2019).

242 Hedman, H. *et al.* LRIG2 in contrast to LRIG1 predicts poor survival in early-stage squamous cell carcinoma of the uterine cervix. *Acta Oncol.* **49**, 812-815, (2010).

243 Hellberg, D. & Tot, T. Tumor marker score for prognostication of early-stage squamous cell cervical cancer. *Anticancer Res.* **34**, 887-892, (2014).

244 Lindstrom, A. K. & Hellberg, D. Immunohistochemical LRIG3 expression in cervical intraepithelial neoplasia and invasive squamous cell cervical cancer: association with expression of tumor markers, hormones, high-risk HPV-infection, smoking and patient outcome. *Eur. J. Histochem.* **58**, 2227, (2014).

245 Muller, S. *et al.* Expression of LRIG1 and LRIG3 correlates with human papillomavirus status and patient survival in cervical adenocarcinoma. *Int. J. Oncol.* **42**, 247-252, (2013).

246 Kvarnbrink, S. *et al.* LRIG1 is a prognostic biomarker in non-small cell lung cancer. *Acta Oncol.* **54**, 1113-1119, (2015).

247 Ostroff, R. M. *et al.* Unlocking biomarker discovery: large scale application of aptamer proteomic technology for early detection of lung cancer. *PLoS One* **5**, e15003, (2010).

248 Tanemura, A., Nagasawa, T., Inui, S. & Itami, S. LRIG-1 provides a novel prognostic predictor in squamous cell carcinoma of the skin: immunohistochemical analysis for 38 cases. *Dermatol. Surg.* **31**, 423-430, (2005).

249 Thompson, P. A. *et al.* Loss of LRIG1 Locus Increases Risk of Early and Late Relapse of Stage I/II Breast Cancer. *Cancer Res.* **74**, 2928-2935, (2014).

250 Chang, L. *et al.* Restoration of LRIG1 suppresses bladder cancer cell growth by directly targeting EGFR activity. *J. Exp. Clin. Cancer Res.* **32**, 101, (2013).

251 Sheu, J. J. *et al.* LRIG1 modulates aggressiveness of head and neck cancers by regulating EGFR-MAPK-SPHK1 signaling and extracellular matrix remodeling. *Oncogene* **33**, 1375-1384, (2014).

252 Mao, F. *et al.* Lrig1 is a haploinsufficient tumor suppressor gene in malignant glioma. *Oncogenesis* **7**, 13, (2018).

253 Wikstrand, C. J., McLendon, R. E., Friedman, A. H. & Bigner, D. D. Cell Surface Localization and Density of the Tumor-associated Variant of the Epidermal Growth Factor Receptor, EGFRvIII. *Cancer Res.* **57**, 4130-4140, (1997).

254 Stutz, M. A., Shattuck, D. L., Laederich, M. B., Carraway, K. L., 3rd & Sweeney, C. LRIG1 negatively regulates the oncogenic EGF receptor mutant EGFRvIII. *Oncogene* **27**, 5741-5752, (2008).

255 Guo, D. *et al.* LRIG3 modulates proliferation, apoptosis and invasion of glioblastoma cells as a potent tumor suppressor. *J. Neurol. Sci.* **350**, 61-68, (2015).
256 Gassmann, M. *et al.* Aberrant neural and cardiac development in mice lacking the ErbB4 neuregulin receptor. *Nature* **378**, 390-394, (1995).
257 Jones, F. E., Welte, T., Fu, X. Y. & Stern, D. F. ErbB4 signaling in the mammary gland is required for lobuloalveolar development and Stat5 activation during lactation. *J. Cell Biol.* **147**, 77-88, (1999).
258 Kurppa, K. J., Denessiouk, K., Johnson, M. S. & Elenius, K. Activating ERBB4 mutations in non-small cell lung cancer. *Oncogene* **35**, 1283, (2015).
259 Bacus, S. S., Chin, D., Yarden, Y., Zelnick, C. R. & Stern, D. F. Type 1 receptor tyrosine kinases are differentially phosphorylated in mammary carcinoma and differentially associated with steroid receptors. *Am. J. Pathol.* **148**, 549-558, (1996).
260 Kew, T. Y. *et al.* c-erbB-4 protein expression in human breast cancer. *Br. J. Cancer* **82**, 1163-1170, (2000).
261 Srinivasan, R., Gillett, C. E., Barnes, D. M. & Gullick, W. J. Nuclear expression of the c-erbB-4/HER-4 growth factor receptor in invasive breast cancers. *Cancer Res.* **60**, 1483-1487, (2000).
262 Williams, C. S. *et al.* ERBB4 is over-expressed in human colon cancer and enhances cellular transformation. *Carcinogenesis* **36**, 710-718, (2015).
263 Ohashi, Y. *et al.* Overexpression of ErbB4 is an independent marker for lymph node metastasis in Japanese patients with oral squamous cell carcinoma. *Oral Surg, Oral Med. Oral Pathol. Oral Radiol.* **122**, 313-321, (2016).
264 Panchal, H., Wansbury, O., Parry, S., Ashworth, A. & Howard, B. Neuregulin3 alters cell fate in the epidermis and mammary gland. *BMC Dev. Biol.* **7**, 105, (2007).
265 Threadgill, D. W. *et al.* Targeted disruption of mouse EGF receptor: effect of genetic background on mutant phenotype. *Science* **269**, 230-234, (1995).
266 Sibilia, M. & Wagner, E. F. Strain-dependent epithelial defects in mice lacking the EGF receptor. *Science* **269**, 234-238, (1995).
267 Nielsen, T. O., Poulsen, S. S., Journe, F., Ghanem, G. & Sorensen, B. S. HER4 and its cytoplasmic isoforms are associated with progression-free survival of malignant melanoma. *Melanoma Res.* **24**, 88-91, (2014).
268 Fujiwara, S. *et al.* The localization of HER4 intracellular domain and expression of its alternately-spliced isoforms have prognostic significance in ER+ HER2- breast cancer. *Oncotarget* **5**, 3919-3930, (2014).
269 Junttila, T. T. *et al.* Cleavable ErbB4 isoform in estrogen receptor-regulated growth of breast cancer cells. *Cancer Res.* **65**, 1384-1393, (2005).
270 Jensen, K. B. & Watt, F. M. Single-cell expression profiling of human epidermal stem and transit-amplifying cells: Lrig1 is a regulator of stem cell quiescence. *Proc. Natl. Acad. Sci. U. S. A.* **103**, 11958-11963, (2006).
271 Doma, E., Rupp, C. & Baccarini, M. EGFR-ras-raf signaling in epidermal stem cells: roles in hair follicle development, regeneration, tissue remodeling and epidermal cancers. *Int. J. Mol. Sci.* **14**, 19361-19384, (2013).
272 Vassar, R. & Fuchs, E. Transgenic mice provide new insights into the role of TGF-alpha during epidermal development and differentiation. *Genes Dev.* **5**, 714-727, (1991).
273 Cook, P. W. *et al.* Transgenic expression of the human amphiregulin gene induces a psoriasis-like phenotype. *J. Clin. Invest.* **100**, 2286-2294, (1997).
274 Dahlhoff, M. *et al.* Overexpression of Epigen during Embryonic Development Induces Reversible, Epidermal Growth Factor Receptor-Dependent Sebaceous Gland Hyperplasia. *Mol. Cell. Biol.* **34**, 3086-3095, (2014).
275 Tizek, L. *et al.* Skin diseases are more common than we think: screening results of an unreferred population at the Munich Oktoberfest. *J. Eur. Acad. Dermatol. Venereol.*, (2019).

276 Artavanis-Tsakonas, S., Rand, M. D. & Lake, R. J. Notch Signaling: Cell Fate Control and Signal Integration in Development. *Science* **284**, 770-776, (1999).
277 Rishikaysh, P. *et al.* Signaling involved in hair follicle morphogenesis and development. *Int. J. Mol. Sci.* **15**, 1647-1670, (2014).
278 Hay, R. J. *et al.* The global burden of skin disease in 2010: an analysis of the prevalence and impact of skin conditions. *J. Invest. Dermatol.* **134**, 1527-1534, (2014).
279 Dekoninck, S. & Blanpain, C. Stem cell dynamics, migration and plasticity during wound healing. *Nat. Cell Biol.* **21**, 18-24, (2019).
280 Diamond, I., Owolabi, T., Marco, M., Lam, C. & Glick, A. Conditional gene expression in the epidermis of transgenic mice using the tetracycline-regulated transactivators tTA and rTA linked to the keratin 5 promoter. *J. Invest. Dermatol.* **115**, 788-794, (2000).
281 Paus, R. *et al.* A comprehensive guide for the recognition and classification of distinct stages of hair follicle morphogenesis. *J. Invest. Dermatol.* **113**, 523-532, (1999).
282 Brou, C. *et al.* A novel proteolytic cleavage involved in Notch signaling: the role of the disintegrin-metalloprotease TACE. *Mol. Cell* **5**, 207-216, (2000).
283 Ando, K., Ajchenbaum-Cymbalista, F. & Griffin, J. D. Regulation of G1/S transition by cyclins D2 and D3 in hematopoietic cells. *Proc. Natl. Acad. Sci. U. S. A.* **90**, 9571-9575, (1993).
284 Rhee, H., Polak, L. & Fuchs, E. Lhx2 Maintains Stem Cell Character in Hair Follicles. *Science* **312**, 1946-1949, (2006).
285 Snippert, H. J. *et al.* Lgr6 marks stem cells in the hair follicle that generate all cell lineages of the skin. *Science* **327**, 1385-1389, (2010).
286 Horsley, V., Aliprantis, A. O., Polak, L., Glimcher, L. H. & Fuchs, E. NFATc1 Balances Quiescence and Proliferation of Skin Stem Cells. *Cell* **132**, 299-310, (2008).
287 Jaks, V. *et al.* Lgr5 marks cycling, yet long-lived, hair follicle stem cells. *Nat. Genet.* **40**, 1291-1299, (2008).
288 Natsuga, K. Epidermal barriers. *Cold Spring Harbor Perspect. Med.* **4**, a018218, (2014).
289 Furuse, M. *et al.* Claudin-based tight junctions are crucial for the mammalian epidermal barrier: a lesson from claudin-1-deficient mice. *J. Cell Biol.* **156**, 1099-1111, (2002).
290 Tunggal, J. A. *et al.* E-cadherin is essential for in vivo epidermal barrier function by regulating tight junctions. *EMBO J.* **24**, 1146-1156, (2005).
291 Graus-Porta, D., Beerli, R. R., Daly, J. M. & Hynes, N. E. ErbB-2, the preferred heterodimerization partner of all ErbB receptors, is a mediator of lateral signaling. *EMBO J.* **16**, 1647-1655, (1997).
292 Nanba, D., Toki, F., Barrandon, Y. & Higashiyama, S. Recent advances in the epidermal growth factor receptor/ligand system biology on skin homeostasis and keratinocyte stem cell regulation. *J. Dermatol. Sci.* **72**, 81-86, (2013).
293 Mak, K. K. & Chan, S. Y. Epidermal growth factor as a biologic switch in hair growth cycle. *J. Biol. Chem.* **278**, 26120-26126, (2003).
294 Peus, D., Hamacher, L. & Pittelkow, M. R. EGF-receptor tyrosine kinase inhibition induces keratinocyte growth arrest and terminal differentiation. *J. Invest. Dermatol.* **109**, 751-756, (1997).
295 Di Fiore, P. *et al.* erbB-2 is a potent oncogene when overexpressed in NIH/3T3 cells. *Science* **237**, 178-182, (1987).
296 Barnes, L., Puenchera, J., Saurat, J. H. & Kaya, G. Lrig1 and CD44v3 Expression in the Human Folliculosebaceous Unit. *Dermatology* **231**, 116-118, (2015).
297 Gandarillas, A. & Watt, F. M. c-Myc promotes differentiation of human epidermal stem cells. *Genes Dev.* **11**, 2869-2882, (1997).

298 Waikel, R. L., Kawachi, Y., Waikel, P. A., Wang, X. J. & Roop, D. R. Deregulated expression of c-Myc depletes epidermal stem cells. *Nat. Genet.* **28**, 165-168, (2001).
299 Hynes, N. E. & Lane, H. A. ERBB receptors and cancer: the complexity of targeted inhibitors. *Nat. Rev. Cancer* **5**, 341-354, (2005).
300 Glick, A. B. & Yuspa, S. H. in *The Molecular Basis of Cancer (Third Edition)* (eds John Mendelsohn *et al.*) 495-502 (W.B. Saunders, 2008).
301 Abel, E. L., Angel, J. M., Kiguchi, K. & Digiovanni, J. Multi-stage chemical carcinogenesis in mouse skin: fundamentals and applications. *Nat. Protoc.* **4**, 1350-1362, (2009).
302 Ise, K. *et al.* Targeted deletion of the H-ras gene decreases tumor formation in mouse skin carcinogenesis. *Oncogene* **19**, 2951-2956, (2000).
303 Witsch, E., Sela, M. & Yarden, Y. Roles for growth factors in cancer progression. *Physiology (Bethesda)* **25**, 85-101, (2010).
304 Chan, K. S. *et al.* Epidermal growth factor receptor-mediated activation of Stat3 during multistage skin carcinogenesis. *Cancer Res.* **64**, 2382-2389, (2004).
305 Califano JA, L. W., Nehal KS, et al. . in *Cutaneous Squamous Cell Carcinoma of the Head and Neck AJCC Cancer Staging Manual* Ch. 15, 171–181 (NY: Springer, 2017).
306 Reiter, F. P. *et al.* 1,25-(OH)(2)-vitamin D(3) prevents activation of hepatic stellate cells in vitro and ameliorates inflammatory liver damage but not fibrosis in the Abcb4(-/-) model. *Biochem. Biophys. Res. Commun.* **459**, 227-233, (2015).
307 Huang, T., Sun, L., Yuan, X. & Qiu, H. Thrombospondin-1 is a multifaceted player in tumor progression. *Oncotarget* **8**, 84546-84558, (2017).
308 Donnini, S., Morbidelli, L., Taraboletti, G. & Ziche, M. ERK1-2 and p38 MAPK regulate MMP/TIMP balance and function in response to thrombospondin-1 fragments in the microvascular endothelium. *Life Sci.* **74**, 2975-2985, (2004).
309 Larcher, F. *et al.* Aberrant expression of the simple epithelial type II keratin 8 by mouse skin carcinomas but not papillomas. *Mol. Carcinog.* **6**, 112-121, (1992).
310 Carlson, C. B., Lawler, J. & Mosher, D. F. Structures of thrombospondins. *Cell. Mol. Life Sci.* **65**, 672-686, (2008).
311 Qian, X., Wang, T. N., Rothman, V. L., Nicosia, R. F. & Tuszynski, G. P. Thrombospondin-1 modulates angiogenesis in vitro by up-regulation of matrix metalloproteinase-9 in endothelial cells. *Exp. Cell Res.* **235**, 403-412, (1997).
312 Tan, K. & Lawler, J. The interaction of Thrombospondins with extracellular matrix proteins. *J. Cell Commun. Signal.* **3**, 177-187, (2009).
313 Hernandez-Perez, M., El-hajahmad, M., Massaro, J. & Mahalingam, M. Expression of gelatinases (MMP-2, MMP-9) and gelatinase activator (MMP-14) in actinic keratosis and in in situ and invasive squamous cell carcinoma. *Am. J. Dermatopathol.* **34**, 723-728, (2012).
314 Kang, Y. & Massague, J. Epithelial-mesenchymal transitions: twist in development and metastasis. *Cell* **118**, 277-279, (2004).
315 Navarro, P. *et al.* A role for the E-cadherin cell-cell adhesion molecule during tumor progression of mouse epidermal carcinogenesis. *J. Cell Biol.* **115**, 517-533, (1991).
316 Haskins, J. W., Nguyen, D. X. & Stern, D. F. Neuregulin 1-activated ERBB4 interacts with YAP to induce Hippo pathway target genes and promote cell migration. *Sci Signal* **7**, ra116, (2014).
317 Segrelles, C. *et al.* Functional roles of Akt signaling in mouse skin tumorigenesis. *Oncogene* **21**, 53-64, (2002).
318 Yang, Z. *et al.* Phosphorylation and inactivation of PTEN at residues Ser380/Thr382/383 induced by Helicobacter pylori promotes gastric epithelial cell survival through PI3K/Akt pathway. *Oncotarget* **6**, 31916-31926, (2015).
319 Salven, P., Hattori, K., Heissig, B. & Rafii, S. Interleukin-1alpha promotes angiogenesis in vivo via VEGFR-2 pathway by inducing inflammatory cell VEGF synthesis and secretion. *FASEB J.* **16**, 1471-1473, (2002).

320 Darido, C. *et al.* Stage-dependent therapeutic efficacy in PI3K/mTOR-driven squamous cell carcinoma of the skin. *Cell Death Differ.* **25**, 1146-1159, (2018).
321 Hertzler-Schaefer, K. *et al.* Pten loss induces autocrine FGF signaling to promote skin tumorigenesis. *Cell Rep.* **6**, 818-826, (2014).
322 Tuszynski, G. P. & Nicosia, R. F. The role of thrombospondin-1 in tumor progression and angiogenesis. *Bioessays* **18**, 71-76, (1996).
323 Liu, A. *et al.* Epidermal growth factor-like repeats of thrombospondins activate phospholipase Cgamma and increase epithelial cell migration through indirect epidermal growth factor receptor activation. *J. Biol. Chem.* **284**, 6389-6402, (2009).
324 Lopez-Dee, Z., Pidcock, K. & Gutierrez, L. S. Thrombospondin-1: multiple paths to inflammation. *Mediators Inflamm* **2011**, 296069, (2011).
325 Dumas, V. *et al.* Expression of basement membrane antigens and matrix metalloproteinases 2 and 9 in cutaneous basal and squamous cell carcinomas. *Anticancer Res* **19**, 2929-2938, (1999).
326 Dittmann, K., Mayer, C. & Rodemann, H. P. Nuclear EGFR as novel therapeutic target: insights into nuclear translocation and function. *Strahlenther. Onkol.* **186**, 1-6, (2010).
327 Li, F. *et al.* LRIG1 combined with cisplatin enhances bladder cancer lesions via a novel pathway. *Oncol. Rep.* **25**, 1629-1637, (2011).

Appendix

A) List of figures

B) List of tables

C) List of abbreviations

ADAM	a disintegrin and metalloproteinase domain-containing protein
AK	actinic keratoses
AKT	RAC-alpha serine/threonine-protein kinase
APM	arrector pili muscle
AREG	amphiregulin

BCC	basal cell carcinoma
BLIMP1	PR domain zinc finger protein 1
BM	basement membrane
BME	beta-mercaptoethanol
BrdU	bromodexoyuridine
BTC	betacellulin
CASP3	caspase-3
CBL	E3 ubiquitin-protein ligase CBL
CCND3	G1/S-specific cyclin-D3
CD34	hematopoietic progenitor cell antigen CD34
CDH1	E-cadherin
CDKN2A	cyclin-dependent kinase inhibitor 2A
CE	cornified envelope
CNS	central nervous system
Co	control
cSCC	cutaneous squamous cell carcinoma
C_T	threshold cycle number
CYT	cytoplasmic tail
D	dermis
DEP1	density-enhanced phosphatase-1
DMBA	7,12-dimethylbenz(a)anthracene
Dox	doxycycline
DP	dermal papilla
E	embryonic day
ECD	extracellular domain
ECM	extracellular matrix
ED	epidermis
EGF	epidermal growth factor
EGFR	epidermal growth factor receptor
EMT	epithelial-mesenchymal transition
EPGN	epigen
EPU	epidermal proliferative unit
ERBB	erythroblastic leukemia viral oncogene homolog
EREG	epiregulin
FLG	filaggrin
GAPDH	glyceraldehyde-3-phosphate dehydrogenase
GATA3	trans-acting T-cell-specific transcription factor GATA-3
GRB2	growth-factor-receptor bound-2
H3F3A	histone H3.3
HBEGF	heparin-binding EGF-like grwoth factor
HD	hypodermis
HES1	transcription factor HES-1
HF	hair follicle
HG	hair germ
HIV	human immunodeficiency virus
IB	immunoblotted
ICD	intracellular domain
IF	immunofluorescence
IFE	interfollicular epidermis
Ig	immunoglobulin-like domain

IHC	immunohistochemistry
IL1A	interleukin-1-alpha
IL6	interleukin-6
INF	infundibulum
IP	immunoprecipitation
IRS	inner root sheath
IVL	involucrin
JM	juxtamembrane domain
Kek	kekkon
KO	knockout
KRT	keratin
LEF1	lymphoid enhancer-binding factor 1
LHX2	LIM homeobox 2
LOR	loricrin
LRIG	leucine-rich repeats and immunoglobulin-like domains
LRR	leucine-rich repeats
MAML1	mastermind-like protein 1
MAPK	mitogen-activated protein kinase
MET	hepatocyte growth factor receptor
MG	mammary gland
MKI67	proliferation marker protein Ki-67
MMP	matrix-metalloproteinase
MYC	myc proto-oncogene protein
NEDD8	neural precursor cell expressed developmentally downregulated protein 8
NMSC	non-melanoma skin cancer
NOTCH	neurogenic locus notch homolog protein
NRG	neuregulin
NSCLC	non-small cell lung cancer
OCLN	occludin
ORS	outer root sheath
P	post partum
PBS	phosphate-buffered saline
PC	progenitor cell
PCNA	proliferating cell nuclear antigen
PCR	polymerase chain reaction
PDGFB	platelet-derived growth factor subunit B
PDGFRA	platelet-derived growth factor receptor alpha
PI3K	phosphatidylinositol 3-kinase
PKB	protein kinase B
PLET1	placenta-expressed transcript 1 protein
PTEN	phosphatidylinositol 3,4,5-triphosphate 3-phosphatase and dual specificity protein phosphatase PTEN
PTGS2	prostaglandin G/H synthase 2
PTP1B	protein tyrosine phosphatase-1B
qPCR	quantitative real time PCR
RAS	GTPase Ras
RBPJ	recombining binding protein suppressor of hairless
RET	proto-oncogene tyrosine-protein kinase receptor Ret
RPL30	ribosomal protein L30
RTK	receptor tyrosine kinase

RT-PCR	reverse transcription PCR
SC	stem cell
SCC	squamous cell carcinoma
SD	standard deviation
SEM	standard error of the mean
SG	sebaceous gland
SH	SRC homology domain
SHC	Shc transforming protein
SOS	son of sevenless homolog 1
SPRY	sprouty
SRC	proto-oncogene tyrosine-protein kinase Src
STAT	signal transducer and activator of transcription
TG	transgenic
TGFA	transforming growth factor alpha
THBS1	thrombospondin-1
TM	transmembrane domain
TP53	cellular tumor antigen p53
TPA	12-O-tetra-decanoylphorbol-13-acetate
tTA	tetracycline-regulated transcriptional transactivator
TUBA1A	tublin alpha-1a chain
UV	ultraviolet
VIM	vimentin
WB	Western blot
YAP1	transcriptional coactivator YAP1

Acknowledgement

Danksagung

Während der gesamten Zeit meiner Promotion haben mich zahlreiche Personen unterstützt. An dieser Stelle möchte ich mich herzlichst bei allen bedanken.

Mein erster Dank geht an meinen Doktorvater PD Dr. Dietmar Martin für die Annahme meiner externen Promotion und die Unterstützung.

Weiter möchte ich mich bei Herrn Prof. Dr. Eckhard Wolf für die Betreuung meiner Promotion, die Unterstützung und die hervorragenden Arbeitsbedingungen bedanken.

Ein besonderer Dank gilt PD Dr. Maik Dahlhoff, der mir die Promotion unter seiner Anleitung und Betreuung ermöglicht hat. Vielen Dank für die interessante und spannende Aufgabenstellung die Organisation aller Rahmenbedingungen, die stetige Unterstützung und die zahlreichen wissenschaftlichen Diskussionen und Anregungen. Ich hatte alle Freiheiten um meine eigenen Ideen einzubringen und umzusetzen und ich durfte meine Ergebnisse auf verschiedenen Konferenzen präsentieren. Herzlichen Dank, ich konnte in der Zeit der Promotion sehr viel lernen!

Außerdem möchte ich mich bei allen weiteren Mitgliedern der Prüfungskommission herzlich bedanken: Prof. Dr. Klaus Förstemann, Prof. Dr. Julian Stingele und Prof. Dr. Karl-Peter Hopfner.

Einen sehr großen Dank richte ich auch an die gesamte AG Wolf. Besonders Sepp Millauer, Franziska Kress, Max Marschall, Anna Lutz, Tamara Holy, Silja Zettler und Nicole Wegmann haben mich bei der Durchführung meiner Experimente und Analysen stetig unterstützt. Danke für die tolle Zusammenarbeit und das angenehme Arbeitsklima!

Weiter möchte ich dem gesamten Personal in der Tierhaltung danken. Petra Renner und Dr. Ingrid Renner-Müller haben es mir ermöglicht, dass ich alle Maus-Experimente reibungslos durchführen konnte. Vielen lieben Dank! Auch den Tierpflegern möchte ich an dieser Stelle dafür danken!

Danke auch an meine Praktikantinnen Jennifer Steiner und Caterina Iuliano. Ich bin an der Aufgabe als Betreuer während der Bachelorarbeit bzw. des F-Praktikums gewachsen und konnte dabei auch viel lernen.

Sylvia Hornig danke ich für die Hilfe bei allen organisatorischen Angelegenheiten.

Außerdem gilt mein Dank auch allen, die an den verschiedenen Projekten während meiner Promotion beteiligt waren, mit mir zusammen gearbeitet und mich unterstützt haben: PD Dr. Marlon Schneider, PD Dr. Ronald Wolf, Enrica Zanuttigh, Jennifer Röhrl, Dr. Thomas Fröhlich, Miwako Köster, Prof. Dr. Mathias Goebeler, Dr. Hermann Kneitz, Prof. Dr. Jennifer Hundt, Nadine Merg, PD Dr. Christian Rose, Dr. Christian Posch, Dr. Julia Philippou-Massier, Dr. Stefan Krebs und Dr. Helmut Blum. Vielen Dank für die gute Zusammenarbeit!

Weiter möchte ich mich bei allen Mitarbeitern des Genzentrums bedanken, die stets für die hervorragenden Arbeitsbedingungen sorgen. Danke auch an Leslie Heinz, der bei IT Fragen immer zur Stelle war und mir den perfekten Schreibplatz vermittelt hat.

Von ganzem Herzen möchte ich mich auch bei Kathrin Hedegger bedanken. Ihre Unterstützung in allen Bereichen und die fachlichen Diskussionen und Anregungen waren mir eine große Hilfe. Danke für die kleinen gemeinsamen Auszeiten, die Pausen auf dem Dach, den rettenden Kuchen oder auch den gelegentlichen G&T. „We are…“ - Du warst ein toller Lab-partner in crime! Vielen lieben Dank!

Mareike Czuppa, Kathrin Hedegger und Jessica Smith danke ich herzlich für das Korrekturlesen von Teilen dieser Arbeit.

Ein außerordentliches Dankeschön gilt auch all meinen Freunden, ohne sie alle namentlich zu nennen. Ihr habt mich während meiner Promotion immer unterstützt und motiviert. Ich schätze mich sehr glücklich so wunderbare Menschen, wie euch, an meiner Seite zu haben. Bei Hannelore Hartmann möchte ich mich für die sportlichen Herausforderungen bedanken. Unsere Challenges und das Training haben mich immer wieder aus dem Laboralltag herausgeholt und mir im wahrsten Sinne des Wortes viel Kraft gegeben. Du hast mir wissenschaftlich und privat immer Mut gemacht, danke! Danke möchte ich auch den ganzen „Senioren“ sagen! Ihr habt sowohl meine Studienzeit als auch diese besondere Zeit der Promotion enorm bereichert! Schön, dass bei uns die Chemie gestimmt hat! Ein ganz großer Dank gilt auch meinen Ex-Homies Gundula Hölzel und Katharina Iwan. Es war immer schön, nach auch noch so stressigen Tagen im Labor, nach Hause zu kommen. Ihr habt mich immer unterstützt und Verständnis gehabt. Ich habe es sehr genossen mit euch! Kathi, Du hast mich v.a. jetzt in der Endphase immer motiviert und beruhigt, auch aus der Ferne, vielen herzlichen Dank!

Vor allem aber möchte ich mich bei meiner Familie für ihre bedingungslose Unterstützung und ihr Verständnis bedanken. Mein größter und von ganzem Herzen kommender Dank gilt meinen Eltern. Sie haben mich immer sowohl emotional als auch finanziell unterstützt und sind mir in jeder Situation zur Seite gestanden. Ohne euch stünde ich heute nicht hier. Danke für alles was ihr für mich getan habt! Für euer immer offenes Ohr, eure Liebe und euren unermüdlichen Beistand bin ich zu tiefst dankbar!